

2016

Laboratory and field-scale studies of corn stover degradation, and implications for feedstock cost to lignocellulosic biorefineries

Rachel Anne Bearden
Iowa State University

Follow this and additional works at: <http://lib.dr.iastate.edu/etd>

 Part of the [Agriculture Commons](#), [Bioresource and Agricultural Engineering Commons](#), and the [Microbiology Commons](#)

Recommended Citation

Bearden, Rachel Anne, "Laboratory and field-scale studies of corn stover degradation, and implications for feedstock cost to lignocellulosic biorefineries" (2016). *Graduate Theses and Dissertations*. 15876.
<http://lib.dr.iastate.edu/etd/15876>

This Thesis is brought to you for free and open access by the Iowa State University Capstones, Theses and Dissertations at Iowa State University Digital Repository. It has been accepted for inclusion in Graduate Theses and Dissertations by an authorized administrator of Iowa State University Digital Repository. For more information, please contact digirep@iastate.edu.

**Laboratory and field-scale studies of corn stover degradation, and implications for
feedstock cost to lignocellulosic biorefineries**

by

Rachel Anne Bearden

A thesis submitted to the graduate faculty
in partial fulfillment of the requirements for the degree of
MASTER OF SCIENCE

Co-majors: Agricultural and Biosystems Engineering, Biorenewable Resources and Technology

Program of Study Committee:
Matthew J. Darr, Major Professor
D. Raj Raman
Thomas J. Brumm

Iowa State University
Ames, Iowa
2016

Copyright © Rachel Anne Bearden, 2016. All rights reserved.

TABLE OF CONTENTS

LIST OF EQUATIONS	vi
LIST OF FIGURES	viii
LIST OF TABLES	xiii
ACKNOWLEDGEMENTS	xv
ABSTRACT	xvi
CHAPTER 1: GENERAL INTRODUCTION	1
1.1 Problem Identification	1
1.2 Thesis Organization	4
CHAPTER 2: LITERATURE REVIEW	5
2.1 Lignocellulosic Biomass	5
2.2 Lignocellulosic Structure	5
2.3 Lignocellulosic Composition	6
2.4 Biological Degradation	8
2.4.1 Enzyme Production and Function	9
2.4.2 Metabolic Conversion	9
2.4.3 Rate Influencing Factors	10
2.4.4 Degradation Inefficiencies	12
2.5 Storage Methods to Minimize Degradation Rates	13

2.6	Gap Analysis.....	15	
2.7	Research Objectives.....	21	
CHAPTER 3: INFLUENCE OF STORAGE MOISTURE AND TEMPERATURE ON			
LIGNOCELLULOSIC DEGRADATION.....			22
3.1	Introduction.....	22	
3.2	Methods.....	23	
3.2.1	Design of Experiment (DOE)	23	
3.2.2	Sample Preparation	24	
3.2.3	Controlled Environment Chambers Set Up	25	
3.2.4	Assessment Parameters.....	26	
3.3	Results and Discussion	29	
3.3.1	Impact of Moisture on Dry Matter Loss	29	
3.3.2	Effect of Temperature on DML	34	
3.3.3	Carbohydrate Analysis.....	36	
3.4	Conclusions.....	45	
3.5	Recommendations for Future Work.....	47	
CHAPTER 4: ASSESSING STORAGE DYNAMICS AND MAGNITUDE OF			
LIGNOCELLULOSIC DEGRADATION.....			48
4.1	Introduction.....	48	
4.2	Methods.....	49	

4.2.1	Material	49
4.2.2	Stack Design	50
4.2.3	Stack Coverage	50
4.2.4	Instrumentation Design.....	51
4.2.5	Top Bale Sampling Design	52
4.2.6	Full Stack Bale Sampling Design	53
4.2.7	Assessment Parameters	54
4.3	Results and Discussion	57
4.3.1	Initial Stack Conditions.....	57
4.3.2	Central Iowa Weather Patterns	59
4.3.1	Stack Temperature Gradients.....	61
4.3.2	Sampling to Understand Moisture Migration	67
4.3.1	Stack Moisture Migration	72
4.4	Conclusions.....	83
APPENDIX A. FEED ANALYSIS METHODOLOGY FOR ANALYZING		
CARBOHYDRATE STRUTURE OF CORN STOVER		
5.1	Laboratory Analysis of Forage	90
5.2	Sample Preparation for Structural Carbohydrate Analysis.....	91
5.3	Neutral Detergent Fiber Analysis	92
5.4	Acid Detergent Fiber Analysis.....	92

5.5	Acid Detergent Lignin Analysis	93
5.6	Determination of Lignocellulosic Composition.....	95
5.7	Influence of Detergent Insoluble Ash.....	95
 APPENDIX B: MODELING MICROBIAL GROWTH AND SUBSTRATE UTILIZATION		
		98

LIST OF EQUATIONS

Equation 2.1: Molecular equation for aerobic respiration	12
Equation 2.2: Aerobic respiration efficiency	13
Equation 2.3: Oxidation of glucose within chains of cellulose	13
Equation 2.4: Bale dry matter calculation.....	17
Equation 3.1: Moisture content calculation, wet basis	27
Equation 3.2: Initial dry matter	28
Equation 3.3: Final dry matter	28
Equation 3.4: Percent dry matter loss (DML %)	28
Equation 3.5: Sample density	28
Equation 3.6: Difference between final % Carbohydrate and the estimated mean initial % Carbohydrate composition	38
Equation 3.7: Corrected % cellulose composition using detergent insoluble ash (DI ash)	39
Equation 3.8: Cellulose estimation error	39
Equation 4.1: Moisture content calculation, wet basis	55
Equation 4.2: Ash content calculation	55
Equation 4.3: Bale dry matter calculation.....	56
Equation 4.4: Dry matter loss calculation.....	56
Equation 4.5: (a,b,c,d): Modifications to Figure 2.10 from literature review, assessing feedstock contribution to ethanol production cost (FCEPC).....	80
Equation 4.6: Feedstock contribution to ethanol production cost (FCEPC) equation	81
Equation 5.1: Reported percent neutral detergent fiber calculation	92
Equation 5.2: Reported percent acid detergent fiber calculation	93

Equation 5.3: Reported percent Lignin calculation	94
Equation 5.4: Percent hemicellulose calculation	95
Equation 5.5: Percent cellulose calculation	95
Equation 5.6: Percent lignin calculation	95
Equation 5.7: Percent total carbohydrate calculation	95
Equation 5.8: Corrected percent cellulose calculation.....	96
Equation 5.9: % Cellulose error calculated with the corrected cellulose content.....	96
Equation 6.1: Microbial growth rate equation (Jang and Chou, 2012).....	100
Equation 6.2: Glucose rate equation (Jang and Chou, 2012).....	100
Equation 6.3: Ethanol rate equation (Jang and Chou, 2012)	100
Equation 6.4: Starch rate equation (Jang and Chou, 2012).....	100
Equation 6.5: Enzyme rate equation (Jang and Chou, 2012).....	100

LIST OF FIGURES

Figure 2.1: Structure of woody lignocellulosic biomass, ETHzürich Institute of Process Engineering. (Rohr, 2016)	6
Figure 2.2: Metabolic conversion of glucose. Adapted from Pearson Education Inc, publishing as Benjamin Cummings	10
Figure 2.3: Categories of bacteria based on pH ranges (Todar, n.d.)	11
Figure 2.4: Categories of bacteria based on temperature ranges (Todar, n.d.)	12
Figure 2.5: Change in moisture content of protected bales during storage (Schon et al., 2013).	15
Figure 2.6: Breakdown of feedstock supply chain cost for 2014 harvest (Darr, 2014).....	16
Figure 2.7: Distribution of average DML% results based on storage type from 32 published studies. Adapted from (Emery et al., 2015)	18
Figure 2.8: Dry matter loss for varying storage methods and biomass moisture contents. Adapted from (Shah and Webster, 2014).	19
Figure 2.9: Final moisture profile for one year of field edge storage. Average bale moisture by vertical row. (Darr et al., 2015).....	19
Figure 2.10: Feedstock supply chain cost equation (Darr, et al., 2015)	20
Figure 3.1: Hydraulic press and resultant tubes of densified corn stover.	25
Figure 3.2: Environmental chamber set up	26
Figure 3.3: Influence of biomass moisture content and storage duration on final dry matter. Combined temperatures of 23°C, 45°C, and 60°C	31

Figure 3.4: Trend of final dry matter with storage duration. Combined 30% and 60% moisture content levels. The R^2 of 84.3% value indicates how well the data fits the quadratic regression.	32
Figure 3.5: The effect of temperature on final dry matter. Combined 30% and 60% moisture content levels at 27 days of storage. Bars indicate 95% confidence intervals.....	36
Figure 3.6: Influence of storage duration on final composition of hemicellulose, cellulose, and lignin. Combined 30% and 60% moisture content levels. Bars indicate 95% confidence intervals.....	37
Figure 3.7: Influence of ash level on detergent insoluble ash content, DI ash/total ash ratio, and cellulose error. Average refers to ash content <12.5% and High refers to ash content >12.5%. Bars indicate 95% confidence intervals.	40
Figure 3.8: Positive linear relationship between total ash content and detergent insoluble ash. The R^2 is 84.0%, indicating how well the data fits the linear regression.	41
Figure 3.9: Linear regression between total ash content and cellulose estimation error. The R^2 is 84.0%, indicating how well the data fits the linear regression.	41
Figure 3.10: Cumulative distribution of field average ash content from 2015 harvest (Darr et al., 2015)	43
Figure 3.11: Lack of relationship between dry matter loss to percent convertible material. Combined all moisture levels and temperatures >0°C.....	44
Figure 3.12: Corn stover composition before and after 30% DML.....	44
Figure 4.1: Map of field locations, Biocentury Research Farm, and DuPont Biorefinery	49
Figure 4.2: 2015 Experimental field edge stack configuration with four coverage methods: A: peaked tarp, B: wrapped top bales, C: flat tarp, and D: no coverage.....	50

Figure 4.3: Coverage treatments and probe locations for six-bale-high stacks	51
Figure 4.4: Top bale sampling bale locations, similar placement for all four treatments.....	52
Figure 4.5: Auger coring unit capable of coring 1.2m (4ft) in depth.....	52
Figure 4.6: Top bale composite sampling three sections.....	53
Figure 4.7: Stationary scale and coring unit	54
Figure 4.8: Side moisture penetration measurement and separated sample	55
Figure 4.9: Estimated initial moisture and ash content by field ID. Bars indicate 95% confidence intervals.	58
Figure 4.10: Completed field edge storage trial stack, fall 2015	58
Figure 4.11: Historical precipitation for central Iowa (Iowa Environmental Mesonet, 2015)	60
Figure 4.12: Cumulative distribution for central Iowa December precipitation (Iowa Environmental Mesonet, 2015).....	61
Figure 4.13: Example of temperature profile, one treatment of one six-bale-high stack	62
Figure 4.14: Probe placement for six and four-bale high stacks.....	62
Figure 4.15: Fields F08465 (left) and F08454 (right), temperature profiles, stacking day to beginning of December 2015.....	64
Figure 4.16: One field site, all four treatment temperature profiles. Probes 1, 5, 8, plotted with ambient temperature.	66
Figure 4.17: Temperature profile of uncovered treatment. Probes 5 and 6 are bolded.	67
Figure 4.18: March top bale sampling moisture content. Combined four fields. Composite profiles of top bale (section 1: top 1ft, section 2: second ft, section 3: bottom ft). Bars indicate 95% confidence intervals.	68

Figure 4.19: March top bale moisture content, fields split by initial moisture content. A: peaked tarp, B: wrapped top bales, C: flat tarp, and D: no coverage. Bars indicate 95% confidence intervals.	69
Figure 4.20: July top bale moisture content by sections. Composite profiles of top bale (section 1: top 1ft, section 2: second ft, section 3: bottom ft) Section 4 in treatment D refers to the top ft of the second bale from the top. Bars indicate 95% confidence intervals.....	70
Figure 4.21: August top bale moisture content by sections. Composite profiles of top bale (section 1: top 1ft, section 2: second ft, section 3: bottom ft) Section 4 in treatment D refers to the top ft of the second bale from the top. Bars indicate 95% confidence intervals.....	71
Figure 4.22: Treatment top bale moisture contents over time. Averaged three sections.....	72
Figure 4.23: Final vertical moisture profiles for each coverage treatment, combined all four fields. “Bottom” refers to the dry upper portion of the bottom bale. “Wicking” refers to the saturated base portion of the bottom bale.	74
Figure 4.24: Telehandler attempting to pick up a top bale post storage, highlighting loss of integrity	74
Figure 4.25: Distribution of wicking height. Combined all fields and all treatments	75
Figure 4.26: Treatment and bale location influence on side moisture penetration. Bars indicate 95% confidence intervals.	75
Figure 4.27: Map of moisture migration- all four fields aggregated.	76
Figure 4.28: Stack site treatment cross sections. Columns indicate treatments: A: peaked tarp, B: wrapped top bales, C: flat tarp, and D: no coverage. Rows indicate field ID’s.....	77
Figure 4.29: Dry matter loss results by vertical bale position for treatments A, C, and D. Bars indicate 95% confidence intervals.....	78

Figure 4.30: Theoretical biomass dry matter composition after 30% DML.....	79
Figure 5.1: Forage analysis breakdown (Schroeder, 2008).	91
Figure 5.2: Forage fraction classification based on Van Soest method (Schroeder, 2008).....	91
Figure 5.3: Summary flow chart of ADF, NDF, and AD Lignin analysis methods	94
Figure 5.4: Description of carbohydrate analysis tests from Midwest Laboratorie Inc.....	97
Figure 6.1: Microbial growth curve, log scale	98
Figure 6.2: Modeling Simultaneous Saccharification/Fermentation reactor using (Jang and Chou, 2012) model. S: starch concentration, E: ethanol concentration, G: glucose concentration, and X: microbial concentration.....	99
Figure 6.3: Simultaneous Saccharification/Fermentation modeling variables (Jang, Chou 2012)	101

LIST OF TABLES

Table 2.1: Composition of lignocellulosic crops (dry basis)	7
Table 2.2: Lignocellulosic composition of corn plant fractions	7
Table 2.3: Structural composition of corn stalk and leaf varying with plant maturity	8
Table 3.1: Summary table of treatment factors, matrix values indicate replications.....	24
Table 3.2: Tukey's test results for mean dry matter loss based on moisture content for various storage durations. Combined temperatures of 23°C, 45°C, and 60°C	30
Table 3.3: Relating Simultaneous Saccharification/Fermentation (SSF) rate equations to biomass degradation.....	33
Table 3.4: Tukey's test results for mean final dry matter for -20°C temperature level. Combined 9, 18, and 27 storage days	34
Table 3.5: Tukey's test results for mean final dry matter based on temperature level. 27 day storage duration. Combined 30% and 60% moisture levels	35
Table 3.6: Tukey's test results for final composition from day 0 to day 54 of storage	37
Table 3.7: Average compositional change after 54 days of storage	38
Table 3.8: Secondary test ash content influence results	39
Table 3.9: Ash variability within individual bales of corn stover (Schon, 2012).....	42
Table 4.1: Tukey's test results for mean estimation of initial moisture and ash content by field ID	58
Table 4.2: Tukey's test for March top bale sampling moisture (averaged three sections) by treatment.	68
Table 4.3: Tukey's test results for average March top bale moisture based on treatment. Separated by initial field average moisture content.....	69

Table 4.4: Tukey’s test for final average top bale moisture content by treatment and field	72
Table 4.5: Moisture content summary by treatment	77
Table 4.6: Tukey’s test results for dry matter loss based on treatment and vertical bale location.....	78
Table 4.7: Tukey’s test results for mean dry matter loss based on vertical bale location for. Combined treatments A, C, and D.....	79
Table 4.8: Comparing feedstock contribution to ethanol production cost (FCEPC) and annual FCEPC for protected storage and field edge storage	82

ACKNOWLEDGEMENTS

I would like to thank DuPont along with central Iowa farmers for providing the means to complete this project. I am extremely grateful to Iowa State University and the Agricultural and Biological Systems Engineering department for providing me with the resources necessary to pursue this research. I owe thanks to each faculty, staff, and team member I have encountered, who have equipped me with the education and knowledge I have today. I want to individually thank my major professor, Dr. Matthew Darr, for his guidance and continued optimism throughout this project. He furnished this opportunity for me to not only be part of an incredible project and research team, but make an impact towards a much larger goal. I also owe special thanks to Keith Webster for the time, effort, and passion he contributed to this research.

I want to thank my friends and loved ones for their patience and support during my graduate program. To my Mom and Dad for fostering my drive for knowledge at an early age and providing me with a solid foundation. I would not have had this opportunity if not for your support from day one. To my grandparents for inspiring me to work hard each day and to stay humble. And to my boyfriend, Andrew, for the encouragement to pursue things to which I have passion for.

Lastly, I want to thank God for the strength summoned to complete this research, and for laying the path forward for me to be where I am today.

ABSTRACT

Industrial producers of biorenewable products require an economically stable biomass feedstock in order to compete with petroleum based products. All components of the supply chain (harvest, transportation, and storage) must each be implemented at the lowest cost. This research is focused on reducing the storage cost of baled corn stover. Uncovered field-edge storage of baled corn stover may be cheaper than aggregated satellite storage, because field-edge storage eliminates material cost to tarp stacks as well as level, drain, and lay a rock base on undeveloped land. Furthermore, field-edge storage eliminates transportation to a satellite location, significantly reducing the total transportation cost. Offsetting these beneficial cost savings is the potential degradation of field-edge storage, due to lessened protection.

Chapters 3 and 4 of this thesis focus on evaluating the tradeoff of reduced storage cost to increased cost associated with loss of material and decreased material quality. Environmentally controlled furnaces were used to simulate the degradation of baled corn stover and evaluate the impact that two rate-influencing factors of microbial metabolism have on material quality. Production scale stacks of bales were monitored to evaluate commercial scale degradation within field edge storage for various methods of coverage. Dynamic trends of degradation were monitored using a thermistor temperature logging system and real time vertical temperature profiles were generated to evaluate the spread of microbial activity within the bale stacks. Weather data and moisture sampling results indicate that temperature shifts within the bale stacks coincided with rainfall events and increased moisture content. Deconstruction of the stacks generated final moisture profiles and permitted assessments of dry matter loss after one year of storage. The trends and profiles developed from these findings were used to assess the impact of degradation on the feedstock contribution of ethanol production cost (FCEPC).

CHAPTER 1: GENERAL INTRODUCTION

1.1 Problem Identification

As recent as 150 years ago, the Western society thrived as a bioeconomy; biomass or organic material from recent biological origin (Brown and Brown, 2014) provided basic energy needs and building blocks for industry. Since then, the introduction of coal, natural gas, and petroleum as consumable resources has outperformed biological materials both in cost and convenience in providing these needs.(Brown and Brown, 2014). Beyond basic needs, modern society moved into a 'petro economy', where developed countries embed petroleum-based products into their everyday lives from fossil fuels for transportation to petroleum based materials and chemicals. Concerns regarding health and environmental impacts (Wang, 2016a), as well as energy security and sustainability (Wang, 2016b) have raised flags to continuing such rates of petroleum consumption. In developed countries, legislation in the form of tax credits, direct and indirect payments, and mandates have been implemented to drive production and consumption of clean biofuels (Brown and Brown, 2014).

Driving this market of biofuels and other biorenewable products relies on the advancement of technology. Progress has been made towards the development of a modern bioeconomy including implementation of advanced biofuel production such as cellulosic based fuels and products. Carbon-rich, lignocellulosic biomass can be either thermochemically or biochemically converted and upgraded into valuable products (Brown and Brown, 2014). Thermochemical processes such as gasification and pyrolysis utilize combinations of heat and pressure to convert biomass (Brown and Brown, 2014). Biochemical production of cellulosic ethanol via fermentation is currently the frontrunner for commercial implementation of lignocellulosic material conversion to fuel. There are currently six major commercial plants in

various stages of startup and production. Two plants are located in Brazil: GranBio Biofelx in São Miguel dos Campos, Alagoas, and Raizen in Piracicaba, São Paulo. These two companies utilize sugar cane bagasse and straw as biomass feedstocks. There are four plants in the United States: DuPont in Nevada, Iowa, Poet in Emmetsburg, Iowa, Quad County Corn Processers in Galva, Iowa, and Abengoa in Hugoton, Kansas (currently undergoing a purchasing agreement for new ownership). Quad County Corn Processers utilize corn kernel fiber and the other three companies utilize corn stover: the leaves, stalks, cobs, and husks left behind after grain harvest. The Midwest United States, producing high yielding corn crops, contains a generous supply of herbaceous corn stover. Corn stover material itself is categorized as a “waste” or co-product feedstock within the biorenewables industry, often seen as a lower cost option compared to energy crops (Brown and Brown, 2014). Regardless of its low-economic value, the collection, transportation, and storage of waste biomass causes logistical challenges that add cost to utilize these feedstocks (Darr, 2014). Additionally, the nature of the material causes issues, specifically its low density, high moisture content, and susceptibility to degradation (Brown and Brown, 2014). As cellulosic ethanol plants come into commission and scale to capacity production, providing a high quality, economically sustainable feedstock is crucial to stabilize output.

The challenge lies within the logistics of continuously supplying a quality harvested product to a plant in a timely, cost effective manner. The corn stover collection industry is starting with modern technology and utilizes windrowing and baling machinery from the well-developed hay and forage industry. A low density material must be collected and packaged to reduce its transport costs as well as storage footprint. Even utilizing developed equipment, “transition costs” are inevitable in a newly developing industry; experience and process development take time, but play a significant role in an industry becoming profitable (Parker,

2016). Since 2010, corn stover feedstock supply chain costs have decreased by approximately 40% (Darr, 2014) . Substantial improvements have been made to the operations section of the supply chain; through equipment telemetry data collection and feedback systems, both machines and operators improve efficiency (Darr, 2014).

Efficiently collecting and transporting a dense package of corn stover has been key to reducing costs within the supply chain. As research continues, the gap for improvement in these areas begins to shrink. Comparable to increasing the efficiency of operations, there is value in optimizing storage methods to both maximize the quality of the material and eliminate non-value-adding costs. Due to climate limitations in many regions, corn stover must be collected in a relatively short window and stored to support an annual supply. If exposed to an adverse environment, material degradation is inevitable (Brown and Brown, 2014). Degradation of corn stover both reduces the amount of available dry material as well as lessens the quality of the material that is left in terms of convertible mass and potential ethanol yield. Degradation can be avoided almost completely if the material is stored properly, but upgraded protection during storage increases the cost of the feedstock. Accurately assessing the tradeoff costs of protection vs material quality highlights potential areas to reduce the cost in that section of the supply chain. From there, informed decisions can be made regarding storage methods.

1.2 Thesis Organization

This thesis begins with an introduction and literature review to focus current knowledge in this area and highlight the need for this particular study. This is followed by two technical chapters. The first technical chapter evaluates the influence of storage moisture and temperature on lignocellulosic degradation. The second technical chapter examines the storage dynamics of moisture migration and bale degradation in response to environmental factors during long term storage. This chapter also evaluates the impact of degradation on the feedstock contribution to ethanol production cost (FCEPC) for a biorefinery.

CHAPTER 2: LITERATURE REVIEW

2.1 Lignocellulosic Biomass

Biomass, or bio renewable resource, is defined as “organic material of recent biological origin” (Brown and Brown, 2014) and is generally split into two categories: wastes and dedicated crops. Biomass materials that are traditionally discarded due to their lack of use or low value are categorized as wastes and include yard waste, municipal solid waste, food processing waste, manure, and agricultural residues (Brown and Brown, 2014). Energy crops, grown for a specific purpose, include varieties of both terrestrial and aquatic species. Terrestrial biomass can be processed to utilize starch, sugar, and oil resources, but lignocellulose comprises the majority of the plant’s structure, making it the world’s most abundant component of biomass available. Terrestrial crops grown specifically for lignocellulosic material fall into two categories: herbaceous crops composed of grasses, both annual and perennial, or woody crops composed of short rotation trees harvested every 3 to 10 years (Brown and Brown, 2014). Crops in both categories produce lignocellulose as a means of energy storage, support, and resistance to degradation, but vary in composition.

2.2 Lignocellulosic Structure

Lignocellulose, making up plant cell wall, can be broken down into three main components: cellulose, hemicellulose, and lignin (Figure 2.1). Cellulose and hemicellulose are sugar-based polymers (polysaccharides) and act as energy storage in the form of carbohydrates. As described by (Aro et al., 2005), cellulose is a homogeneous polymer comprised of solely six-carbon glucose monomers connected by β -1, 4 linkages in a linear chain fashion. These chains, often 8,000-12,000 glucose units long, are often closely packed by hydrogen bonds, forming a strong crystalline structure. Hemicellulose is a heterogeneous polysaccharide containing

combinations of a variety of sugar units with various α and β linkages. The five-carbon sugars can include xylose, mannose, galactose, rhamnose, and arabinose. Often hemicellulose is identified by a specific sugar backbone with differing side chains providing variability and an amorphous structure. Lignin is a heterogeneous polymer composed of phenolic units held together by ether and carbon-carbon bonds. These linkages and the complex branching arrangement forms a matrix surrounding cellulose and hemicellulose, providing structural support and resistance to biological degradation (Aro et al., 2005).

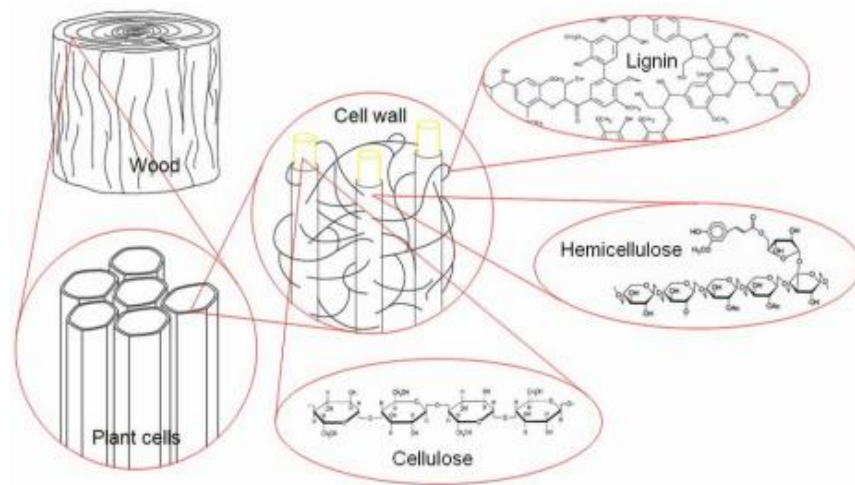


Figure 2.1: Structure of woody lignocellulosic biomass, ETHzürich Institute of Process Engineering. (Rohr, 2016)

2.3 Lignocellulosic Composition

The composition of cellulose, hemicellulose, and lignin within cell walls varies between plant species (Table 2.1). For example, woody plants such as softwood and hardwood species, contain approximately 27% to 32% lignin (Chen, 2014). Whereas herbaceous plants like straws and grasses have lower lignin concentrations near 14% to 25% (Chen, 2014). Lignocellulosic composition can also vary between anatomical fractions of a plant. Crop residue collected as biomass is often a non-homogeneous material. Modern baled (densified) corn stover, for

example is composed of the residual leaves, husks, stalks, and cobs, and components can vary from bale to bale. Beyond that, each plant fraction is composed of differing concentrations of cellulose, hemicellulose, and lignin. Different fractions of a corn plant's biomass maintains their own lignocellulosic composition (Table 2.2). Lastly, the composition of lignocellulose heavily depends on the maturity of a plant. The composition of both corn leaf and corn stalk change as they mature through the growing season (Table 2.3). The heterogeneous nature of crop residue and structural change with maturity provides an extremely variable feedstock in terms of carbohydrate availability.

Table 2.1: Composition of lignocellulosic crops (dry basis)

Feedstock	Cellulose (wt %)	Hemicellulose (wt %)	Lignin (wt %)	Other ^a (wt %)
Bagasse	35	25	20	20
Corn Stover	53	15	16	16
Corn Cob	32	44	13	11
Wheat straw	38	36	16	10
Wheat chaff	38	36	16	11
SRWC	50	23	22	5
HEC	45	30	15	10
Waste Paper	76	13	11	0

Source: Adapted from (Brown and Brown, 2014)^aIncludes protein, oils, and mineral matter, such as silica and alkali

Table 2.2: Lignocellulosic composition of corn plant fractions

Plant fraction	Stover (%)	Bottom (%)	Top (%)	Cob (%)	Above-ear (%)
Cellulose	41.37	42.59	38.67	38.73	38.68
Hemicellulose	25.56	20.17	28.30	33.76	29.93
Lignin	6.34	8.43	5.32	4.89	5.19

Source: Adapted from (Mourtzinis et al., 2014)* Bottom refers to stover material below the ear. Top refers to stover material above the ear, excluding cobs. Above the ear refers to combined top and cob fractions. Grain was removed from cobs.

Table 2.3: Structural composition of corn stalk and leaf varying with plant maturity

	<i>Late dent (110d^a)</i>	<i>Physiological maturity (153d)</i>	<i>Post physiological maturity (220d)</i>
	<i>% of dry matter</i>		
Corn Stalk			
Structural glucon	35	35	35
Xylan	16	22	23
Lignin	15	20	19
Protein	3	4	4
Soluble solids	15	4	4
Corn Leaf			
Structural glucon	18	23	32
Xylan	2	17	22
Lignin	4	13	16
Protein	8	8	4
Soluble solids	35	8	6

Source: Adapted from (Lee et al., 2007) ^aDays after planting

2.4 Biological Degradation

The compositional makeup of lignocellulose within a type of biomass plays a large role in how that material is biologically broken down. Low lignin concentrations, seen with herbaceous biomass, are easier to delignify and access carbohydrate (Brown and Brown, 2014). Herbaceous hemicellulose is composed mainly of xylan which is relatively easy to break down (Bajpai, 2016). These two traits can ease the pretreatment process for herbaceous biomass in chemical and fuel production, but also leaves the biomass more susceptible to environmental degradation (Brown and Brown, 2014). Bacteria and fungi in the environment produce enzymes capable of breaking down organic plant material. Depending on the oxygen content within the environment, the sugars from the plants' carbohydrates can be anaerobically or aerobically metabolized into energy for survival and reproduction of the microorganisms.

2.4.1 Enzyme Production and Function

The breakdown of crop residue on a crop field, or the composting process, are examples of the biological decomposition of organic materials. These processes utilize natural enzymes produced and secreted by microorganisms to degrade the cell wall and its polysaccharides to release monomer sugars. Specific species of fungi and few bacteria are capable of producing lignin-degrading enzymes: laccases and heme peroxidases groups (Aro et al., 2005). More abundant species of fungi and bacteria do not produce these enzymes well, but do produce enzymes that break down cellulose and hemicellulose. Cellulose requires three classes of enzymes for its degradation and must utilize the amorphous regions of the cellulose structure (Aro et al., 2005). Hemicellulose requires different types of endo-enzymes, exo-enzymes, and accessory enzymes (de Souza, 2013). The specific enzymes required depend on the monomer sugars within the hemicellulose.

2.4.2 Metabolic Conversion

Living cells, in this case microorganisms, metabolize organic molecules to obtain energy and release waste products. Two common modes cells use to produce adenosine triphosphate (ATP) energy are aerobic respiration and fermentation as described by (Brooker et al., 2011) (Figure 2.2). One defining contrast between these metabolic processes is the amount of ATP produced, which is directly associated with the availability of oxygen or another electron acceptor. Both pathways begin with glycolysis, converting glucose into pyruvic acid, releasing NADH and 2 ATP. Respiration then moves through the Krebs cycle, producing more NADH, and because there is an electron acceptor (usually oxygen), the NADH is oxidized through oxidative phosphorylation to produce a maximum of 34 more ATP. Fermentation is a less efficient means to produce cellular energy. Without the presence of the electron accepting

oxygen, ATP is formed solely from glycolysis. To keep NADH produced in glycolysis from building up, pyruvic acid is reduced or broken down to help oxidize NADH and produce other products like alcohols or lactic acid.

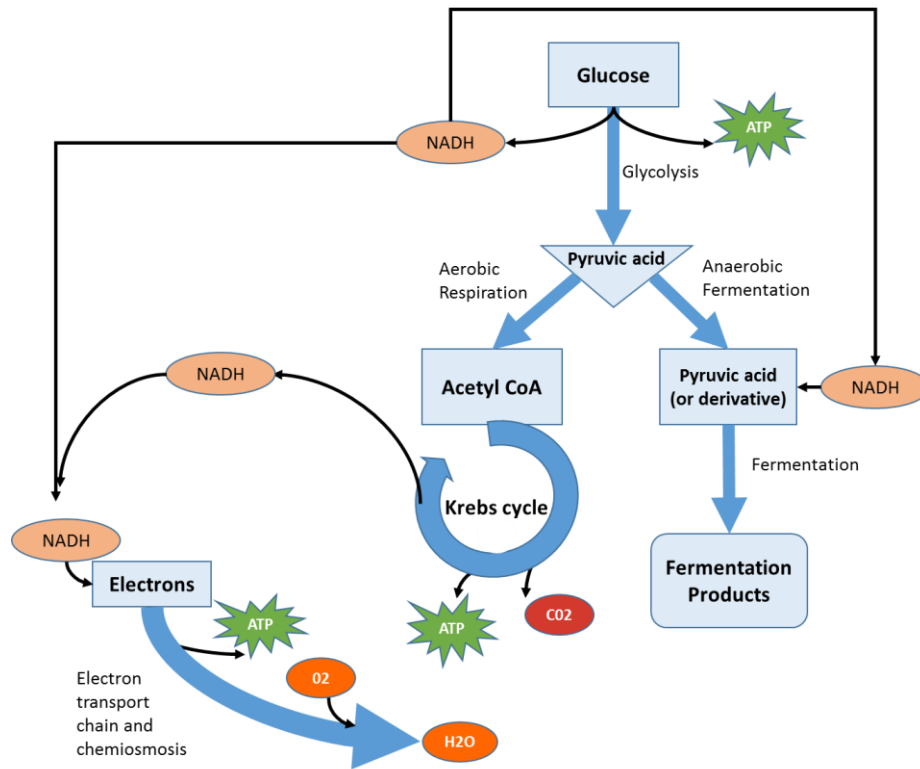


Figure 2.2: Metabolic conversion of glucose. Adapted from Pearson Education Inc, publishing as Benjamin Cummings

2.4.3 Rate Influencing Factors

Many environmental factors influence the breakdown of organic material. Factors include the surrounding substrate, moisture level, oxygen level, pH, and temperature (Hubbe et al., 2010). Properties of the substrate such as the C: N (carbon to nitrogen) ratio and particle size can also affect degradation of the organic material. Microorganisms require nitrogen, specifically proteins, to function and carbon is the basis for sugars needed for energy production (Hubbe et al., 2010). A smaller material particle size increases the accessible area for enzymes (Hubbe et al., 2010). The moisture content or water availability is also important because it “facilitates

substrate decomposition through mobilizing microorganism activities” (Hubbe et al., 2010). For composting, a specific form of microbial degradation of organic materials, a moisture content of 40% to 60% is recommended to optimize degradation. (Hubbe et al., 2010). Too much water can over saturate compost material and limit oxygen availability. Oxygen, pH, and temperature levels influence which species of organisms survive. As mentioned, oxygen influences whether respiration or fermentation is used as the metabolic pathway and the energy a cell can produce, which is needed to further break down sugars. Inadequate oxygen supply can slow down biodegradation (Hubbe et al., 2010). Different species of microorganisms have their own range of pH levels that they can survive in and an optimum pH at which they thrive. Species are categorized based on their ranges; Acidophiles prefer pH between 1 and 5, Neutrophiles prefer levels between 5 and 9, and Akaliphiles prefer pH between 7 and 12 (Figure 2.3) (Todar n.d.). The same type of categorization exists for temperature ranges. Psychrophiles prefer temperatures between 0°C and 20°C (32°F and 68°F), mesophiles prefer 10°C to 45°C (50°F to 113°F), and thermophiles prefer 40°C to 70°C (104°F to 158°F) (Figure 2.4) (Todar, n.d.). Increases or decreases in these three factors: oxygen, pH, and temperature do not necessarily halt organic degradation but influence which species survive and the rate degradation occurs.

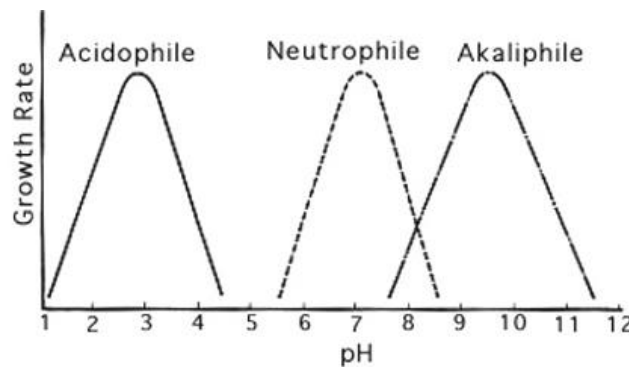


Figure 2.3: Categories of bacteria based on pH ranges (Todar, n.d.)

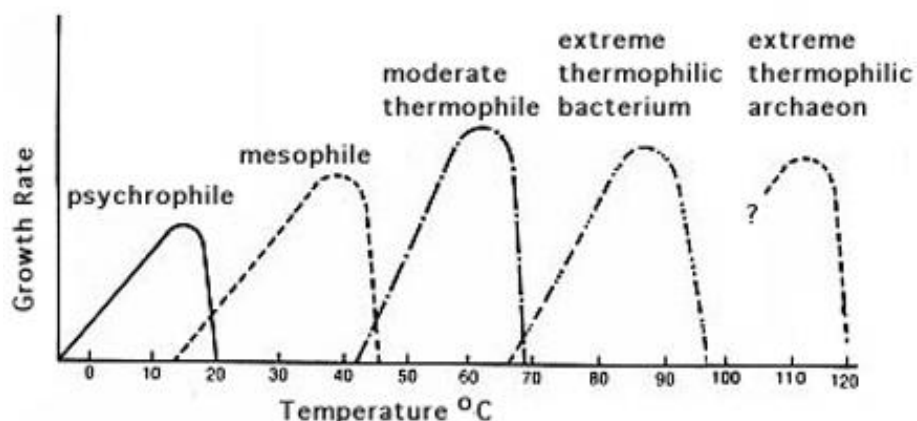
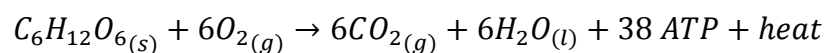


Figure 2.4: Categories of bacteria based on temperature ranges (Todar, n.d.)

2.4.4 Degradation Inefficiencies

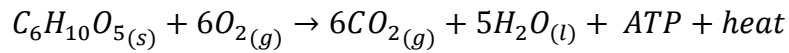
System inefficiencies are noticeable when converting one form of energy into another. In cellular respiration, metabolic pathways convert the caloric value of 1 mol of glucose into a maximum of 38 ATP (Brooker et al., 2011). During aerobic respiration there are 686 kcal released when glucose reacts with oxygen to produce CO₂, H₂O, and ATP (Equation 2.1) (Brooker et al., 2011). The obtainable energy within one formed ATP, represented by the by the hydrolysis of ATP to ADP, is 7.3 kCal (Brooker et al. 2011). This makes the maximum energy conversion efficiency 40% (Equation 2.2). The other 60% or other 412 kCal are released from the reaction in the form of heat. Inefficiencies of decomposition reactions such as the oxidation of glucose within cellulose (long chains of glucose with β 1-4 linkages) (Equation 2.3), could be calculated similarly.

Equation 2.1: Molecular equation for aerobic respiration



Equation 2.2: Aerobic respiration efficiency

$$Efficiency = \frac{(7.3 * 38)}{686} * 100 = 40.4\%$$

Equation 2.3: Oxidation of glucose within chains of cellulose

Decaying organic matter, such as compost, highlights the inefficiency of aerobic respiration well, where enough metabolism occurs to significantly increase temperatures (Hubbe et al., 2010). Composting generally has three phases as described by Hubbe (2010). These phases are best defined by temperature and the types of microorganisms thriving in said temperature. Psychrophiles are able to thrive at lower temperatures, but produce enough heat to raise the composting temperature to levels comfortable for mesophiles. Mesophiles, being more efficient decomposers raise the temperatures up to thermophilic range: 45°C -68°C (113°F to 155°F). During composting, temperature increases correlate with CO₂ production, evidence that oxidation is taking place and organic material is being consumed (Hubbe et al., 2010). Commonly temperatures peak in the thermophilic range and then experience a decrease, indicating the maturation phase (Hubbe et al., 2010). After a spiking in heating, less than thermophilic temperatures does not necessarily indicate decomposition has ceased.

2.5 Storage Methods to Minimize Degradation Rates

In processes like composting or crop residue management, the objective is to speed up degradation by optimizing the conditions of those rate influences factors; moisture, temperature, oxygen, and pH. Conversely, these rates must be minimized in storing biomass to utilize in biorenewable products. Due to the seasonal climate in some regions, temperature is the most

difficult factor to control over one year of storage. Cold storage is a very successful way to prevent biomass degradation, but is not practical for commodity crops with low economic value (Brown and Brown, 2014). Commercial scale implementation of cold storage of corn stover in regions with warm climates would not be economical.

Controlling oxygen and pH is another method of minimizing degradation. Restricting oxygen levels inhibits the growth and consumption of aerobic bacteria, and allows anaerobic bacteria to take over as consuming organisms (Brooker et al., 2011). As mentioned, the consumption rates are much lower for anaerobes because they gain ATP energy from glycolysis only, slowing their growth and reproduction. Anaerobic bacteria also produce various organic acids during the fermentation process which can further inhibit the growth of microorganisms and provide long term storage (Brown and Brown, 2014). This method of storage is referred to as ensiling, and is often used with wet, freshly cut biomass. Ensiling wet corn stover in plastic tube wrap has seen dry matter losses as low as 1.1% (Shinners et al., 2006).

For lower moisture biomass, drying can be used to limit storage losses. “Successful preservation of plant material may require drying to as little as 10% moisture” (Brown and Brown 2014). Mechanical drying consumes a large amount of energy; drying 1 ton of fresh green biomass from 50% moisture to 10% moisture would require about 1.5 GJ (1.4M BTU’s) of energy (Brown and Brown, 2014). In-field drying, takes advantage of solar energy, and is often used for grass crops. Crops can be left in-field beyond maturity to dry, or green crops may be chopped and left to dry before being collected. In the hay industry it is also common to condition the material, crushing the stalks to speed and align drying with that of leaves.

Dry biomass is often baled for storage and may or may not be covered with plastic or net wrap. Uncovered bales are exposed to the risk of taking on moisture during rain events. Sets of

bales can be stacked and covered with a single tarp to minimize coverage material and footprint. Dry bales that are not exposed to rainfall will see minimal degradation. Interior bales of an outside stack experience the same losses as those stored indoors (Schon et al., 2013). Ideally field drying would take place before baling of material, but situations may require biomass to be harvested and baled at a higher than ideal moisture content. Corn stover bales with higher initial moisture content will experience a degree of losses, but properly stored bales will heat, release moisture, and reach a steady state moisture content of ~15%, limiting further degradation (Figure 2.5) (Schon et al., 2013).

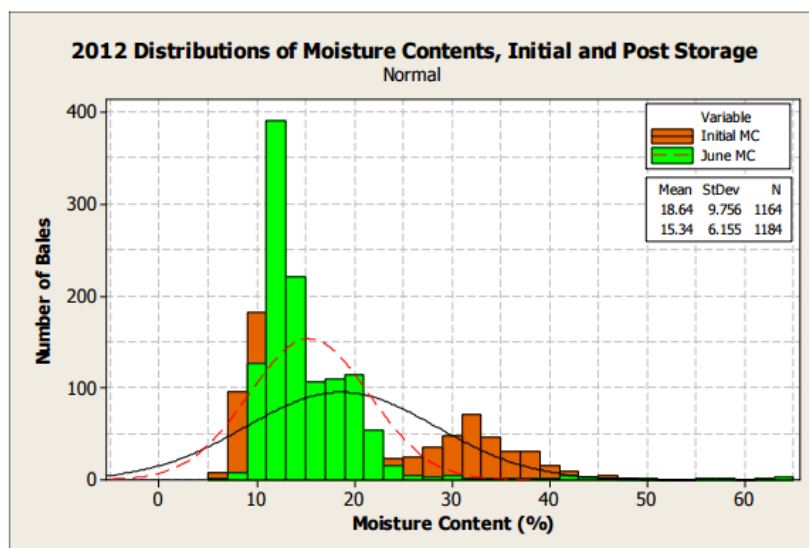


Figure 2.5: Change in moisture content of protected bales during storage (Schon et al., 2013).

2.6 Gap Analysis

Cost efficient feedstock plays a crucial role in making cellulosic-based fuels economically viable and competitive within the energy market. This cost is not simply applied to the purchase of the feedstock from a grower, but also includes the equipment and operations cost

to harvest and bale (densify) the feedstock, as well as the means to transport and store the material (Figure 2.6).

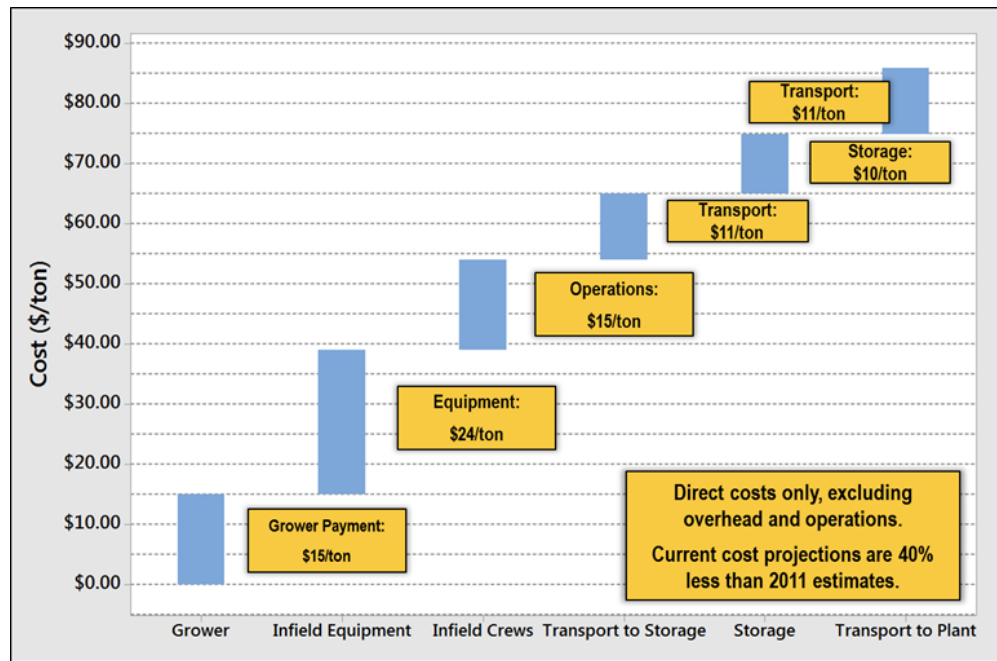


Figure 2.6: Breakdown of feedstock supply chain cost for 2014 harvest (Darr, 2014)

The overall cost of the feedstock supply chain in this model has decreased by roughly 40% since 2011, much attributed to the optimization of the harvest and transportation components (Darr, 2014). The gap for improvements in equipment and operator efficiency will narrow, and savings in other supply chains must be pursued to continue decreasing feedstock costs. One model for bale storage aggregates bales from multiple fields, transporting them to a satellite location for long term storage. Over the course of a year, bales are pulled out of the satellite locations and transported to a biorefinery (Shah et al., 2011). It is common for such satellite locations to be leveled, drained, and have a rock base. Tarping stacks in storage protects material from sunlight and rainfall (Shah et al., 2011). These storage areas provide a high level of protection for biomass, but naturally increase the cost of storage. Field-edge storage has the potential to decrease this cost. Storing smaller bale stacks on the edge of the field they were

harvested from avoids the cost of improving a site. Additionally, bales would be taken directly to the plant from field edge, eliminating transportation to a satellite storage location and a second handling of the bales. A potential \$21/ton decrease in feedstock cost is substantial. A supply chain will not see the full savings if the quality of the material is jeopardized due to decreased protection. The resulting quality and material losses must not outweigh the savings in material and transportation.

Current methods of associating cost to material lost in storage is limited to an analysis of dry matter loss (DML). The dry matter of a bale is calculated using its respective weight and moisture content (Equation 2.4).

Equation 2.4: Bale dry matter calculation

$$\text{Dry Matter} = \text{Bale Weight} - (\text{MC}\% * \text{Bale Weight})$$

Dry matter loss is an evaluation of the dry tons remaining after material is taken out of storage compared to what went into storage. Loss of dry matter is typical due to either handling, or biological degradation and will depend on the moisture of biomass at the time of storage, and the method used to protect the material. Past storage studies show high variability in DML results. Emery (2015) collected DML results for various storage methods from 32 studies of grass crop storage and presented distributions for each (Figure 2.7). Common storage method categories included both loose and baled silage, as well as indoor, covered, and uncovered large square bales (LSB). Uncovered storage results have a wide distribution ranging from DML results of 6% to 42%.

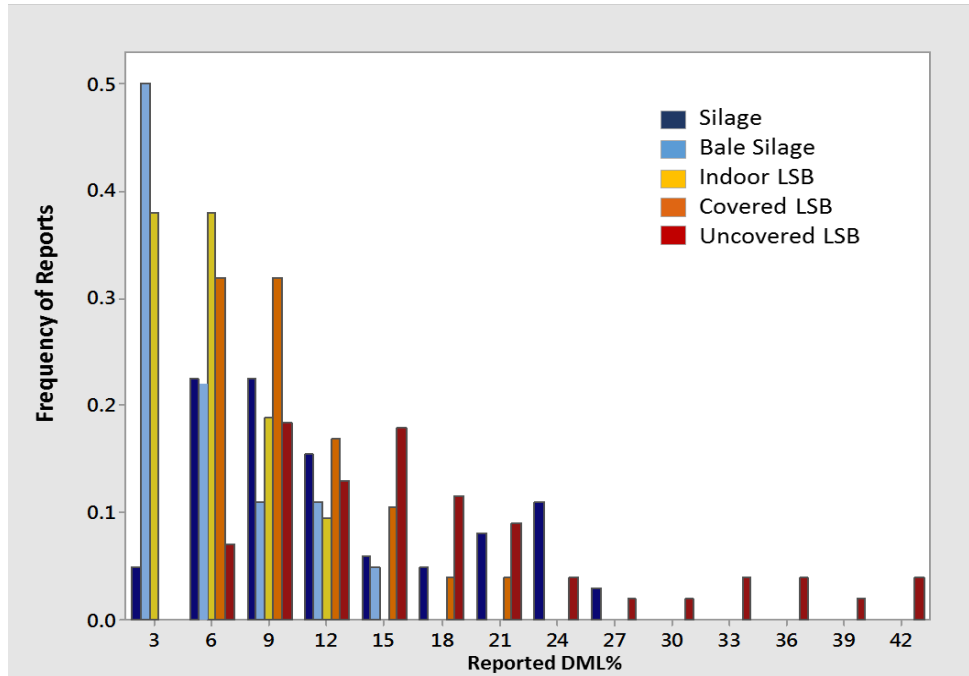


Figure 2.7: Distribution of average DML% results based on storage type from 32 published studies. Adapted from (Emery et al., 2015)

Dry matter loss results will depend on the initial moisture content of the stored biomass. Baled material going into storage with >25% moisture content experiences nearly double the dry matter loss in tarpred and roofed stacks than those < 25% (Shah and Webster, 2014)(Figure 2.8). Losses with ensiled storage are not affected by the initial moisture content of biomass (Figure 2.8) Results will also differ depending on the bales evaluated to represent the stack. Some studies have only analyzed dry matter loss of interior bales; bales within the stack not exposed directly to external moisture. Exposed bales often vary in final moisture content, making it difficult to measure final dry matter to calculate loss (Schon et al., 2013).

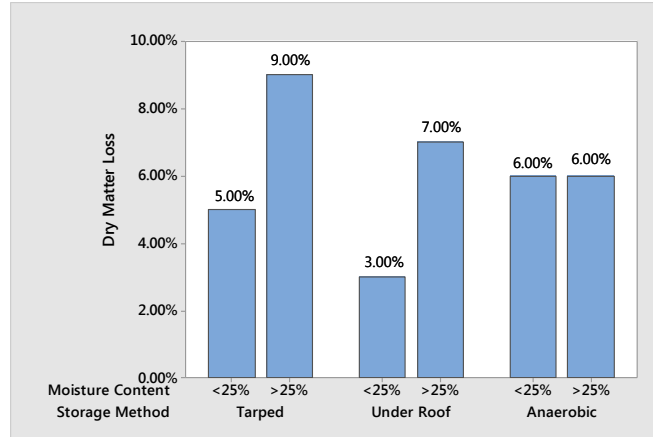


Figure 2.8: Dry matter loss for varying storage methods and biomass moisture contents. Adapted from (Shah and Webster, 2014).

To fully understand the impact of different storage methods on degradation, uncovered in particular, it is necessary to evaluate degradation within the entire stack. Uncovered stacks will also be the most affected by the duration of the storage trial. Typically, field edge stored biomass would be taken to a biorefinery before the next harvest, a one year maximum storage period. Corn stover bales stacked six-high on field edge for one year experience moisture penetration through the top bale, the second bale from the top, and the bottom portion of the bottom bale (Figure 2.9). All material in between measure moisture contents similar to the initial field average and below stable limits (Darr et al., 2015).

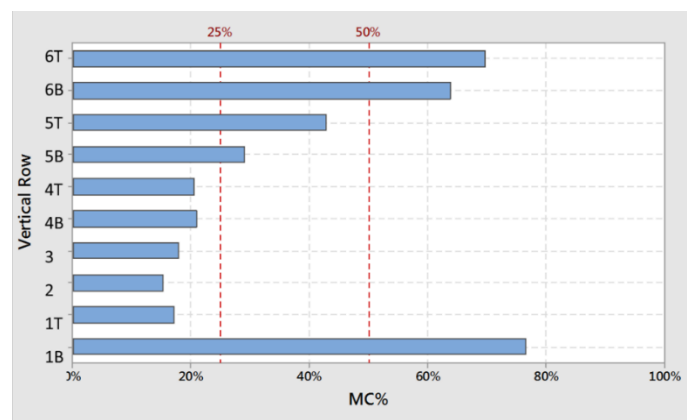


Figure 2.9: Final moisture profile for one year of field edge storage. Average bale moisture by vertical row. (Darr et al., 2015)

The material in top exposed bales near saturation, and experience significant degradation, changing in color, and texture. Top bales can lose over 20% dry matter loss and nearly all structural integrity during one year of exposed storage (Darr et al., 2015).

Dry matter, composed mainly of cellulose, hemicellulose, lignin, and ash will experience selective degradation. If given the right environment, microorganisms selectively degrade the sugar-based carbohydrate components of hemicellulose and cellulose for their energy needs, leaving behind a concentration of non-biodegradable components in the remaining biomass. Not only is less dry material being sent into the biorefinery per bale, but that material, if biologically degraded, contains less convertible carbohydrates. Underperforming reactions, due to feedstock quality loss, will increase the feedstock contribution to ethanol production cost (FCEPC) and annual ethanol production costs for a biorefinery. When assessing the overall FCEPC for a biorefinery, the cost impact of degradation should be included with the cost to collect, store, and transport the feedstock. (Figure 2.10).

$$FCEPC = \frac{\$Cost_{HST}}{1 \text{ Ton}_{DM_i}} * \frac{1 \text{ Ton}_{DM_i}}{\text{Ton}_{DM_f}} * \frac{1 \text{ Ton}_{DM_f}}{\text{Ton}_{Carbohydrate}} * \frac{1 \text{ Ton}_{Carbohydrate}}{\text{Gal}_{EtOH}} = \frac{\$}{\text{Gal}}$$

Figure 2.10: Feedstock supply chain cost equation (Darr, et al., 2015)

Biomass that is protected from environmental factors measures little to no loss in dry matter, and maintains its original quality (Schon et al. 2013). The level of degradation is directly related to the available moisture within the material, dependent on the coverage method and duration of storage. It's necessary to evaluate the impact of various levels of protection to understand the tradeoff and timing of biomass degradation to a bio refinery.

2.7 Research Objectives

The potential \$21/ton reduction in feedstock supply chain costs is what motivated this research, along with the one unknown to field-edge storage: the effect on biomass quality. Field-edge storage will be more susceptible to degradation and responsive to environmental conditions. The severity of decreased quality and material loss will dictate whether field-edge conditions are economically viable for long term storage. This research will provide a means to quantify how environmental conditions impact degradation of corn stover in field edge storage by completing two objectives:

- Objective #1: Analyze the influence of storage moisture and temperature on degradation of densified corn stover.
- Objective #2: Assess the dynamics of moisture migration and degradation within field edge stacks during storage.

CHAPTER 3: INFLUENCE OF STORAGE MOISTURE AND TEMPERATURE ON LIGNOCELLULOSIC DEGRADATION

3.1 Introduction

The dynamics of densified biomass storage degradation, especially carbohydrate structure, are not well known. In freshly harvested lignocellulosic material, ~70% of the material is biodegradable. Due to its structure, the remaining 30% composed of lignin, ash, and other components will not be readily consumed by environmental microbes. Microbial degradation that occurs is the breakdown and consumption of the sugar-based components of dry matter: cellulose and hemicellulose, which are the same components currently sought after for bioprocessing of renewable products.

Past studies have addressed storage losses by quantifying dry matter loss (DML) associated with protected, baled corn stover. Results from dry matter loss studies on unprotected bales are highly variable, partially due to the difficulty in assessing material loss in bales that experience absorbance of moisture. Microorganisms require minimum thresholds of moisture and temperature to maintain and optimize metabolism; levels of these factors affect the rate of growth and substrate utilization. The objective of this research is to identify dynamic trends in corn stover degradation and quantify the effects that moisture and temperature have on these trends in terms of dry matter loss and carbohydrate composition. This is accomplished in Chapter 3 by:

- Preparing densified corn stover units to degrade in moisture and temperature controlled environments.
- Evaluating the dry matter and carbohydrate structure changes in each experimental unit.

3.2 Methods

3.2.1 Design of Experiment (DOE)

The treatment factors for this controlled degradation experiment consisted of varying moisture contents, temperatures, and storage durations. Both temperatures levels and material moisture content levels were chosen to represent values typically experienced in production field edge storage stacks or those critical to microbial activity. Stover moisture levels of 0%, 10%, 15%, 20%, 30%, and 60% were selected. The levels of 15%, 20%, 30%, and 60% were selected to reflect final bale moistures measured during ISU's field edge stack deconstruction for material harvested in 2014 (Darr et al., 2015). Moistures of 0% and 10% were included to evaluate moistures that are generally thought to be low enough to prevent microbial degradation (Brown and Brown 2014). Temperatures of -20°C (-4°F), 23°C (73°F), 45°C (113°F), and 60°C (140°F) were chosen based on bale heating curves measured by Schon in 2013 (Schon et al., 2013) and those critical ranges for bacterial growth. A -20°C (-4°F) cooler was used to simulate frozen material during the winter months. 23°C (73°F) represents the lower temperature range of mesophilic bacteria and simulates an average Iowa summer. 45°C (113°F) and 60°C (140°F) are common temperature seen in past research focused on the heating of high moisture corn stover bales (Schon et al., 2013). Experimental units were allowed to degrade for set durations. Most combinations of temperature and moisture content degraded for durations of 9, 18, and 27 days. Experimental unit capacity and time limitations dictated the set durations.

A full factorial experiment including five replications requires 360 experimental units. An initial test was implemented: testing moistures of 0% and 10% degrading at 60°C (140°F) for a storage duration of 27 days. Showing statistically no dry matter loss at the temperature and duration theoretically most at risk for degradation among the factors, it was concluded

unnecessary to test those moistures at the remaining temperature and duration levels. Total experiment unit population was reduced to 250 (Table 3.1).

In addition to the DOE previously described, after evaluating results from the 27 day durations, two moisture/temperature combinations were selected for a continuation test.

Moistures of 30% and 60% were set up to degrade at 45°C (113°F) for a 54 day storage duration.

Table 3.1: Summary table of treatment factors, matrix values indicate replications

		Temperature °C (°F)															
		-20 (-4)				23 (73)				45 (113)				60 (140)			
Moisture Content %	0	-	-	-	-	-	-	-	-	-	-	-	-	-	-	5	-
	10	-	-	-	-	-	-	-	-	-	-	-	-	-	-	5	-
	15	5	5	5	-	5	5	5	-	5	5	5	-	5	5	5	-
	20	5	5	5	-	5	5	5	-	5	5	5	-	5	5	5	-
	30	5	5	5	-	5	5	5	-	5	5	5	10	5	5	5	-
	60	5	5	5	-	5	5	5	-	5	5	5	10	5	5	5	-
		9	18	27	54	9	18	27	54	9	18	27	54	9	18	27	54
		Storage Duration (Days)															

3.2.2 Sample Preparation

A single bale of non-degraded corn stover from Story County, Iowa, was pulled apart to provide material for this experiment. This provided material of the same partial size as shredded stover ahead of baling. To simulate dense, baled corn stover, 260 g (0.57 lbs) of dry stover was compacted into a 8 cm (3 in) diameter, 30 cm (12 in) long, clear tube with a hydraulic cylinder plunger (Figure 3.1). This reached an average dry density of 184 g/cm³ (11.5 lb/ft³), similar to infield bale density (Darr, 2014). A predetermined volume of water was added during the compaction process to reach specified moisture levels. After densification, tubes were capped and stored in a cooler at 5°C (41°F) to limit degradation until the material preparation process

was finished for each round of tests (less than two days). As experimental units were positioned to start the test, holes were drilled into the capped ends to allow O₂ and CO₂ exchange to occur.



Figure 3.1: Hydraulic press and resultant tubes of densified corn stover.

3.2.3 Controlled Environment Chambers Set Up

Thermo Scientific Tabletop Muffle Furnaces provided a controlled environment for the experimental unit corn stover tubes to degrade. These furnaces are temperature controlled. To maintain moisture content within the experimental units, the relative humidity within the furnaces was brought up to and kept between 75% and 95% using a two pan watering system (Figure 3.2). Water would naturally transfer through a tube filled with cotton cloth into the chamber through a 3cm (1in) hole and into a second pan. The inside pan was lined with a towel to increase surface area. Before the experiment was started, furnaces were run to reach desired temperature and relative humidity. HOBO U23 Pro v2 Temperature/Relative Humidity Data Loggers were used to monitor relative humidity (RH) until it reached a steady 75% to 95%. The top pan was periodically refilled to maintain this environment. Depending on the treatment

temperature, the top pan was refilled every three to four days once at equilibrium. Experimental units were also covered with a burlap sack to act as another means to hold in moisture. The environmental chambers themselves allowed limited air exchange through two 3 cm (1in) holes filled with steel wool, providing oxygen and carbon dioxide flow throughout the environmental chamber, but limiting heat and moisture fluctuation. Each chamber housed five packed units of corn stover.

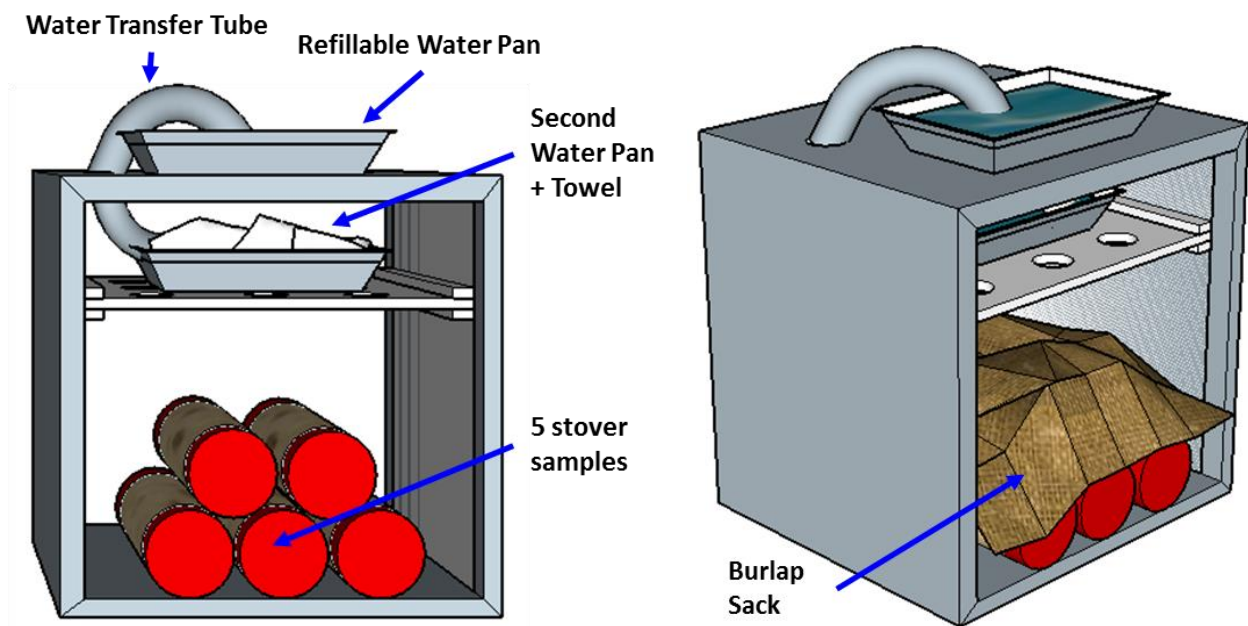


Figure 3.2: Environmental chamber set up

3.2.4 Assessment Parameters

3.2.4.1 Moisture Content

Experimental units were prepped to specific moisture contents with predetermined masses of dry stover and water. Final moisture contents were analyzed for whole experimental units post degradation using the ANSI/ASAE S358.3 standard (ASABE, 1988) for moisture measurements of forage material, modified slightly for corn stover. First an initial wet moisture

was recorded and sample was dried in a ventilated oven at 105°C (221°F) for 24 hours. A dry weight was taken, and Equation 3.1 was used to determine the percent moisture.

Equation 3.1: Moisture content calculation, wet basis

$$\text{Moisture Content}_{\text{wet basis}}(\%) = \frac{(\text{Wet weight} - \text{Dry weight})}{\text{Wet weight}} * 100$$

3.2.4.2 Mass and Volume

A scale reading to the nearest 0.01 g was used to record all weights. During preparation, weights of the following were recorded separately for each experimental unit: empty clear tube (T), end caps (L₁, L₂), initial dry stover (S_i), and initial water (W_i). The initial mass of each completed unit was also recorded (C_i). All tubes were 8cm (3.0 in) in diameter and 30 cm (12 in) long, giving an initial and final volume (V) of 1400cm³ (0.05 ft³). At test completion, each experimental unit was weighed ahead of drying (C_f). The final mass of water (W_f) was determined for each unit using the moisture content standard above.

3.2.4.3 Dry Matter Loss

The initial dry matter target for each experimental unit was estimated at 260 g (0.57 lbs), but the actual dry matter weight for each unique unit was determined using Equation 3.2. At the completion of the storage duration final moisture content, masses of the unit, tube, end caps, and final water were used to calculate the final dry matter (Equation 3.3). Dry matter loss was calculated on a percent mass basis with equation (Equation 3.4).

Equation 3.2: Initial dry matter

$$\text{Dry Matter}_i(g) = (C_i - T - L_1 - L_2 - W_i)$$

Equation 3.3: Final dry matter

$$\text{Dry Matter}_f(g) = (C_f - T - L_1 - L_2 - W_f)$$

Equation 3.4: Percent dry matter loss (DML %)

$$\text{Dry Matter Loss}(\%) = \frac{\text{Dry Matter}_i - \text{Dry Matter}_f}{\text{Dry Matter}_i} * 100$$

3.2.4.4 Density

Initial and final density was recorded on a dry mass basis. The mass of dry matter and set sample volume of 1400cm³ (0.05 ft³) were used in Equation 3.5 to calculate both initial and final experimental unit densities.

Equation 3.5: Sample density

$$\text{Sample Density} \left(\frac{g}{cm^3} \right) = \frac{\text{Sample Dry Matter}(g)}{1390 cm^3}$$

3.2.4.5 Structural Carbohydrate Analysis

Wet chemistry typically used for forage quality analysis was performed by Midwest Laboratories, Inc to evaluate the neutral detergent fiber, acid detergent fiber, and acid detergent lignin composition of a subsample from each experimental unit. These residue test results were used to calculate the composition of structural carbohydrate components of hemicellulose, cellulose, and lignin (Appendix A). All material in this experiment was from a single bale. 20 subsamples of the initial material were analyzed for NDF, ADF, and AD Lignin to estimate the average initial carbohydrate concentration. Results from the forage quality tests prompted a detailed look at the influence of ash content on the methods for the NDF, ADF, and AD Lignin tests. A subset of experimental units were evaluated for total ash content and detergent insoluble ash content (Appendix A).

3.2.4.6 Statistical Analysis

Minitab 17 Statistical Software was used to interpret the results in this chapter. The Analysis of Variance (ANOVA) function was used to determine if means differed among treatment factors such as temperature, moisture, and storage duration. The null hypothesis tested: the mean values do not differ between treatments. At α value of 0.05 for a confidence interval of 95%, if a P-value less than 0.05 is obtained, there is enough evidence to reject the null hypothesis, indicating that at least one mean is statistically different. To further determine which treatments differed from one another, a Tukey's test was performed. In the Tukey grouping, means that do not share a letter are significantly different. All ANOVA's with over 2 levels were followed by a Tukey's test and the Tukey's test results are displayed in this writing.

3.3 Results and Discussion

3.3.1 Impact of Moisture on Dry Matter Loss

Excluding storage duration, moisture content was the greatest driver in dry matter loss in this experiment. Data from the three temperature levels above freezing: 23°C (73°F), 45°C (113°F), and 60°C (140°F), were aggregated to analyzed the difference in average dry matter loss for the different moisture content levels (Table 3.2). Reasoning is explained in 3.3.2. Experimental units with starting moisture contents of 0%, 10%, 15%, and 20% showed little to no dry matter loss within 27 days of storage, and those treatments ended with the originally scheduled longest storage duration: 27 days (Figure 3.3). The experimental units with 30% and 60% moisture content, after 27 days measured statistically higher DML than the other four moisture levels. Though statistically different from the lower moistures, the loss was small relative to the amount of dry matter remaining. The tests for these two levels of moisture content

were extended into a 54 day storage duration to better understand the trend in loss measured in degrading experimental units. The two combinations continued to show loss throughout the additional storage duration (Figure 3.3).

Table 3.2: Tukey’s test results for mean dry matter loss based on moisture content for various storage durations. Combined temperatures of 23°C, 45°C, and 60°C

Initial MC (%)	9 Day Storage Duration				18 Day Storage Duration				27 Day Storage Duration			
	N	Dry Matter Loss %		Tukey Grouping*	N	Dry Matter Loss %		Tukey Grouping*	N	Dry Matter Loss %		Tukey Grouping*
		Mean	StDev			Mean	StDev			Mean	StDev	
0	-	-	-	-	-	-	-	-	5	1.1	0.7	A
10	-	-	-	-	-	-	-	-	5	0.1	0.5	A
15	9	2.3	0.8	A	15	-0.2	1.0	A	15	0.5	0.9	A
20	9	2.4	0.7	A	15	1.1	1.3	A B	15	1.2	1.1	A
30	9	2.6	0.8	A	15	2.5	2.6	B	15	3.8	2.2	B
60	9	2.0	1.6	A	15	1.5	1.6	A B	15	5.8	1.5	C

*Means that do not share a letter are significantly different.

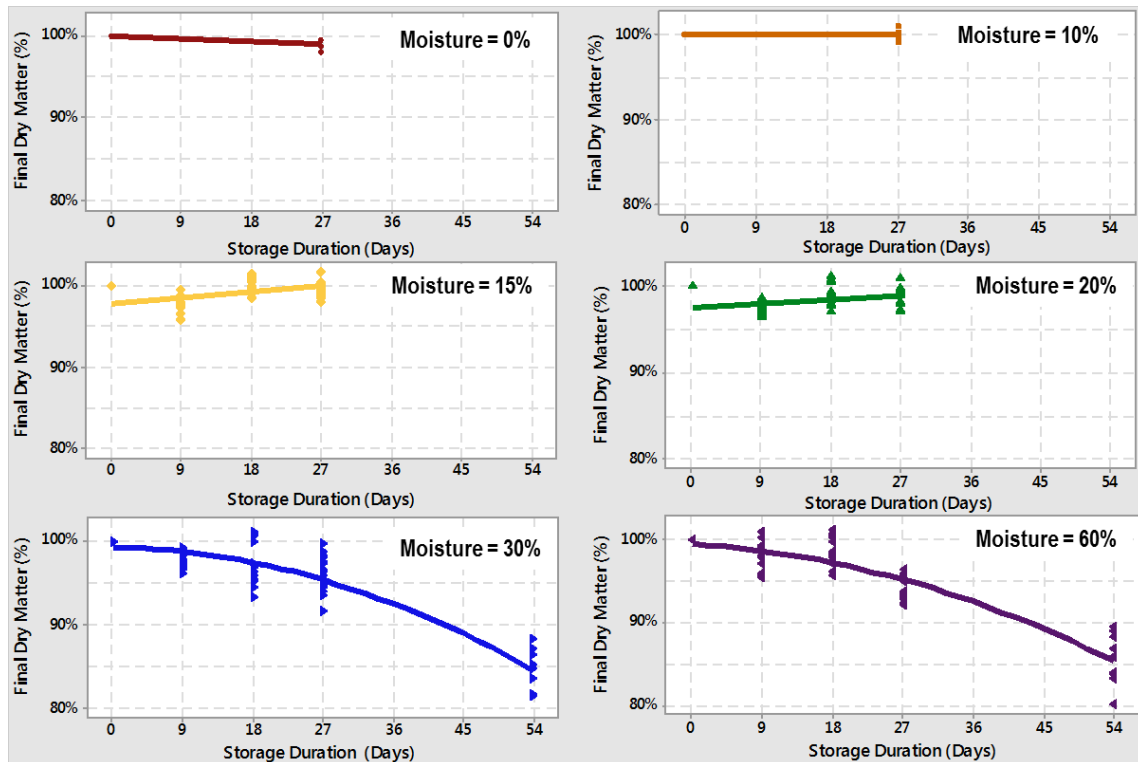


Figure 3.3: Influence of biomass moisture content and storage duration on final dry matter. Combined temperatures of 23°C, 45°C, and 60°C

The losses from treatments in which degradation was observed (moisture contents of 30% and 60% at temperatures of 23°C, 45°C, and 60°C) did not follow a linear pattern. These moisture treatments, having nearly identical regression lines, were aggregated into a single category. There is a negative correlation between dry matter and time in this data set. The regression fits a quadratic model with an R^2 value of 84.3% (Figure 3.4). The resulting regression equation is: % Dry Matter = $99.28 - 0.03402(x) - 0.004279(x)^2$. X refers to days of storage. Note experimental units measuring over 100% dry matter; this is most likely due to measurement error during sample preparation, final dry matter analysis, or a combination of both.

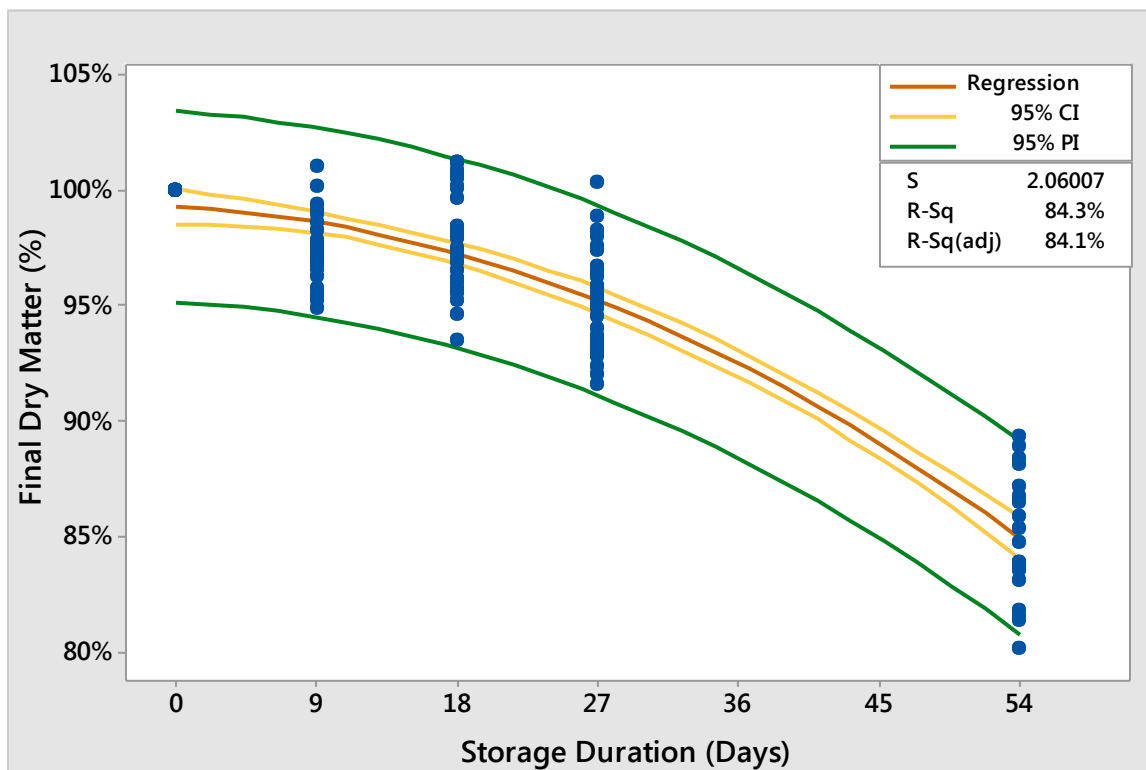


Figure 3.4: Trend of final dry matter with storage duration. Combined 30% and 60% moisture content levels. The R^2 off 84.3% value indicates how well the data fits the quadratic regression.

This model is limited on the x-axis; longer trials of the same experiment would be needed to understand the dynamics of degradation and dry matter loss beyond 54 days. It is impossible

for degradation to continue with this model indefinitely. If extrapolated beyond 54 days with the current model, the remaining dry matter reaches zero and becomes negative in 126 days, approximately 4 months. Realistically, dry matter cannot take on a negative value, and if it were to reach zero that would indicate that the remaining experimental unit is entirely water; all components of cellulose, hemicellulose, lignin, and ash have been degraded, or the unit is empty. The early stages of degradation mimic a quadratic model, but to forecast longer storage durations, the model should contain a minimum dry matter restriction. Under the notion of selective degradation, the combined initial concentrations of lignin and ash would be a logical minimum dry matter estimation.

In theory, the consumption of dry matter is most similar to substrate utilization in a microbial growth model. See Appendix B for modeling a similar complex system: simultaneous saccharification-fermentation (SSF), which includes microbial growth, substrate utilization, and product formation. The concept of decomposing microorganisms consuming dry matter in biomass storage could utilize many of the same dependent rate equations (Table 3.3). Within this system, microorganisms are growing, enzymes are produced, carbohydrate components of lignocellulose are broken into simple sugar monomers, monomers are consumed by microorganisms, and carbon dioxide is produced. An additional rate equation could be created for the substrate level of dry matter.

Table 3.3: Relating Simultaneous Saccharification/Fermentation (SSF) rate equations to biomass degradation

Rate Equation	SSF Reaction	Degradation Reaction
dX/dt	Microbes	Microbes
dG/dt	Glucose	Simple sugars
dS/dt	Starch	Cellulose, hemicellulose, Lignin
dEnz/dt	Enzyme	Enzyme
dE/dt	Ethanol	C02
dDM/dt	NA	Dry Matter

Do note that each rate equation becomes extremely complex for degradation of field stored biomass. In the case of corn stover, substrate uniformity cannot be assumed. Dry matter consists of multiple components, composed of differing monomer structures, some more biodegradable than others. There are relationships among the components that influence the rate of dry matter loss. To accurately model substrate loss it would require at least four individual rate equations. Secondly, the non-homogenous structure of corn stover causes variability within the initial substrate. Finally, material is exposed to various moisture and temperature conditions, and susceptible to numerous microorganism communities. Unable to be controlled or assumed, these growth influencers, along with substrate concentration would need to be closely monitored to understand the growth rate at any given time. Given the results from this test and these various features of biomass degradation, the resulting kinetics could follow models such as a Monod, logistic, or logarithmic to describe the biodegradation (Okpokwasili and Nweke, 2005). In these types of models, substrate utilization starts slow, increases significantly, and then slows down reaching a minimum value, similar to that in the SSF example (Appendix B).

3.3.2 Effect of Temperature on DML

Decomposing microorganisms require a minimum temperature to maintain metabolic rates. If biomass is allowed to freeze, the material will not experience significant dry matter loss.

There was no statistical difference measured in the average final dry matter for all moistures that were frozen for 9, 18, or 27 days (Table 3.4).

Table 3.4: Tukey's test results for mean final dry matter for -20°C temperature level. Combined 9, 18, and 27 storage days

Moisture (%)	N	Final Dry Matter (%)		Tukey Grouping*
		Mean	StDev	
15	15	101	1.0	A
20	15	101	1.0	A
30	15	100	1.1	A
60	15	102	1.1	A

*Means that do not share a letter are significantly different.

Frozen material aggregated together, averaged 101% final dry matter (Figure 3.7). Realistically, dry matter cannot increase. This is most likely due to condensation/frost build up on the outside of containers as frozen experimental units hit humid air while taking a final intact unit weight. After this weight was taken, units were allowed to thaw in a 5°C (41°F) cooler where outside condensation could evaporate. Once thawed, material was taken out of the tube container and whole container, lids, and material were put into a pan for wet weight, dried and taken a dry weight. The final weight of the unit was based off the slightly higher (due to condensation) frozen measurement, but the MC% was based off the thawed wet and dry weights. This could show a slight increase in dry matter for frozen treatments.

For experimental units with moisture levels promoting degradation (30% and 60%), temperature levels tested above freezing: 23°C (73°F), 45°C (113°F), and 60°C (140°F) did not show a statistical difference in mean final dry matter, but were statistically lower than the frozen treatments (Table 3.5 and Figure 3.5). Longer storage durations should be tested to fully conclude the influence of temperature.

Table 3.5: Tukey's test results for mean final dry matter based on temperature level. 27 day storage duration. Combined 30% and 60% moisture levels

Temperature °C (°F)	N	Final Dry Matter (%)		Tukey Grouping*
		Mean	StDev	
-20 (-4)	10	101	1.1	A
23	10	96	2.1	B
45	10	95	1.2	B
60	10	95	1.7	B

*Means that do not share a letter are significantly different.

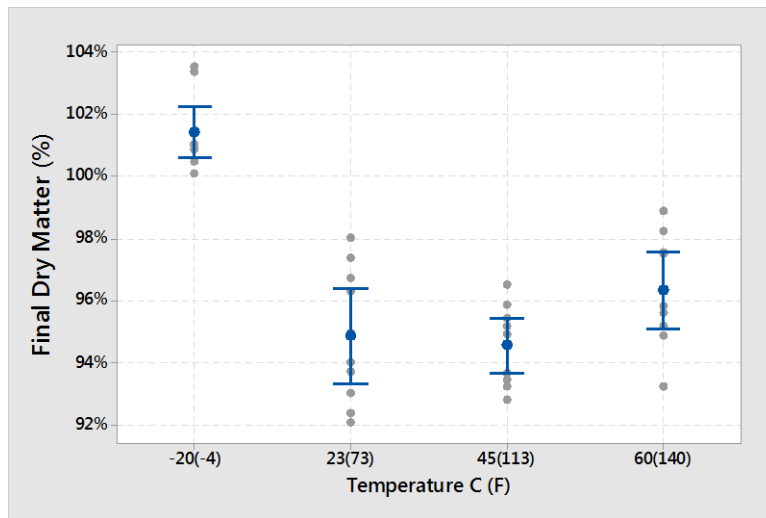


Figure 3.5: The effect of temperature on final dry matter. Combined 30% and 60% moisture content levels at 27 days of storage. Bars indicate 95% confidence intervals.

3.3.3 Carbohydrate Analysis

Experimental units, dried for dry matter loss analysis, were prepared and sent to an external analytical lab to be analyzed for final carbohydrate structure. Three tests: Neutral Detergent Fiber (NDF), Acid Detergent Fiber (ADF), and Acid Detergent (AD) Lignin were performed to quantify the remaining composition of cellulose, hemicellulose, and lignin. See Appendix A for detailed methods for each test. The percent composition of hemicellulose was the only component to correspond to the decreasing trend seen with the results of dry matter loss

(Figure 3.6). Both the composition of cellulose and lignin had no significant change from day zero to day 54 of storage. (Table 3.6).

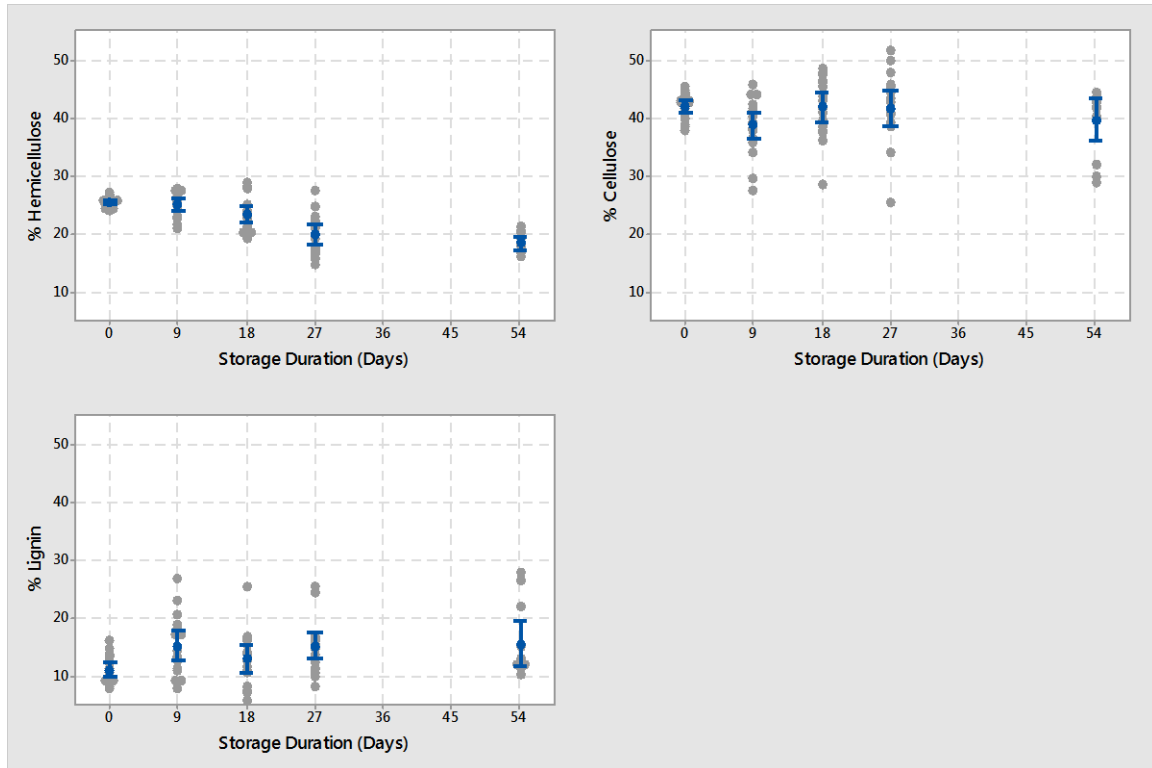


Figure 3.6: Influence of storage duration on final composition of hemicellulose, cellulose, and lignin. Combined 30% and 60% moisture content levels. Bars indicate 95% confidence intervals.

Table 3.6: Tukey's test results for final composition from day 0 to day 54 of storage

Storage Duration (Days)	% Hemicellulose			% Cellulose			% Lignin			% Dry Matter		
	n	Mean	Tukey Grouping*	n	Mean	Tukey Grouping*	n	Mean	Tukey Grouping*	n	Mean	Tukey Grouping*
0	20	25.4	A	20	41.9	A	20	11.0	A	20	100.0	A
54	12	18.3	B	12	39.5	A	12	15.4	A	20	82.1	B

*Means that do not share a letter are significantly different.

Cellulose and hemicellulose, both sugar based molecules, are the components currently sought after for bioprocessing. To track those more valuable components, cellulose and hemicellulose are combined to represent the carbohydrate composition (% carbohydrate) within

an experimental unit. Theoretically the decrease in carbohydrate composition should mirror the decrease in dry matter loss because those components are more likely to biodegrade during storage than the aromatic structure of lignin. The percent loss of carbohydrate composition accounted for only half of the dry matter lost after 54 days of storage (Table 3.7). The values in this table were calculated using the estimated mean initial carbohydrate structure and final carbohydrate structure. Example calculation is provided for % Carbohydrate (Equation 3.6).

Table 3.7: Average compositional change after 54 days of storage

Δ % Lignin	Δ % Hemicellulose	Δ % Cellulose	Δ % Carbohydrate	Δ % Dry Matter
4.4	-7.1	-2.4	-9.5	-17.9

Equation 3.6: Difference between final % Carbohydrate and the estimated mean initial % Carbohydrate composition

$$\Delta \% \text{ Carbohydrate } (\%) = \% \text{ Carbohydrate } - \bar{x}_{(\% \text{ Carbohydrate}_i)}$$

Multi-pass baled corn stover experiences soil contamination (Darr, 2014), increasing its ash content and ash variability. Because feed analysis is often done on relatively clean, consistent feedstock, a secondary test was performed to analyze the effect ash content has on the methods used to report NDF, ADF, and AD Lignin values. 10 of the subsamples sent to Midwest Labs Inc. for carbohydrate analysis were also evaluated for total ash content and detergent insoluble ash (DI ash) (Appendix A). DI ash content results were used to calculate a corrected % cellulose composition and percentage points error in the original cellulose estimation (Equations 3.7 and 3.8). The lower population of the high ash content level widens the 95% confidence interval, but there is still a statistical difference in mean ash content for normal ash (<12.5%) and high ash (>12.5%) levels. Statistical differences were also seen in the results for detergent insoluble ash

(DI), the DI-ash/total ash ratio, and the cellulose estimation error for these two levels of ash content (above and below 12.5%) (Figure 3.7).

Equation 3.7: Corrected % cellulose composition using detergent insoluble ash (DI ash)

$$\text{Corrected \% Cellulose} = (\%ADF - AD \text{ Lignin} - \%DI \text{ Ash})$$

Equation 3.8: Cellulose estimation error

$$\text{Cellulose Estimation Error (\% points)} = \% \text{ Cellulose} - \text{Corrected \% Cellulose}$$

Table 3.8: Secondary test ash content influence results

% Total Ash	% DI Ash	% ADF	% NDF	% AD Lignin	% Hemicellulose	% Cellulose	Corrected % Cellulose	% Cellulose Error	% DI Ash/ Total Ash
7.6	1.6	53.7	76.4	23.6	22.7	30.1	28.5	1.6	20.9
9.7	1.7	53.5	74.2	8.8	20.7	44.7	43	1.7	17.5
10.1	2.3	52.5	74.6	11.9	22.1	40.6	38.3	2.3	22.8
9.5	3.1	50.4	73.8	13.3	23.4	37.1	34	3.1	32.6
10	1.7	46.8	72.2	8.5	25.4	38.3	36.6	1.7	17
10.5	2.3	50.8	74.3	14.7	23.5	36.1	33.8	2.3	21.9
8.9	1.1	52.2	74.2	8.9	22	43.3	42.2	1.1	12.4
14.5	4	53.9	69.4	17.8	15.5	36.1	32.1	4	27.6
16.5	5.2	55.3	71.7	7.7	16.4	47.6	42.4	5.2	31.5
14.9	5	54.1	73.6	11.6	19.5	42.5	37.5	5	33.6

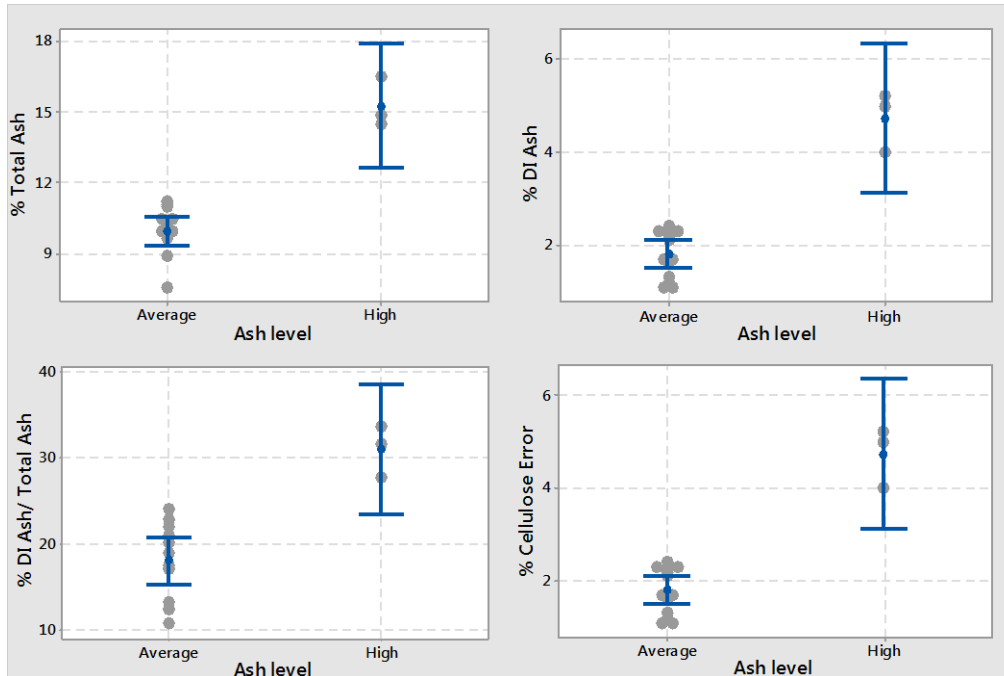


Figure 3.7: Influence of ash level on detergent insoluble ash content, DI ash/total ash ratio, and cellulose error. Average refers to ash content <12.5% and High refers to ash content >12.5%. Bars indicate 95% confidence intervals.

There is a strong positive, linear correlation between the total ash content of a subsample and the detergent insoluble ash remaining in the ADF residuals of that same subsample (Figure 3.8). Soil contamination is the leading factor in increased ash content for multi-pass harvested corn stover. Increasing soil concentration increases silica concentration, a large contributor to detergent insoluble ash. Because the error in cellulose estimation is directly linked to the concentration of detergent insoluble ash, the same linear relationship is seen between total ash content and cellulose estimation error (Figure 3.9). Subsamples below 12.5% total ash, on average, provided less than 2 percentage points of error in cellulose estimation from ADF and AD Lignin results (Figure 3.7). As ash content increases and becomes more variable, the cellulose error increases and is less predictable. Increasing ash content five percentage points over doubled the cellulose estimation error.

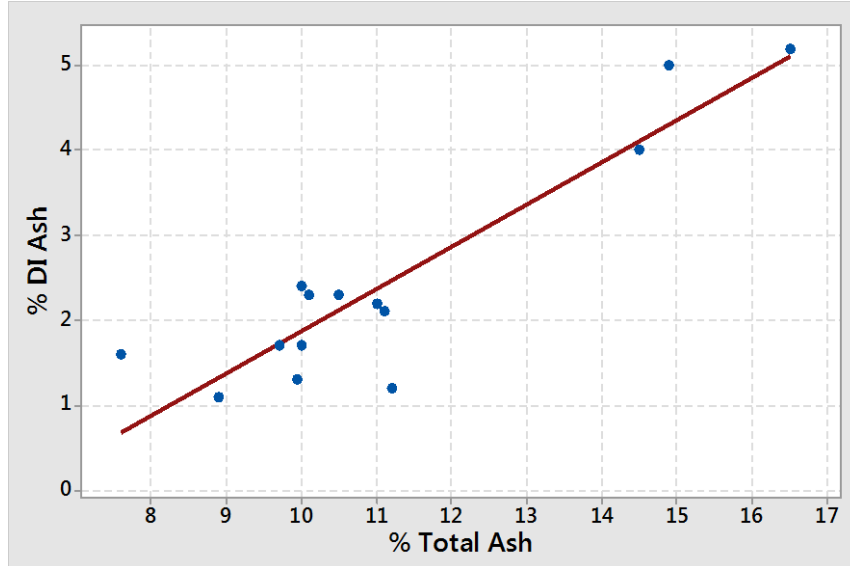


Figure 3.8: Positive linear relationship between total ash content and detergent insoluble ash. The R^2 is 84.0%, indicating how well the data fits the linear regression.

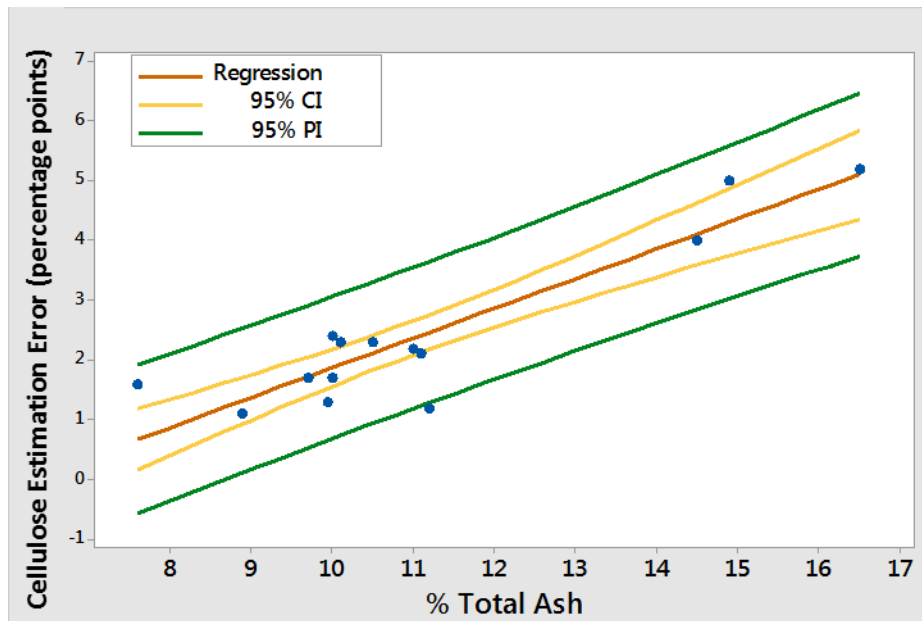


Figure 3.9: Linear regression between total ash content and cellulose estimation error. The R^2 is 84.0%, indicating how well the data fits the linear regression.

Ash content in baled corn stover can be reduced on average with improvements in machinery and operation, but is still highly variable on a bale-by-bale basis (Schon, 2012). The ash variability of a bale increases with increasing mean ash content (Table 3.9) (Schon, 2012). A

large enough population of bale samples must be taken to create an accurate field average. Aggregation of field averages over a harvest season provides a realistic mean ash content of inventory brought into a bio refinery. In 2015, fields showed a cumulative distribution with 70% of fields harvested below 12.5% ash content (Figure 3.10) (Darr et al., 2015). In the secondary test, 70% of the fields contained ash content less than 12.5% ash. From the results, it could be estimated that in a season average, 90% of subsamples tested for carbohydrate composition with this method would have less than 5% error in percent cellulose estimation. Due to the large sample size and relatively low variability in ash content, this method may be suitable for analyzing freshly baled corn stover carbohydrate content with a correction factor for ash content. This assumes that the dry 200-400 g (0.44-0.88 lb) core sample taken from a single bale is representative of the entire bale's carbohydrate composition. A sample taken from a bale and ground contains its own ash variability, and due to differences in density, is difficult to take a perfectly representative 30 g (0.07 lb) subsample to send for carbohydrate analysis. An even smaller sub sample is taken to run the actual carbohydrate composition tests. In summary, a single 0.5 g (0.001 lb) sample is used to analyze carbohydrate composition of a 453,592 g (1000 lb) bale of highly variable biomass. Further testing should be done to verify this is enough to accurately evaluate the carbohydrate composition.

Table 3.9: Ash variability within individual bales of corn stover (Schon, 2012)

Bale Number	Mean Ash Content %	St. Dev Ash Content %
3	27.09	10.27
4	24.4	11.33
5	9.5	2.87
6	10.08	3.98
7	7.9	1.73
8	7.43	1.88

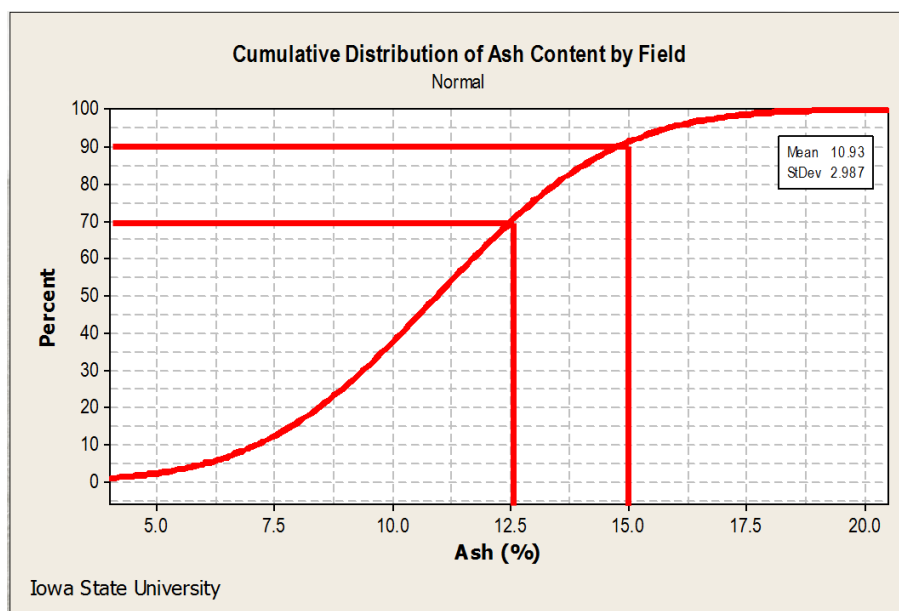


Figure 3.10: Cumulative distribution of field average ash content from 2015 harvest (Darr et al., 2015)

Monitoring carbohydrate structure over 54 days of degradation, the carbohydrate composition was expected to show a closely linear relationship with the percent dry matter loss. No distinct relationship was seen between carbohydrate concentration and dry matter loss for all experimental units analyzed for structural carbohydrate composition (Figure 3.11). Under conditions of high biomass degradation, theoretically ash content will increase significantly due to selective degradation (Figure 3.12). It is suggested that the loss in dry matter increased the ash content of the units, increasing the error in the estimation of cellulose. An overestimation of cellulose would falsify the results for carbohydrate composition. The likely increase in cellulose estimation error with degradation makes this method of carbohydrate analysis not suitable to analyze the carbohydrate dynamics of degrading biomass.

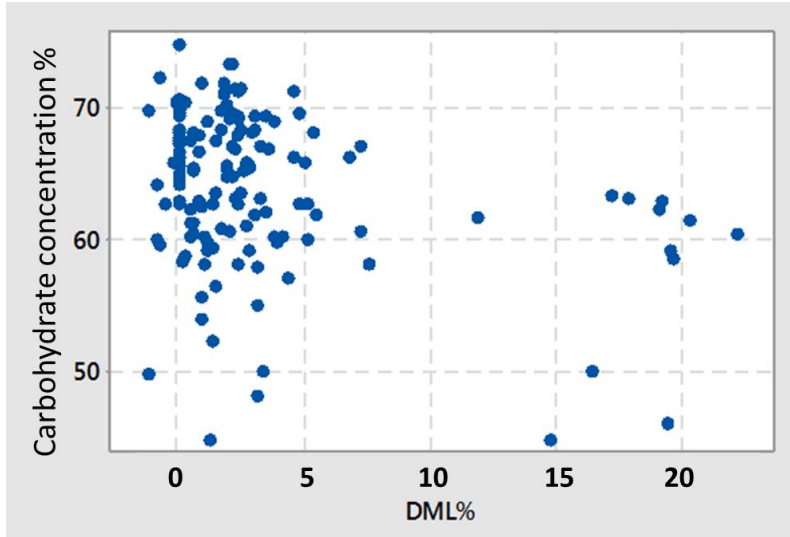


Figure 3.11: Lack of relationship between dry matter loss to percent convertible material. Combined all moisture levels and temperatures >0°C.

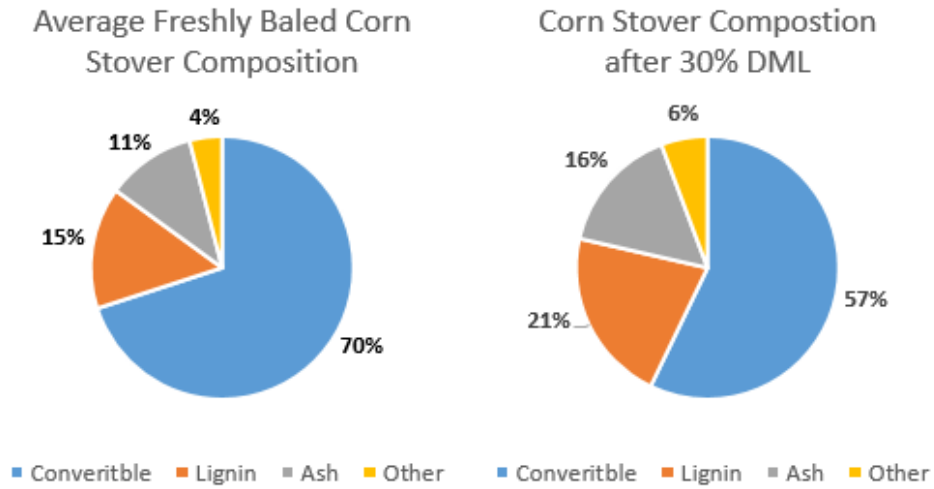


Figure 3.12: Corn stover composition before and after 30% DML

3.4 Conclusions

This experiment provided a controlled simulation of biomass degradation for baled corn stover; regulation of temperature and moisture content was enforced to evaluate trends of impact on decomposition. The influence of sustained moisture content has a threshold trend; the environment either has enough moisture for microbial degradation, or it does not. Biomass with moisture contents below 20% are stable and not fit for microbial consumption, regardless of environmental temperature. Biomass with moisture contents constantly above 20% degrade similarly to one another. Preferably biomass would not be put into long term storage unless its moisture is below 20% moisture content. Environmental temperature impacted degradation in a similar threshold trend. Corn stover that is frozen does not experience dry matter loss. The moisture content of material does not influence degradation of frozen material; units with moisture contents of 15% and those with 60% measured zero dry matter loss. At environmental levels above freezing, material experiences degradation if adequate moisture is present. The influence of environmental temperature above freezing did not measure a distinct trend. Theoretically the temperature of biomass will influence the microbial communities present. Thermophiles are more generally considered most efficient at decomposing lignocellulose, so an environment that supports their needs will measure higher rates of material losses. The storage durations tested may not have been long enough to see this impact. Longer duration replications of the tests are recommended to fully conclude the influence of temperature.

Biomass that experiences high levels of dry matter loss due to biodegradation will decrease in quality in terms of carbohydrate composition. Material will lose convertible components of hemicellulose and cellulose, concentrating the non-convertible components of lignin and ash. Consequently, this concentration of ash content, if not measured, decreases the accuracy of

forage feed analysis in determining concentrations of structural components: cellulose, hemicellulose, and lignin. If omitted from the test method, high ash content will falsely inflate the concentration of cellulose, and inaccurately measure the impact of degradation on carbohydrate content. As ash content increases, the error in these methods increases in a linear fashion. Because degradation concentrates ash, these current methods should not be used to measure the dynamic carbohydrate trend in lignocellulosic degradation.

Biomass with low and consistent ash content measure low levels of error in the feed analysis process. These methods would be relatively accurate in analyzing the initial carbohydrate composition of a freshly harvested feedstock sample. Cleaner feedstocks reduce the variability in the measurements. Feedstocks higher in ash content, but low in ash variability could potentially apply a constant parameter for ash content without needing to measure total ash itself.

Accuracy of the method to analyze the composition of the subsample taken is important, but that test must also be representative of a much larger mass of material. The non-homogenous make up of corn stover bales and varying carbohydrate composition of plant fractionations, genetics, and maturity, naturally provide corn stover bales with high variability in carbohydrate composition. Subsampling non homogenous biomass lessens the accuracy of the analysis. The NDF, ADF, and AD Lignin tests are run on a 0.5 g subsample of biomass. This subsample size must be representative of what the results will be applied to. If a single feed analysis test is applied to a single bale, this sample size is 0.0000276% of the material it is representing. Analysis must be completed to assess the minimum sample population to accurately determine carbohydrate content for a bale of corn stover.

3.5 Recommendations for Future Work

Baled biomass has high variability in both carbohydrate composition and ash content. To accurately analyze feedstock quality, testing methods must account for this variability. Either sampling sizes or sampling populations must increase to decrease the error associated with material variability. Wet chemistry equipment limits the subsample size run, and the turn around and cost of the procedures limit the sample population. To avoid these limitations, it is suggested that sensor-based analysis, such as near infrared (NIR) technology be tested as a more accurate method to assess the quality of corn stover biomass through increased sample populations. An individual test may hold the same or lower accuracy, but increased tests can potentially reduce the overall error. Quality analysis of forage material was first implemented in 1976 (Nutrition, 2003). NIR analysis of ADF and NDF are common methods to analyze energy content of forage today, and calibration equations have been developed further to assess components of hemicellulose, cellulose, and lignin. The sensor-based analysis of multi-pass corn stover, similar to wet chemistry, must account for the magnitude and variability of ash content when detecting characteristic wavelengths and establishing models for these components. The rapid, non-destructive characteristics of NIR, if calibrated accurately, would provide high sample rates and potentially decrease error in carbohydrate composition analysis.

CHAPTER 4: ASSESSING STORAGE DYNAMICS AND MAGNITUDE OF LIGNOCELLULOSIC DEGRADATION

4.1 Introduction

As research advances and cellulosic based products continue to commercialize, the need for clean, economical feedstock increases. As supply chain strategies work to cut cost, they also must drive to maintain feedstock quality. Field edge storage of corn stover bales holds potential to reduce the overall cost of feedstock by reducing storage inputs and eliminating significant transportation logistics. The impact of long term storage on the feedstock quality and integrity is not well understood for commercial supply chains.

Past research has focused on material losses of protected baled biomass, with the assumption that stored material would be set up with coverage, configuration, and location that would allow bale moistures to reach a stable level as well as limit external precipitation. Currently, for long term storage, bales are aggregated from individual fields and stored at a satellite location. These sites are often leveled, drained, and contain a rock base. The long term stacks are covered with tarps in the spring. Protection of biomass will limit material losses and results from Chapter 3 reinforced the concept of limiting moisture to restrict degradation. In the lowest storage cost scenario: an uncovered stack stored on field edge, the top and bottom bales, making up 1/3 of a six-bale-high stack, will experience significant degradation relative to satellite storage. The long-term goal of this research is to quantify the tradeoff of less storage protection in terms of material quality. Chapter 4 accomplishes this with two objectives:

- Evaluate the magnitude of degradation within a field edge stack for multiple coverage scenarios.

- Assess the dynamic behavior of corn stover degradation throughout its storage life relative to environmental conditions.

4.2 Methods

4.2.1 Material

The lignocellulosic material used for this experiment was corn stover from Story County, Iowa. Corn stover was harvested using a multi-pass system and baled into large square bales measuring 0.9 x 1.2 x 2.4 m (3 x 4 x 8 ft) in height, width, and length respectively at approximately 184 kg/m³ (11.5 lb/ft³). Four fields were used to harvest material from and provided the location for the bales to be stacked, with the exception of F08883, whose bales were transported and stacked at the Biocentury Research Farm (Figure 4.1). All four fields were located near Jewell, Iowa, and harvested by a single production scale baling crew.

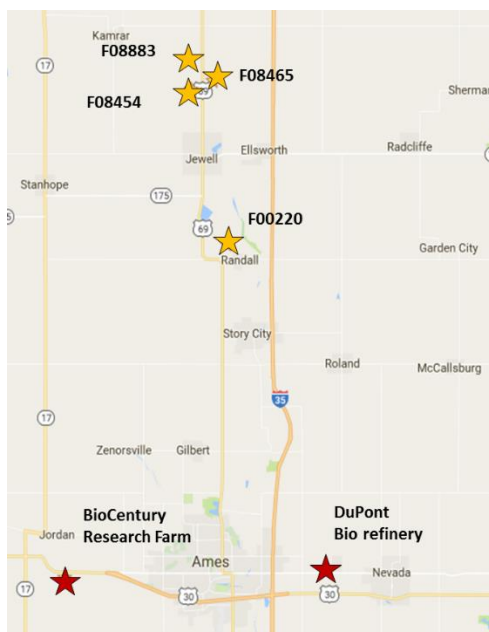


Figure 4.1: Map of field locations, Biocentury Research Farm, and DuPont Biorefinery

4.2.2 Stack Design

This in-field experiment monitors two factors: initial moisture content and stack coverage. The 2015 corn stover harvest in central Iowa was exceptionally dry, limiting the initial moisture content ranges to extremely dry (10% to 15%) and standard to wet (20 to 24%) moisture. Each category was represented by two individual production harvested fields, four total for the experiment. The fields are referred to by their corresponding production field ID's: F00220, F08465, F08883, and F08454. The extremely dry fields were stacked six bales high (F00220 and F08465), and the wetter standard fields were stacked four bales high (F08883 and F08454). All stacks were three bales wide. Each field was used to analyze four stack coverage treatments. The treatment levels included a peaked tarp (A), flat wrap (top bales were individually wrapped) (B), a flat tarp (C), and no coverage (D). All four treatments were stacked together with buffer sections between treatments of ten cross sections (Figure 4.2). Treatments will be referred by their letter assignment throughout this chapter.

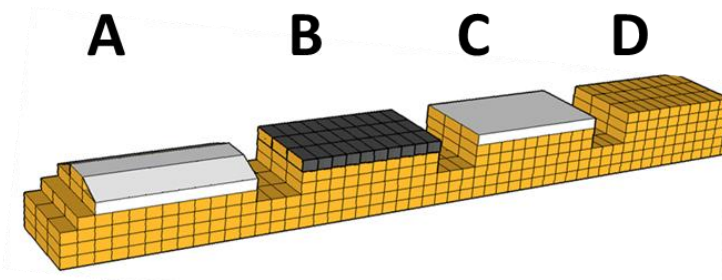


Figure 4.2: 2015 Experimental field edge stack configuration with four coverage methods: A: peaked tarp, B: wrapped top bales, C: flat tarp, and D: no coverage

4.2.3 Stack Coverage

Based on historic rainfall, past tarping strategies, and availability of crews, the two tarped treatments were not covered until Spring of 2016. Iowa Tarping Solutions applied and maintained tarps on these treatments throughout this storage experiment. The treatment with

wrapped top bales were wrapped at harvest, before stacking. The uncovered treatment was exposed to the environment for the full storage trial.

4.2.4 Instrumentation Design

To monitor heat production, an indication of microbial activity, each stack was instrumented with thermistor probes as it was built. Each of the four treatments housed probes in two columns of their fifth cross section. Determining the vertical placement of the probes reflects knowledge gained from field edge storage stack deconstruction data from 2014 harvested bales (Darr et al., 2015). If left uncovered at field edge, within a year of average central Iowa rainfall, the top two bales and the lower half of the bottom bale will be influenced by moisture migration and degradation. Individual columns within a three-bale-wide stack do not see a difference in degradation pattern. Based on these findings, two columns of each treatment were instrumented with eight probes at the specific vertical locations. Probe locations within the six-bale-high stacks are shown below for each treatment (Figure 4.3).

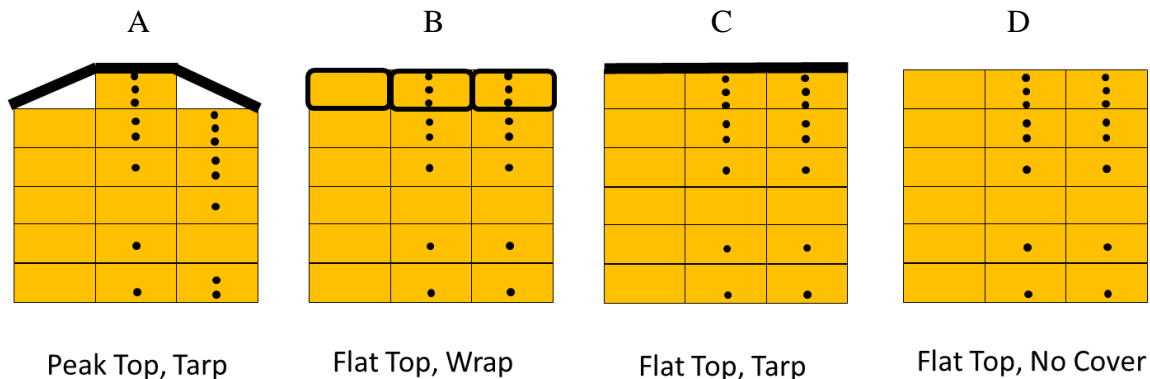


Figure 4.3: Coverage treatments and probe locations for six-bale-high stacks

The instrumentation for this experiment was produced by Pace Scientific. The temperature probes used were PT960 thermistor probes, rated for -40°C to 100°C (-40°F to 212°F) with minimum accuracy of $\pm 0.3^{\circ}$. Each set of eight probes was connected to an individual XR5-SE Data Logger housed in a weather proof box. Each logger recorded

temperature readings every 30 minutes, and data was manually downloaded bi-weekly. Online weather data from Mesonet (Iowa Environmental Mesonet, 2015) was used to track ambient temperature and rainfall amounts.

4.2.5 Top Bale Sampling Design

Throughout the one-year storage trial, samples were taken to monitor material changes within the stacks' top bales. At each stack site, three top bales were sampled from each treatment (Figure 4.4). An auger coring unit with an 8 cm (3 in) diameter coring bit was used to sample vertically from the top of the stack (Figure 4.5). The coring bit and extension rods were marked every 0.3 meters (1 ft) to achieve sample top bales in three 0.3 m (1 ft) sections to obtain a composite profile (Figure 4.6).

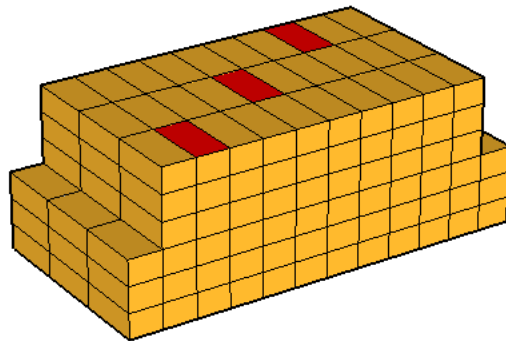


Figure 4.4: Top bale sampling bale locations, similar placement for all four treatments



Figure 4.5: Auger coring unit capable of coring 1.2m (4ft) in depth

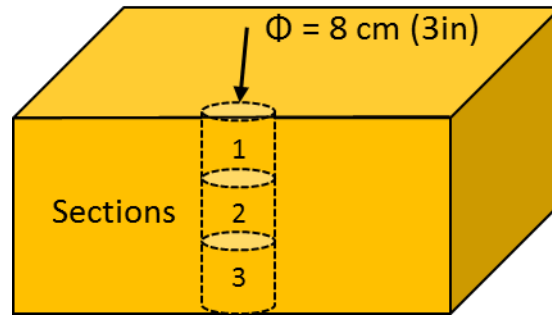


Figure 4.6: Top bale composite sampling three sections

The first set of top samples were taken in March as bales unfroze and before tarps were applied. All four treatments were sampled using the same method. The wrapped top bale treatment holes were patched after sampling. The holes of the remaining three treatments, still uncovered at this time, were filled in with loose stover material. In early July, the same bales from each treatment were sampled again using the same top auger method. The tarped treatments were untarped, sampled, and retarped within the same day. The last set of top samples were taken in late August, again in the same manner. All samples from each batch were analyzed for moisture content. All assessment methodologies are listed at the end of this methods section.

4.2.6 Full Stack Bale Sampling Design

To assess various parameters of bales from all locations within the stacks, initial and final samples and measurements were taken from specific bales. Within one day of harvest, initial samples were taken from the center of the small end of the bale using a 5 cm (2 in) diameter, 61 cm (24 in) long core bit (Figure 4.7). All samples were analyzed for moisture content and a portion for ash content. Initial weight was also recorded for each bale. All four treatments within each stack received 10 to 15 of these bales, depending on stack height, and were distributed equally in all dimensions. Each bale was tagged and the location within the stack was recorded. As stacks were deconstructed after one year of storage, the same bales were core sampled and

weighed once again. Final dimensions of each bale were also recorded. Samples were analyzed for moisture and ash content. Dry matter loss, and final density were calculated as well.



Figure 4.7: Stationary scale and coring unit

(Core: 5 cm (2 in) diameter, 61 cm (24 in) length)

4.2.7 Assessment Parameters

4.2.7.1 Moisture Content and Ash Content

Core samples were analyzed for moisture using the ANSI/ASAE S358.3 standard (ASABE, 1988) for moisture measurements of forage material, modified slightly for corn stover. First an initial wet moisture was recorded and the sample was dried in a ventilated oven at 105°C (221°F) for 24 hours. A dry weight was taken, and Equation 4.1 was used to determine the percent moisture. To analyze ash content, once dry, samples were burned using Thermo Scientific Tabletop Muffle Furnaces following a modified version of National Renewable Energy Laboratory's NREL/TP-510-42622 procedure (Sluiter et al., 2005). A sample was dried, weighed, and placed in a furnace. Furnace temperature stepped up to 570°C (1058°F), dwelled at

that temperature for 8 hours, and then allowed to cool down. The final ash weight was taken. Ash content was calculated using Equation 4.2.

Equation 4.1: Moisture content calculation, wet basis

$$\text{Moisture Content}_{\text{wet basis}}(\%) = \frac{(\text{Wet weight} - \text{Dry weight})}{\text{Wet weight}} * 100$$

Equation 4.2: Ash content calculation

$$\text{Ash Content}(\%) = \frac{\text{Ash weight}}{\text{Dry weight}} * 100$$

4.2.7.2 Side Moisture Penetration

The wrapped and uncovered treatments allow external moisture to fall between bale columns. To analyze the horizontal moisture migration, at the time of deconstruction, side penetration measurements were taken for all four treatments. Samples, taken using stationary coring unit, were ejected into a PVC measurement tool (Figure 4.8). Distinct material quality change was assessed visually by a single person and recorded to the nearest inch. The two quality portions were separated and analyzed for moisture content separately (Figure 4.8).



Figure 4.8: Side moisture penetration measurement and separated sample

4.2.7.3 Bale Weight and Dimensions

Bale weights were taken using a Central City, GT400 scale to the nearest 1 lb. Bales' height, length, and width were measured to assess final bale dimensions and bale volume. A telescoping measurement tool was used to capture these measurements.

4.2.7.4 Dry Matter Loss

Dry matter loss (DML), being a destructive test, was assessed at stack set up and stack deconstruction. Between the harvest of bales and stacking (approximately one day), an assessment of the initial mass of dry matter was conducted using the average sample moisture content and bale weight (Equation 4.3). As stacks were deconstructed, the same bales were assessed for final mass of dry matter using the same method. Dry matter loss was calculated on a percent basis for each bale measured (Equation 4.4).

Equation 4.3: Bale dry matter calculation

$$\text{Dry Matter} = \left(1 - \frac{\text{Moisture Content}}{100}\right) * \text{Bale Weight}$$

Equation 4.4: Dry matter loss calculation

$$\text{Dry Matter Loss} = \frac{\text{Dry Matter}_i - \text{Dry Matter}_f}{\text{Dry Matter}_i} * 100$$

4.2.7.5 Temperature Profiles

Using the constant logging of the thermistor probes, temperature profiles over the course of the year storage trial were generated using Minitab software.

4.2.7.6 Material Coloring

As each stack was deconstructed, photos of each cross section were captured. Individual sample photos were also taken post storage.

4.2.7.7 Statistical Analysis

Minitab 17 Statistical Software was used to interpret the results in this chapter. The Analysis of Variance (ANOVA) function was used to determine if means of resulting values differed among treatment factors and or field ID's. The null hypothesis tested: the mean values did not differ between treatments. At an α value of 0.05 for a confidence interval of 95%, if a P-value less than 0.05 was obtained, there would be enough evidence to reject the null hypothesis, indicating that at least one mean was statistically different. To further determine which treatments differed from one another, a Tukey's test was performed. In the Tukey grouping, means that do not share a letter are significantly different. All ANOVA's with more than two levels tested were followed by a Tukey's test and the Tukey's test results are displayed in this writing.

4.3 Results and Discussion

4.3.1 Initial Stack Conditions

Immediately after harvest, bales were sampled to collect initial material conditions. These bales were then stacked with the remaining bales within one day of sampling, and distributed evenly between treatments and all dimensions of the stack. Dry weather conditions during the 2015 harvest season influenced the levels of bale moisture available for this stack. An ANOVA and Tukey's test (Table 4.1) revealed that the mean field moisture content was found to be statistically different between all four fields tested. Although not an experimental factor, initial bale samples were also analyzed for percent ash content. Field F00220 and field F08465 were the only two fields that did not show a statistical difference in mean initial ash content.

Table 4.1: Tukey's test results for mean estimation of initial moisture and ash content by field ID

Field ID	Moisture Content %				Ash Content %			
	n	Mean	StDev	Tukey Grouping*	n	Mean	StDev	Tukey Grouping*
F08454	78	23.74	6.68	A	33	17.96	8.02	A
F08883	106	19.50	3.27	B	73	12.44	4.85	B
F08465	159	16.67	3.57	C	109	10.41	2.60	C
F00220	158	10.38	1.69	D	111	10.19	3.95	C

*Means that do not share a letter are significantly different.

**Note differences in sample population. F08454 was the first field sampled, and sampling was increased for remaining fields due to adequate time. F08454 and F08883 are four-bale-high stacks and less samples were taken compared to the six-bale high stacks: F08465 and F00220.

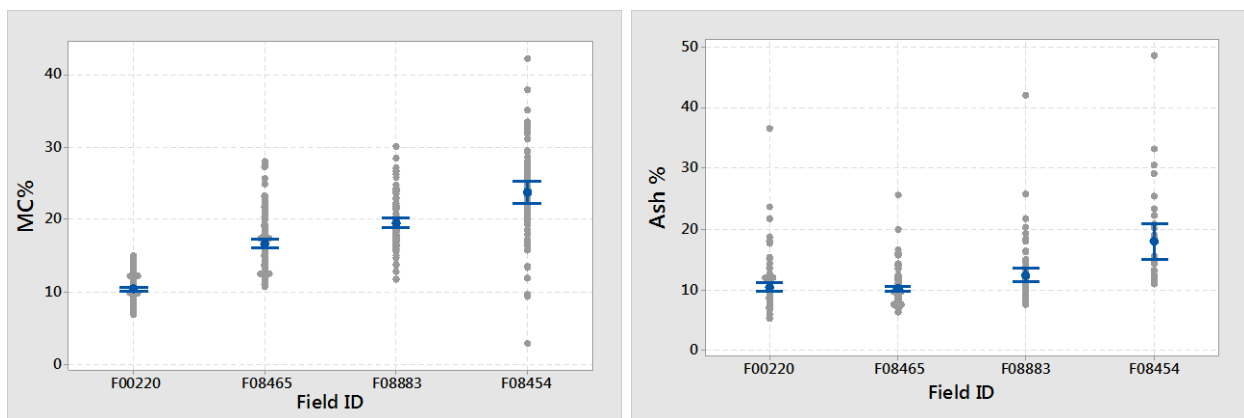


Figure 4.9: Estimated initial moisture and ash content by field ID. Bars indicate 95% confidence intervals.

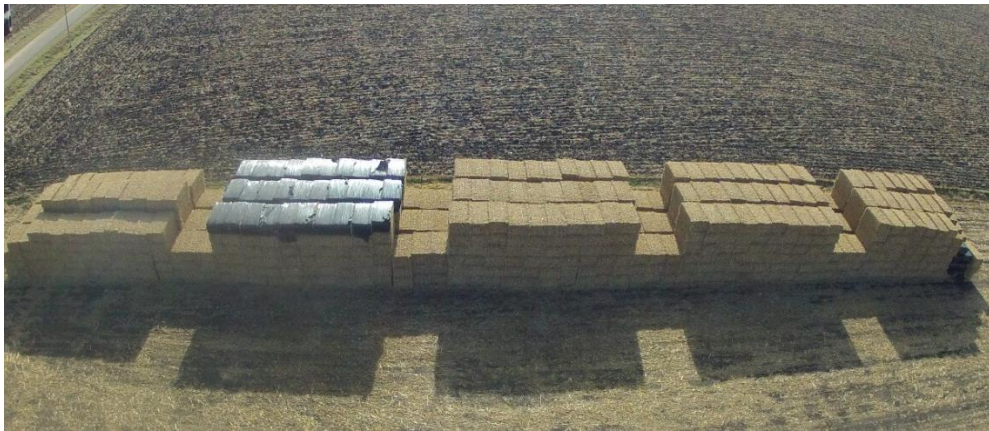


Figure 4.10: Completed field edge storage trial stack, fall 2015

UAV photography: Chris Murphy

4.3.2 Central Iowa Weather Patterns

Weather in central Iowa heavily dictates the available harvest season for corn stover collection. This also dictates how much excess material must be harvested and stored to support an entire year's worth of biomass feedstock to a bio refinery. Iowa averages 81. cm (32 in) of rain per year (1900-2016 recorded average) (Iowa Environmental Mesonet, 2015), indicating that some form of coverage or protection is necessary to minimize degradation of biomass during storage. As typical per the Midwestern United States, Iowa normally receives the bulk of its precipitation during the spring and summer months (Figure 4.11). On average, during late fall and winter (November-February), Iowa receives less than 15% of its annual rainfall. Chapter 3 of this work concluded that microbial activity is not generated at freezing temperatures, and degradation is limited. Low rainfall and freezing temperatures align with the current practice of tarp application in early spring, to limit mechanical wear on tarps caused by high winds and snow loads during winter months.

Fall 2015 weather presented abnormal precipitation that resulted in a unique feedstock storage condition (Figure 4.11). The first abnormal rainfall occurs in December. December, a month that historically has an average of 2.8 cm (1.1 in) of rain precipitation, received 13 cm (5.0 in), five times as much in 2015.

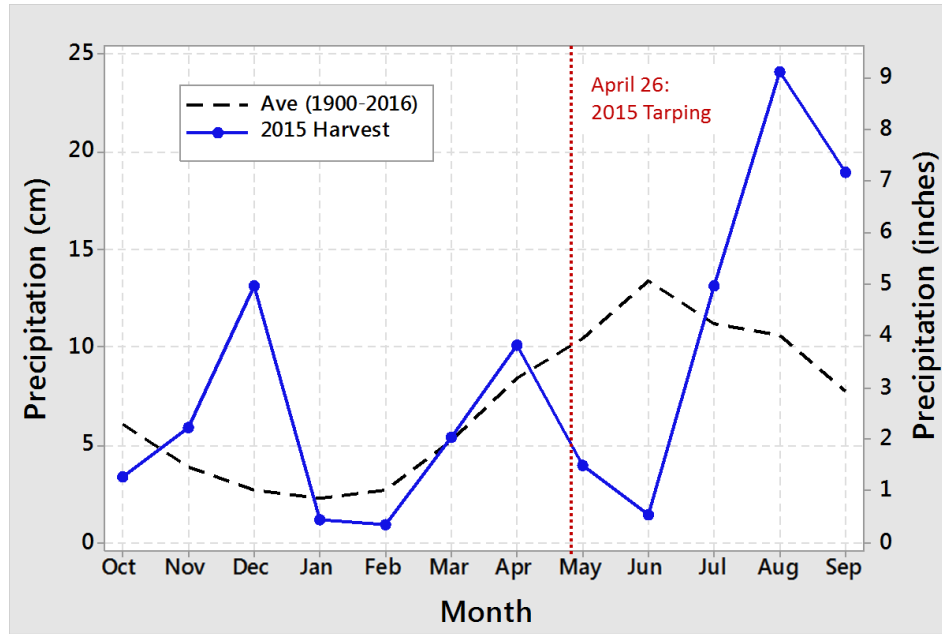


Figure 4.11: Historical precipitation for central Iowa (Iowa Environmental Mesonet, 2015)

If stacks were covered during the suggested February/March timeframe, they would have still been exposed to the extra four inches of rain in December. Weather fluctuates year by year, creating a historical average. A higher than average rainfall is only as extreme as its frequency. Based on the cumulative distribution of December rainfall from 1900 – 2016 the average rainfall for December, 50th percentile, is 2.8cm (1.1 inches) (Figure 4.12). The 13 cm (5.0 in) of rain received in December of 2015 is highlighted at the 100th percentile, indicating that 100% of the years recorded were below this rainfall amount. Furthermore, this rainfall occurred before treatments A and C were tarped in the spring, providing most likely the worst case scenario for those two treatments compared to an average year.

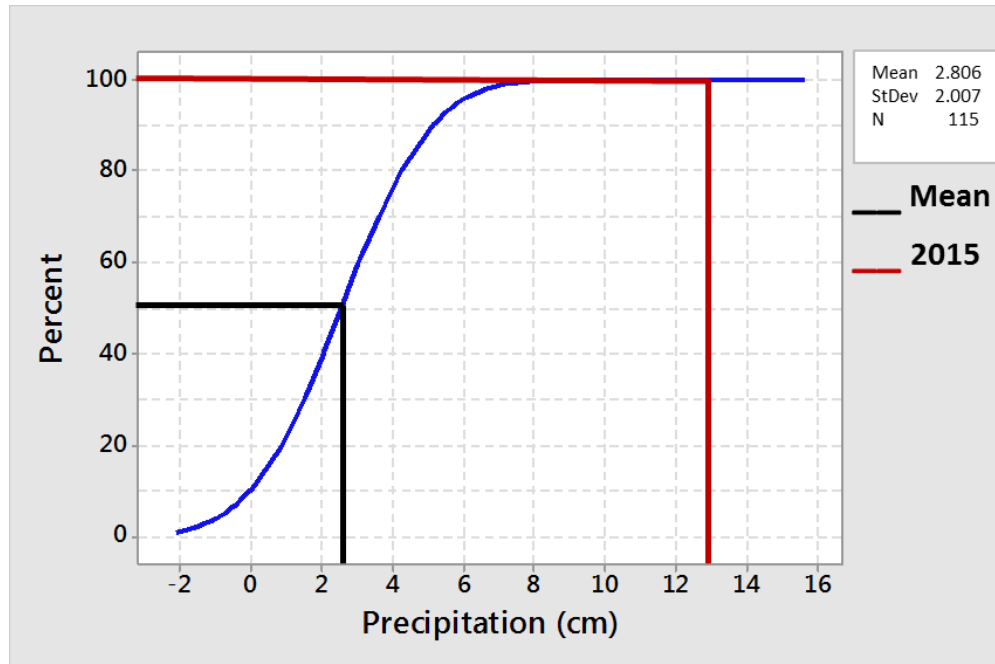


Figure 4.12: Cumulative distribution for central Iowa December precipitation (Iowa Environmental Mesonet, 2015)

4.3.1 Stack Temperature Gradients

4.3.1.1 Generating Vertical Profiles

From the time each field was stacked to the time of deconstruction, thermistor readings were recorded every 30 minutes. Each treatment contained two instrumented columns with eight probes. The columns, being replicates of one another for the most part, were averaged to generate a single vertical temperature profile (Figure 4.13). The profiles are color coded to reference the vertical probe location within each column (Figure 4.14).

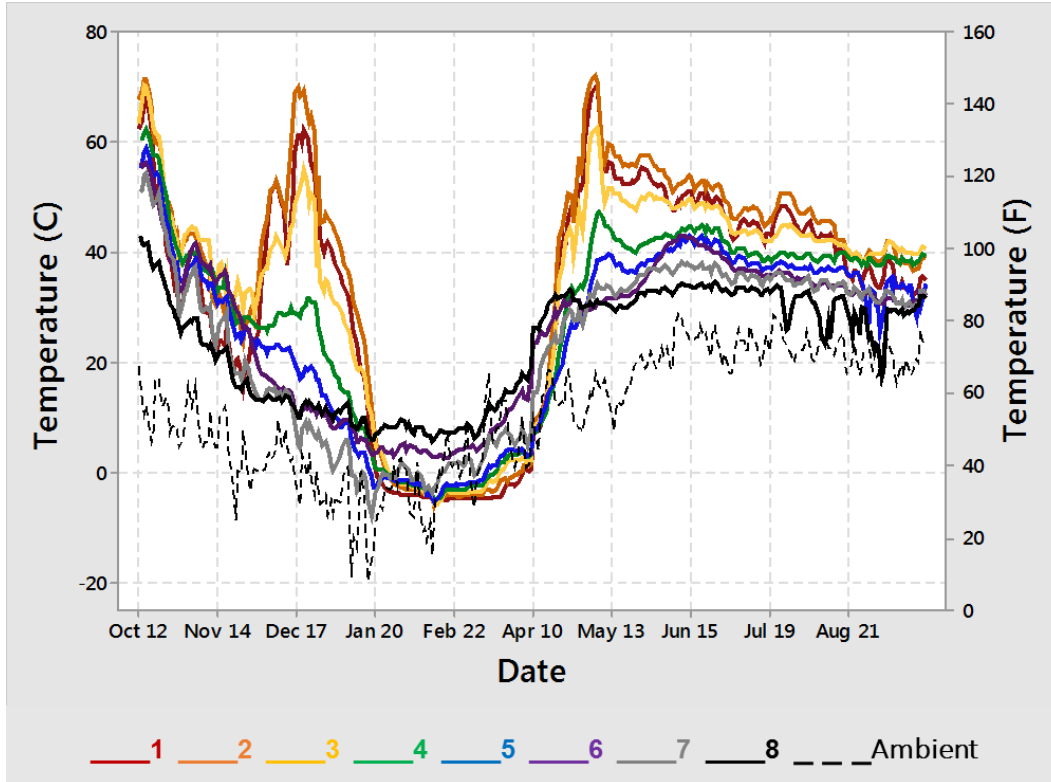


Figure 4.13: Example of temperature profile, one treatment of one six-bale-high stack

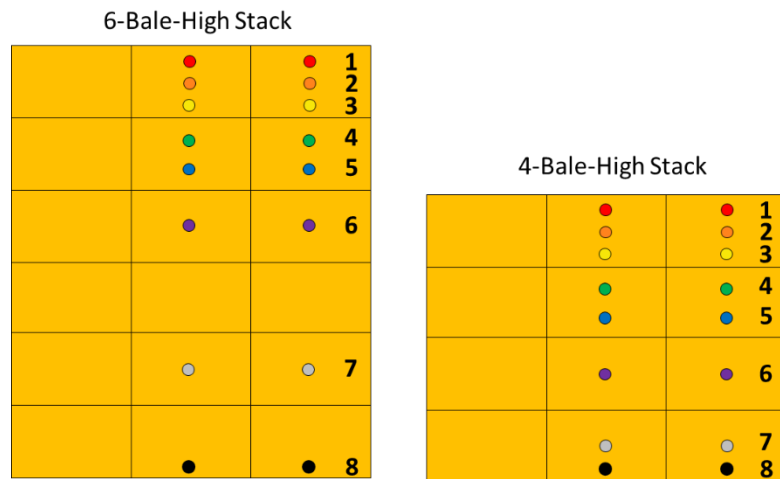


Figure 4.14: Probe placement for six and four-bale high stacks

4.3.1.2 Influence of Initial Moisture Content

Immediately after baling and stacking, biomass with higher initial moisture content began heating. This effect is best highlighted from the date of stacking bales up to the extreme December rainfall (Figure 4.15). Field F08465 was baled at 16% moisture, a level considered stable to limit microbial activity (according to Ch. 3), recorded minimal heating, and tracked ambient in the top six probes. Probes seven and eight held a more constant temperature slightly above ambient, most likely due to the capillary action the bale stacks make on the surface moisture. The same treatment in field F08454, baled at 24% moisture, experienced significant heating above ambient in all eight probes. As Chapter 3 concluded, moistures above 20% are more susceptible to microbial degradation than those at lower moisture contents. The immediate heating in F08454 aligns with past temperature research regarding high moisture stover bales as well as degradation of lignocellulosic material during composting. All four treatments from F08454 experienced this type of initial heating in all eight probes. With the exception of the bottom probe (probe eight), all probes initially heated to the 50°C to 65°C (120°F to 150°F) range before decreasing in temperature. This again follows the basic science behind lignocellulosic degradation and temperature research (Schon et al. 2013). Soon after reaching this heating spike, temperatures began to fall, most likely due to a combination of thermophile population reduction and decrease in moisture content and/or substrate.

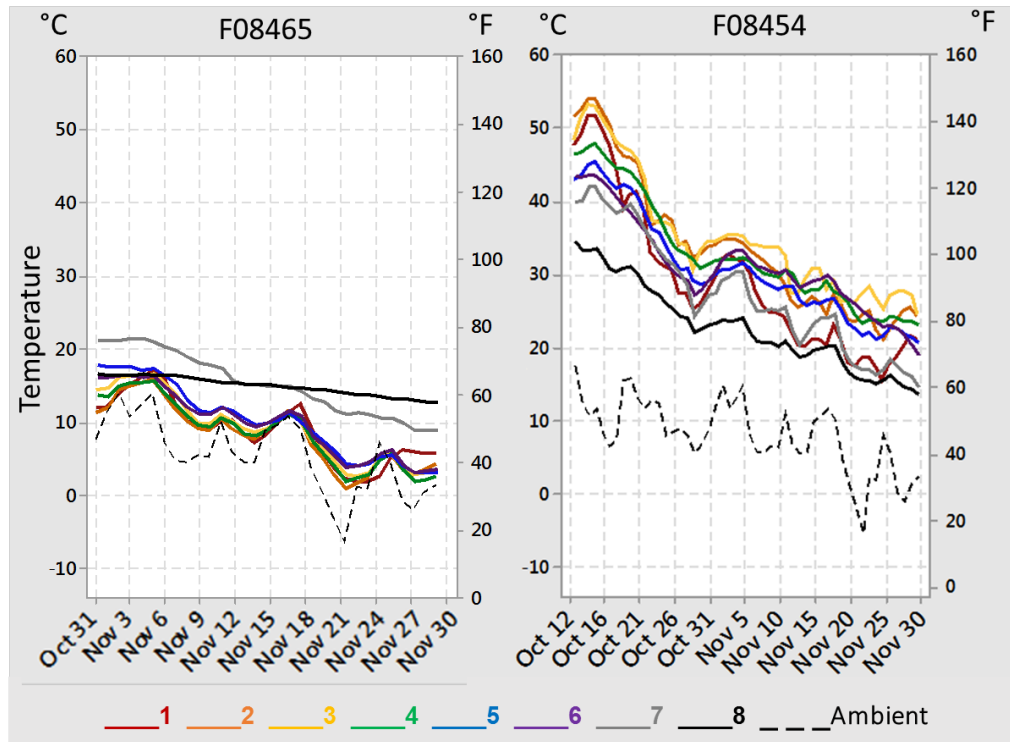


Figure 4.15: Fields F08465 (left) and F08454 (right), temperature profiles, stacking day to beginning of December 2015.

4.3.1.1 Influence of Environment Post Harvest

Adequate moisture content and temperature of biomass generate a habitable environment for heat-generating microbial degradation. Dynamic vertical temperature profiles map post-harvest moisture migration for each treatment of a single stack. Probes one, five, and eight provide a high level map of degradation occurring in the top bale, second from top bale, and bottom bale. (Figure 4.16). The “to-be-tarped” treatments: A and C, and the uncovered treatment D, absorbed the extreme winter rainfall, causing a distinct temperature spike during the month of December. Treatment B, with a top layer of bales wrapped during October harvest, lacks this December peak, indicating moisture did not penetrate the top six inches of the top bale as it did with the other three treatments. Probe five, during this same period of time, does not spike, indicating that the rainfall in December did not penetrate through the second bale from the

top. Common to all four treatments, the top and center bales track ambient from January to March. The bottom probe of each treatment, commonly seen in all fields, does not track ambient during these months. Moisture and/or temperature are below levels that sustain microbial activity in the top and center bales, but are adequate at the base of the stack. Most likely moisture was immediately absorbed from the ground, initiating microbial activity and heating, then was not allowed to escape due to the insulating properties of the ground and bale stack. More research is needed fully conclude on this phenomenon. After tarping in April, temperatures did not suddenly drop, but slowly decrease towards ambient in treatments A and C. Probe five, located in the bottom half of the 2nd bale from the top, measures temperature slightly above ambient, but never spikes to maximum temperatures. Material above probe five in these treatments may house microbial activity and pass on excess thermal energy, but degradation has not yet reached that far down the stack. Treatment D's top probe, still uncovered, experiences heating cycles as it continues to absorb rainfall until deconstruction in September. Probe five in this treatment does begin to spike into the 65°C (150°F) range, indicating that decomposition has penetrated into the second bale from the top in the uncovered treatment.

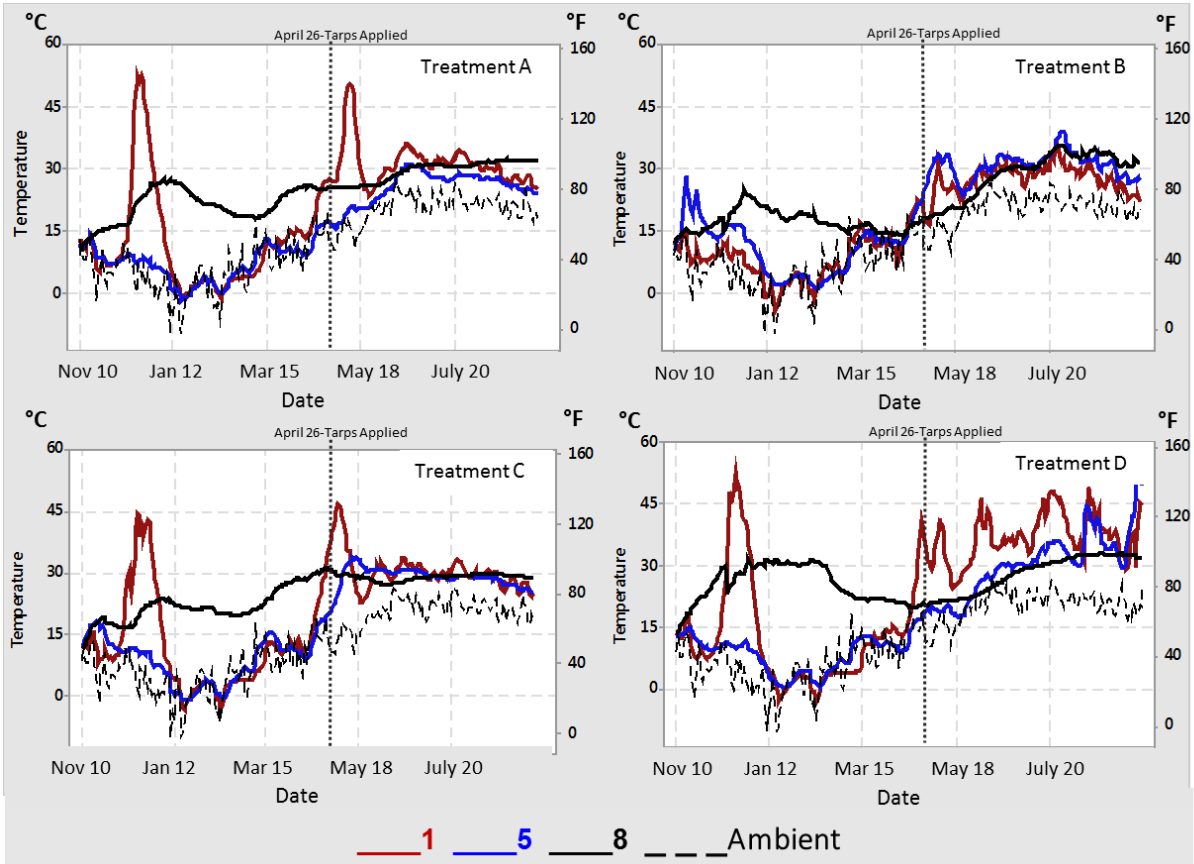


Figure 4.16: One field site, all four treatment temperature profiles. Probes 1, 5, 8, plotted with ambient temperature.

Moisture migrated into the second from the top bale in treatment D, but not the bale below that, indicated by the heating seen in probes five and six. (Figure 4.17) As shown more clearly, probe five does spike into the 65°C (150°F) range. While probe six is constantly above ambient, it does not spike in heat yet.

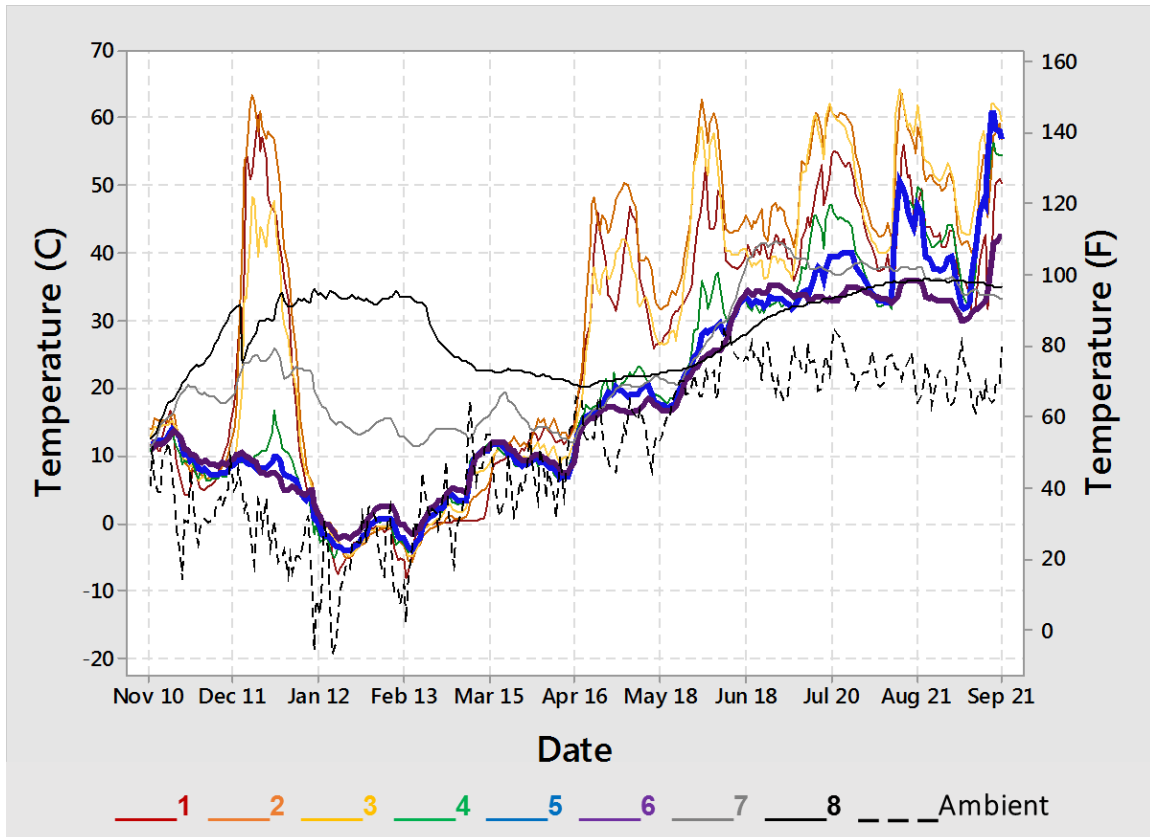


Figure 4.17: Temperature profile of uncovered treatment. Probes 5 and 6 are bolded.

4.3.2 Sampling to Understand Moisture Migration

To verify dynamics of moisture migration through the top of the stack, core samples were taken at each site during the months of March, July, and August. The first set of samples were taken in March, once bales were thawed enough to core after the winter season. This sampling took place before the tarping season, so treatments A, C, and D had been exposed to fall rain events. The levels of moisture in the top bales at this point held any retained rainfall from the harvest season and that in December. All three treatments that were uncovered showed similar trends in moisture levels vertically down the top bale (Figure 4.18). The top section of the top bale had an average moisture content of 75%. The second section had an average moisture content of 55%. And the third or bottom section of the top bales from uncovered treatments had

and average moisture content of 25%. Treatment B, being wrapped early, did not absorb the fall and winter rainfall. The first, second, and third sections of the top bales had average moisture contents of 36%, 21%, and 15% respectively. Combining all four fields' top bale data in March, treatment B is statically different from all other treatments in its mean moisture content (Table 4.2).

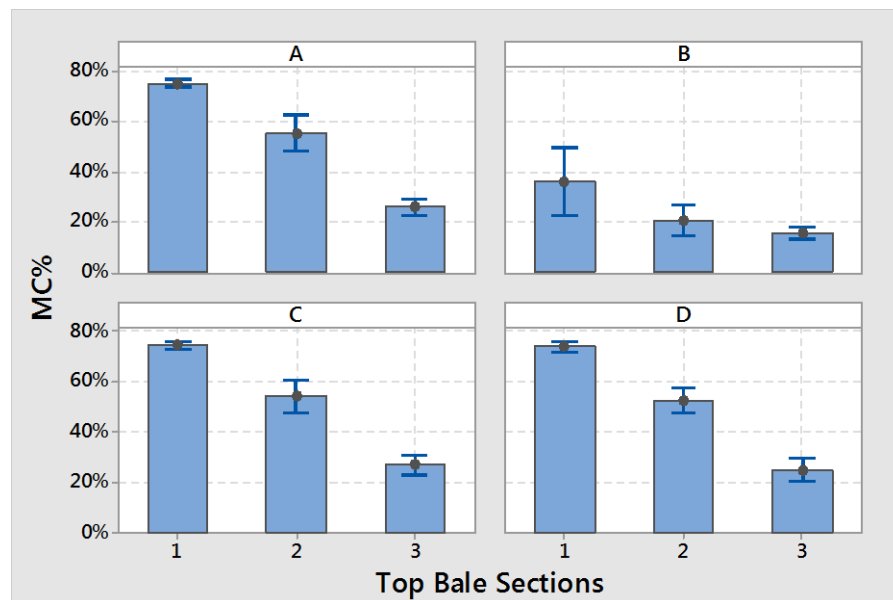


Figure 4.18: March top bale sampling moisture content. Combined four fields. Composite profiles of top bale (section 1: top 1ft, section 2: second ft, section 3: bottom ft). Bars indicate 95% confidence intervals.

Table 4.2: Tukey's test for March top bale sampling moisture (averaged three sections) by treatment.

Treatment	n	Moisture Content %		Tukey Grouping*
		Mean	StDev	
A	34	51.12	21.77	A
B	36	28.85	15.97	B
C	35	51.23	20.79	A
D	35	51.09	20.99	A

A: peaked tarp, B: wrapped top bales, C: flat tarp, and D: no coverage

*Means that do not share a letter are significantly different.

**Note differing sample populations; due to failure in sample transport/processing.

Separating the March top bale samples based on initial field moisture changes the comparison of treatments. Fields with initial moisture content less than 20% follow the aggregated data set: treatment B’s mean March moisture content is statistically lower than the other three treatments (Table 4.3). Field F08454, that had an initial moisture content above 20%, has no statistical difference in mean moisture content among the four treatments (Table 4.3). This material was baled at a higher moisture content, and because the bales were wrapped, moisture may not have been allowed to leave. Note that the Tukey’ test for F08454 alone has a significantly lower population size than the three combined drier fields (Figure 4.19), and will influence its 95% confidence interval.

Table 4.3: Tukey’s test results for average March top bale moisture based on treatment. Separated by initial field average moisture content

F00220, F08883, F08465					F08454			
Treatment	n	Moisture Content %		Tukey Grouping*	n	Moisture Content %		Tukey Grouping*
		Mean	StDev			Mean	StDev	
A	25	49.66	22.09	A	9	55.17	21.57	A
B	27	20.09	10.75	B	9	35.14	23.42	A
C	26	49.48	19.79	A	9	56.29	23.99	A
D	25	49.25	21.08	A	9	53.79	21.43	A

A: peaked tarp, B: wrapped top bales, C: flat tarp, and D: no coverage
 *Means that do not share a letter are significantly different.
 **Note differing sample populations; due to failure in sample transport/processing.

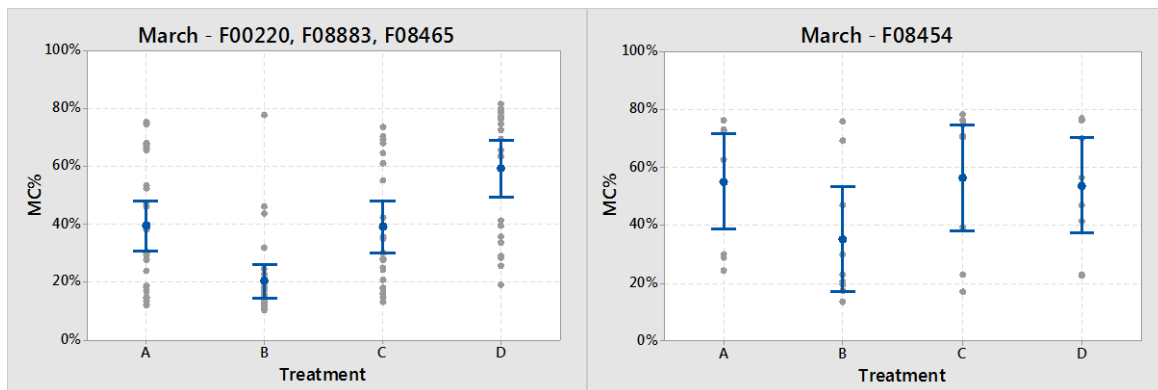


Figure 4.19: March top bale moisture content, fields split by initial moisture content. A: peaked tarp, B: wrapped top bales, C: flat tarp, and D: no coverage. Bars indicate 95% confidence intervals.

The second set of samples were taken at the beginning of July. The two tarped treatments were covered at the end of April, so they had protection from rainfall for just over one month at this point. Treatment D had no coverage, and the second section of this treatment has a significantly higher mean moisture content than any other treatment (Figure 4.20). A fourth section sample was taken in July; representing the top section of the second bale from the top.

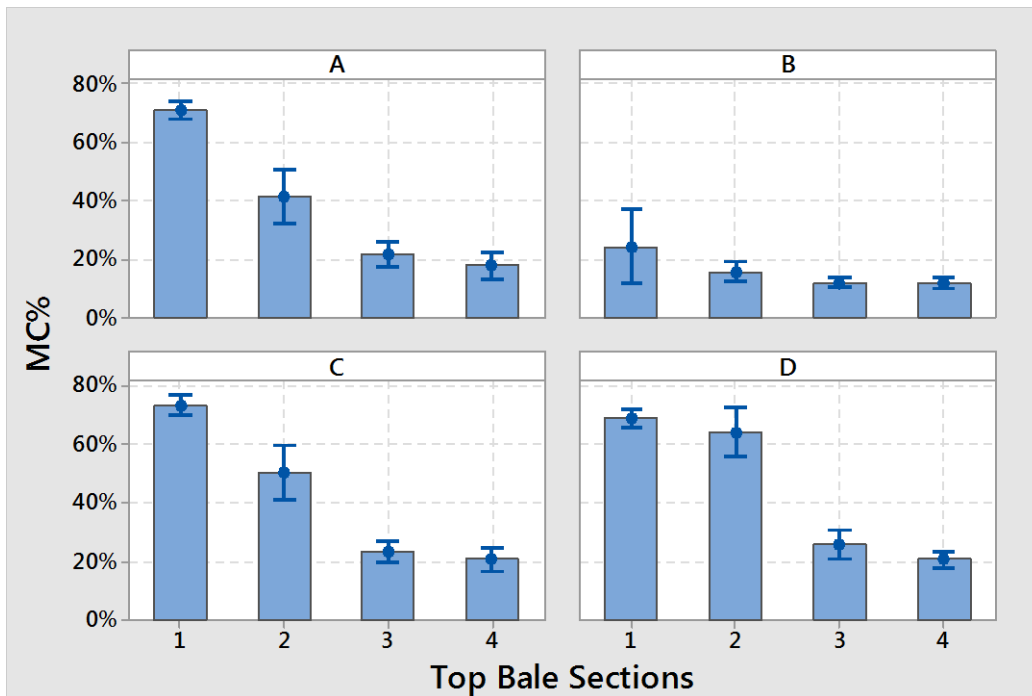


Figure 4.20: July top bale moisture content by sections. Composite profiles of top bale (section 1: top 1ft, section 2: second ft, section 3: bottom ft) Section 4 in treatment D refers to the top ft of the second bale from the top. Bars indicate 95% confidence intervals.

The last set of samples taken from the top of the stack were collected in August, ahead of the stacks being fully deconstructed. Treatment D, again continued to gain moisture in the top bale. In August, all top three sections of treatment D were statistically higher than the corresponding sections in all three other treatments (Figure 4.21). Section 4 samples were only taken for treatment D at this time. Section 4 of treatment D was statistically higher in moisture

content than section 3 in treatments A and C, indicating that moisture penetrated the second bale in only treatment D. Treatments A and C's top bale profiles look very similar in August.

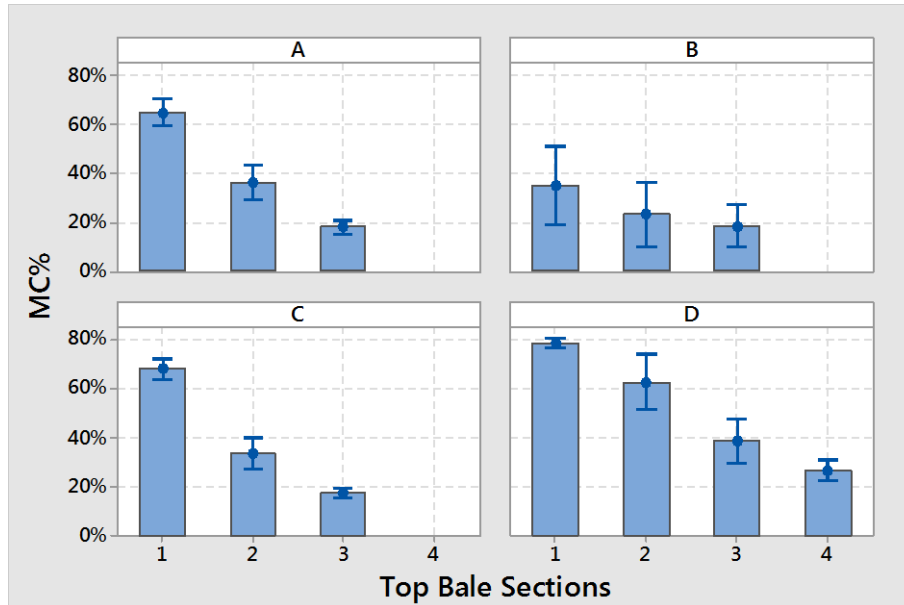


Figure 4.21: August top bale moisture content by sections. Composite profiles of top bale (section 1: top 1ft, section 2: second ft, section 3: bottom ft) Section 4 in treatment D refers to the top ft of the second bale from the top. Bars indicate 95% confidence intervals.

The moisture content within the top bale of a stack depends on the initial moisture content of the material, the type of coverage, and the timing of coverage. Exposed to rainfall early on, the average top bale moisture content of treatments A, C, and D increased dramatically from October to March (Figure 4.22). Once covered, top bales in treatments A and C decreased in average moisture content, while the exposed treatment D continued to increase through August. The wrapped treatment B did not absorb near the moisture as the other treatments, but also held in initial moisture. These trends seen with physical moisture sampling reflect the vertical temperature profile heating patterns.

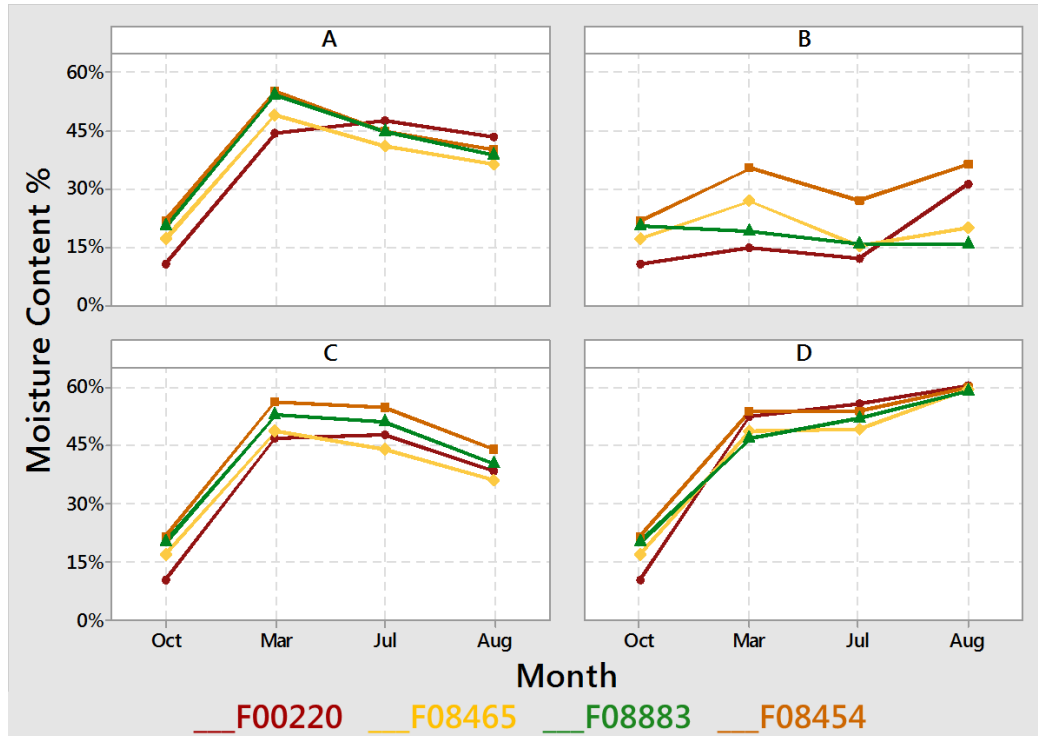


Figure 4.22: Treatment top bale moisture contents over time. Averaged three sections.

4.3.1 Stack Moisture Migration

When sampled for moisture content in August, there was no statistical difference in average top bale moisture content among the four fields (Table 4.4). A one-way ANOVA test was performed, followed by a Tukey's test. On that basis, all four fields were aggregated to evaluate the full vertical moisture profile for each coverage treatment.

Table 4.4: Tukey's test for final average top bale moisture content by treatment and field

Field ID	Top Bale MC% (A)			Top Bale MC% (B)			Top Bale MC% (C)			Top Bale MC% (D)		
	n	Mean	Tukey Grouping*	n	Mean	Tukey Grouping*	n	Mean	Tukey Grouping*	n	Mean	Tukey Grouping*
F00220	9	43.35	A	9	30.99	A	9	38.34	A	9	62.19	A
F08465	9	36.16	A	9	19.82	A	9	35.88	A	9	59.36	A
F08883	9	38.73	A	9	15.34	A	9	40.21	A	9	59.06	A
F08454	9	40.22	A	9	36.20	A	9	44.11	A	9	58.25	A

A: peaked tarp, B: wrapped top bales, C: flat tarp, and D: no coverage

*Means that do not share a letter are significantly different.

During stack deconstruction in the fall of 2016, samples were taken to summarize final bale moisture contents and generate vertical moisture profiles for each treatment (Figure 4.23). The August results for top bale sampling were applied to the profiles for the top bale moisture content. Nearly all top bales from treatments A, C, and D were unable to be picked up singly with the telehandler (Figure 4.24). Due to the lack of integrity, each top bale weight was captured in combination with the bale below it. The “Center” category aggregates all middle bales within a treatment between the second from the top and bottom bales. The bottom bale is split into two categories for moisture content. Through the capillary action experienced by ground moisture directly beneath the stack, moisture is wicked up by the bottom bale. This capillary action, working against gravity, creates a distinct line of separation in quality. The significantly drier, upper portion is listed as the “Bottom” category, and the lower saturated portion is listed as “Wicking”. The largest influencer of wicking height in this experiment was stack location. Treatment mean wicking heights did not differ statistically. Aggregating all 102 bottom bales, wicking height ranged from 5-31cm (2-12in), with a mean of 14 (5.5in) (Figure 4.25). Absorption of moisture from the ground was expected. There is currently little to no past research published to compare the magnitude of wicking height with. Bales were also analyzed for horizontal moisture migration through side penetration measurements. Treatment B experienced significantly higher side penetration than the other three treatments (Figure 4.26).

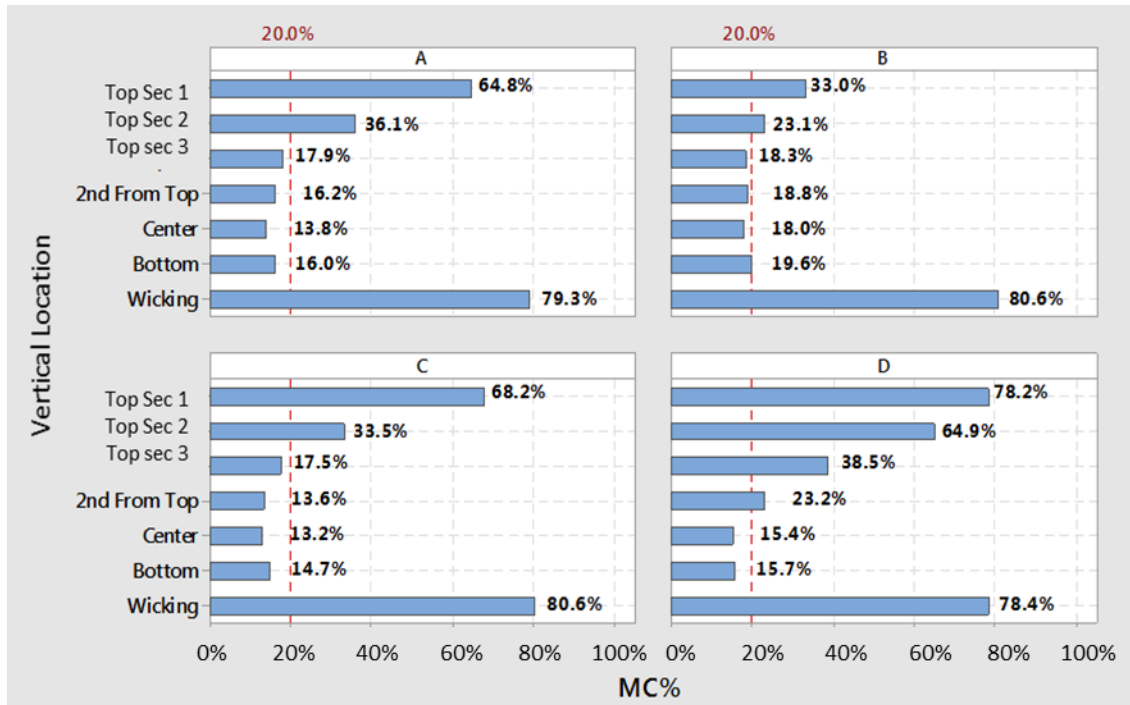


Figure 4.23: Final vertical moisture profiles for each coverage treatment, combined all four fields. “Bottom” refers to the dry upper portion of the bottom bale. “Wicking” refers to the saturated base portion of the bottom bale.



Figure 4.24: Telehandler attempting to pick up a top bale post storage, highlighting loss of integrity

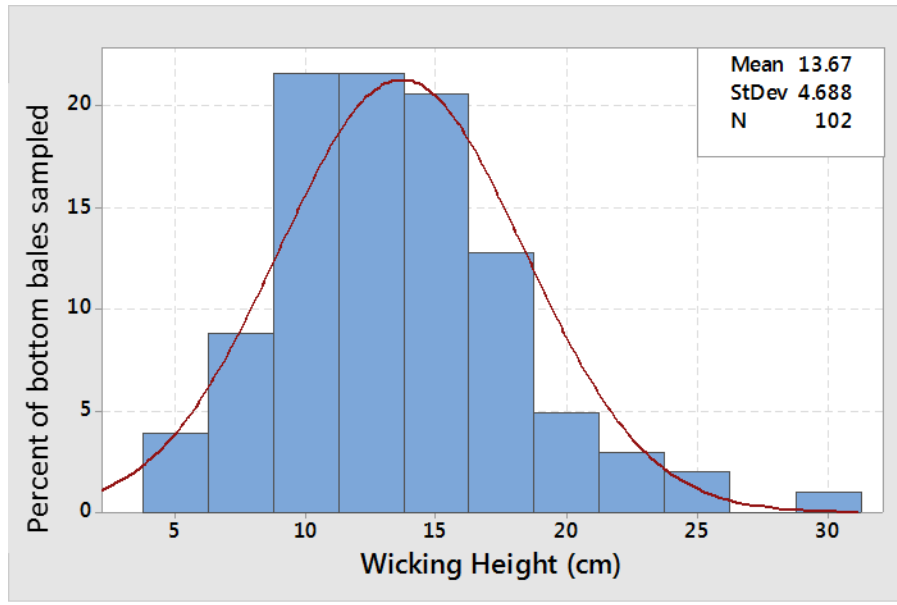


Figure 4.25: Distribution of wicking height. Combined all fields and all treatments

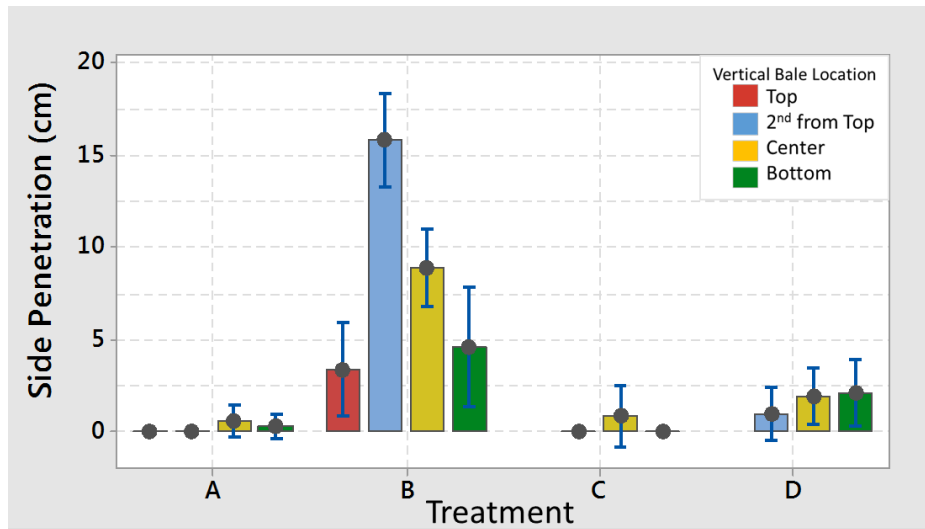


Figure 4.26: Treatment and bale location influence on side moisture penetration. Bars indicate 95% confidence intervals.

Using moisture analysis results from bale sampling, wicking, and side penetration measurements, a moisture penetration map was generated for each treatment (Figure 4.27). With these maps, each treatment's material was aggregated into moisture bins and analyzed to determine the cumulative percentage of dry, stable material in each bale stack (Table 4.5).

Moisture migrates through the stack both vertically and horizontally. Treatment D, uncovered, allowed for the highest moisture absorbance through the top of the stack, resulting in the lowest percentage of dry, stable material make up. The final aggregated material contains nearly 40% higher moisture material (MC > 20%). Treatment B absorbed less moisture through the top bale than the three other treatments, but also experienced the highest horizontal migration into the sides of the stack columns. This moisture collected between the columns leaves treatment B with less dry, stable material than treatments A and C. The high moisture material resulting in treatments A and C is due to the unexpected winter rainfall and absorbance of moisture from the ground, into the bottom bale. The aggregated treatment profile maps were applied to both the four-bale-high and six-bale-high stacks. Naturally, with less center bale material, the percent of dry, stable material increases with decreasing stack height. Treatment D is very unstable with less than half of the material measuring below 20% moisture content. External moisture has greater impact on the average quality of material coming out of shorter stacks. Degradation and discoloration within the stacks follows same pattern as the moisture migration (Figure 4.28).

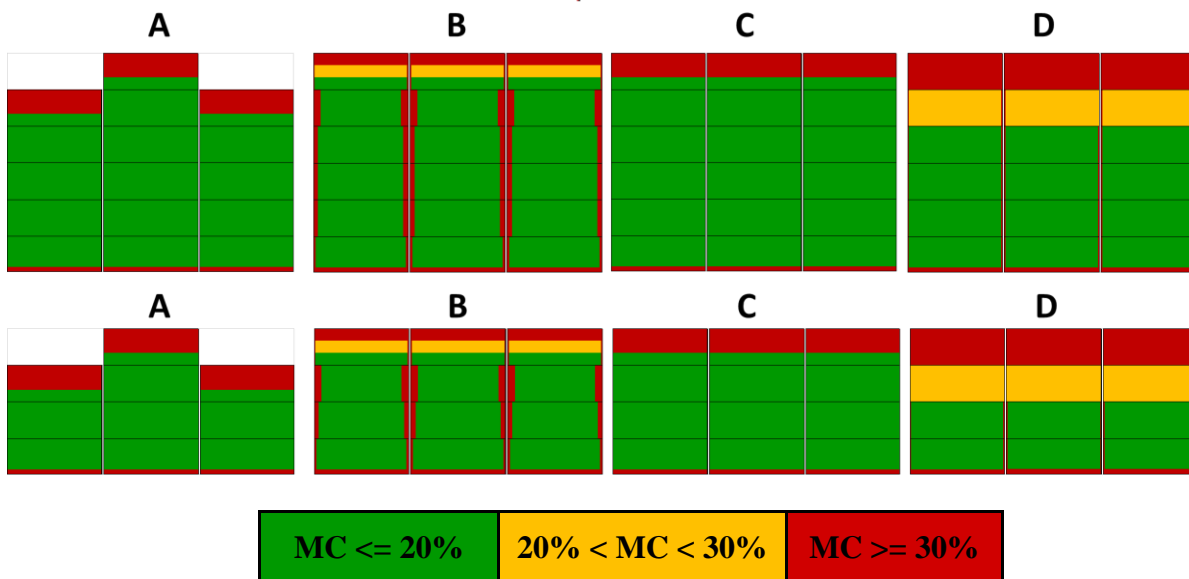


Figure 4.27: Map of moisture migration- all four fields aggregated.

Table 4.5: Moisture content summary by treatment

Moisture Level	6-Bale-High Stack				4-Bale-High Stack			
	Treatment				Treatment			
	A	B	C	D	A	B	C	D
MC ≤ 20%	83%	78%	84%	61%	73%	70%	76%	43%
20% ≤ MC ≤ 30%	0%	6%	0%	17%	0%	8%	0%	25%
MC ≥ 30%	17%	17%	16%	22%	27%	21%	24%	32%

A: peaked tarp, B: wrapped top bales, C: flat tarp, and D: no coverage

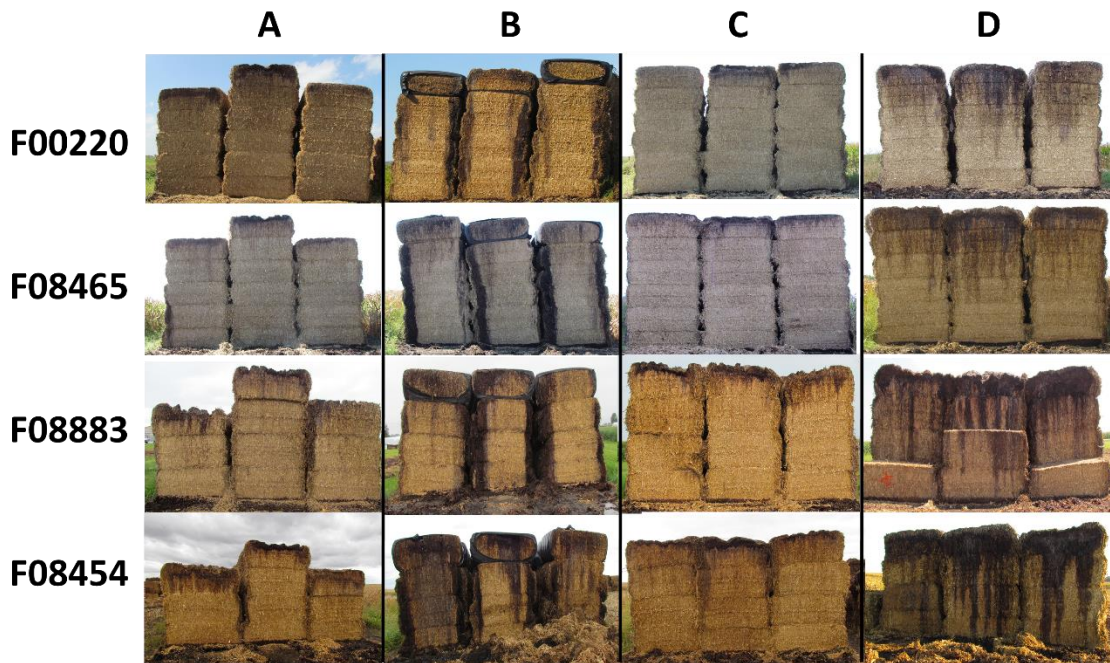


Figure 4.28: Stack site treatment cross sections. Columns indicate treatments: A: peaked tarp, B: wrapped top bales, C: flat tarp, and D: no coverage. Rows indicate field ID's.

There showed difficulty in accurately averaging the final moisture contents of both the bottom bales and bales in treatment B. The dry matter loss for bottom bales is a conservative estimate based on a measurement of the remaining dry, non-degraded material obtained from measurements of height and wicking height, opposed to the analysis based on moisture content and weight. Dry matter loss is not reported for treatment B. There was no statistical difference in mean dry matter loss among treatments for the four vertical bale locations (Table 4.6 and Figure

4.29). Aggregating the three remaining treatments, top and bottom bales measured significantly higher DML than the other two categories (Table 4.7). The top bales of treatments A, C, and D absorbed the most rainfall, and experienced the largest amount of dry matter loss, 31.5% on average, followed by bottom bales averaging 16.3% DML (Table 4.28). The bales second from the top and the center bales averaged approximately 2% DML.

Table 4.6: Tukey’s test results for dry matter loss based on treatment and vertical bale location.

Treatment	n	Top Bale		2nd Bale from Top			Center Bale			Bottom Bale		
		DML%	Tukey Grouping*	n	Mean	Tukey Grouping*	n	Mean	Tukey Grouping*	n	Mean	Tukey Grouping*
A	18	33.2	A	16	5.6	A	26	1.20	A	25	14.5	A
C	20	29.80	A	27	1.1	A	42	2.1	A	30	16.7	A
D	10	31.9	A	16	0.4	A	31	1.9	A	24	17.9	A

A: peaked tarp, B: wrapped top bales, C: flat tarp, and D: no coverage

*Means that do not share a letter are significantly different.

**Note differing sample populations; “center” includes multiple bales. There are also multiple guilty factors including initial sampling and failures in sample collection (moisture and weight), sample recording, sample transport, and lab processing.

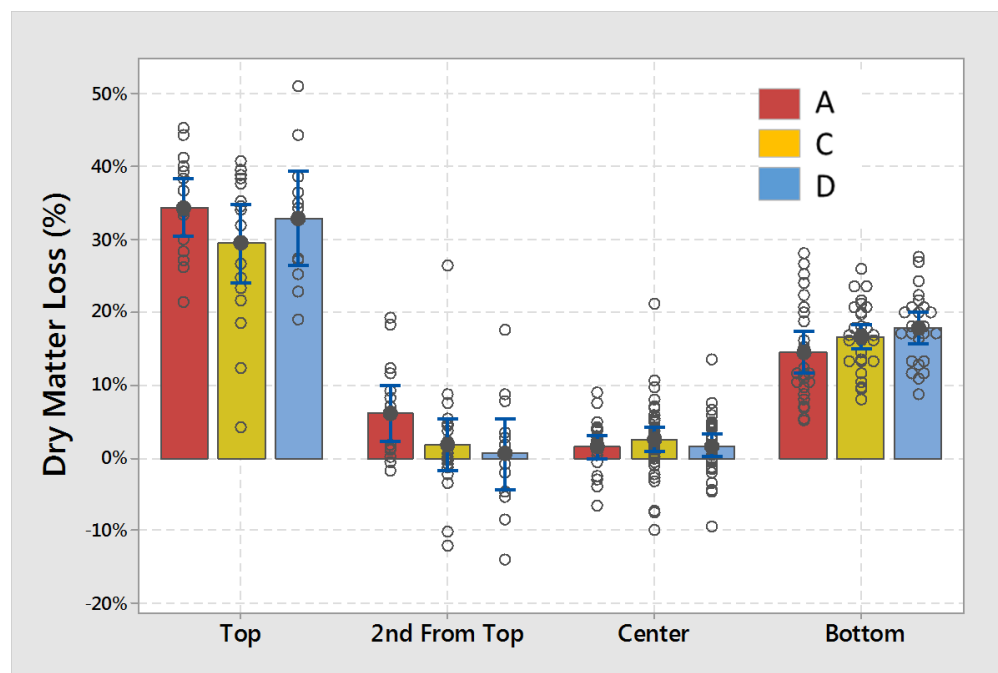


Figure 4.29: Dry matter loss results by vertical bale position for treatments A, C, and D. Bars indicate 95% confidence intervals.

Table 4.7: Tukey’s test results for mean dry matter loss based on vertical bale location for. Combined treatments A, C, and D.

Vertical Location	n	Dry Matter Loss %		Tukey Grouping*
		Mean	StDev	
Top	48	31.5	9.06	A
2nd from Top	59	2.1	7.87	B
Center	99	1.8	4.95	B
Bottom	79	16.3	5.58	C

*Means that do not share a letter are significantly different.

**Note differing sample populations; “center” includes multiple bales. There are also multiple guilty factors including initial sampling and failures in sample collection (moisture and weight), sample recording, sample transport, and lab processing.

Assuming all dry matter loss experienced by top bales is due to biological degradation of sugar-based material, the quality of the remaining dry matter will decrease in terms of carbohydrate concentration. Biomass originally composed of 70% carbohydrate that experiences 30% dry matter loss will provide a biorefinery with 30% less dry material per bale, and the material processed will contain a lower percentage of carbohydrate concentration, under 60%, influencing its fermentation capacity (Figure 4.30).

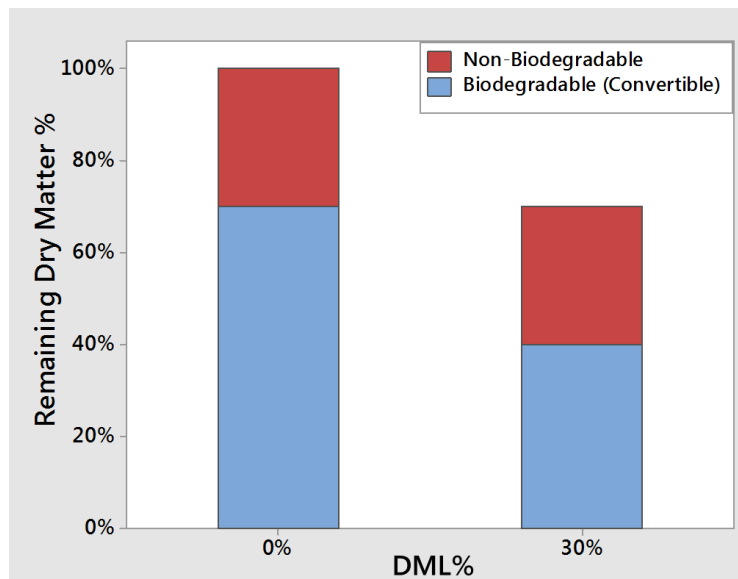


Figure 4.30: Theoretical biomass dry matter composition after 30% DML.

The impact of degradation should be included when evaluating the feedstock contribution to ethanol production cost (FCEPC) for a biorefinery. Figure 2.10, from this literature review (Equation 4.5a) can be modified into a four-input equation to analyze feedstock cost. The inputs include the HST (harvest, storage, and transportation) cost, DML (dry matter loss), BCC_i (initial biomass carbohydrate composition), and reactor product yield. The original equation is configured in terms of initial tons of dry matter (Figure 4.5b), simplified (Figure 4.5c), and the “gallons of ethanol per ton of carbohydrate value” is further broken down allowing a user to need only apply a basic reaction yield to the equation (Equation 4.5d).

Equation 4.5: (a,b,c,d): Modifications to Figure 2.10 from literature review, assessing feedstock contribution to ethanol production cost (FCEPC).

<p>a.) $FCEPC = \frac{\\$Cost_{HST}}{1 \text{ Ton}_{DM_i}} * \frac{1 \text{ Ton}_{DM_i}}{\text{Ton}_{DM_f}} * \frac{1 \text{ Ton}_{DM_f}}{\text{Ton}_{carbohydrate}} * \frac{1 \text{ Ton}_{carbohydrate}}{\text{Gal}_{Ethoh}} = \frac{\\$}{\text{Gal}_{Ethoh}}$</p>
<p>b.) $FCEPC = \frac{\\$Cost_{HST}}{1 \text{ Ton}_{DM_i}} * \frac{1 \text{ Ton}_{DM_i}}{(\text{Ton}_{DM_i} - (\text{Ton}_{DM_i} * DML))} * \frac{(\text{Ton}_{DM_i} - (\text{Ton}_{DM_i} * DML))}{((\text{Ton}_{DM_i} * BCC_i) - (\text{Ton}_{DM_i} * DML))} * \frac{1 \text{ Ton}_{carbohydrate}}{\text{Gal}_{Ethoh}} = \frac{\\$}{\text{Gal}_{Ethoh}}$</p>
<p>c.) $FCEPC = \frac{\\$Cost_{HST}}{1 \text{ Ton}_{DM_i}} * \frac{\cancel{1 \text{ Ton}_{DM_i}}}{(\cancel{\text{Ton}_{DM_i}} - (\cancel{\text{Ton}_{DM_i}} * DML))} * \frac{(\cancel{\text{Ton}_{DM_i}} - (\cancel{\text{Ton}_{DM_i}} * DML))}{((\cancel{\text{Ton}_{DM_i}} * BCC_i) - (\cancel{\text{Ton}_{DM_i}} * DML))} * \frac{1 \text{ Ton}_{carbohydrate}}{\text{Gal}_{Ethoh}} = \frac{\\$}{\text{Gal}_{Ethoh}}$</p> <p>$FCEPC = \frac{\\$Cost_{HST}}{1 \text{ Ton}_{DM_i}} * \frac{1}{(BCC_i - DML)} * \frac{1 \text{ Ton}_{carbohydrate}}{\text{Gal}_{Ethoh}} = \frac{\\$}{\text{Gal}_{Ethoh}}$</p>
<p>d.) $FCEPC = Cost_{HST} \frac{[\\$]}{[\text{Ton}_{DM_i}]} * \frac{1}{(BCC_i - DML)} \frac{[\text{Ton}_{DM_i}]}{[\text{Ton}_{carbohydrate}]} * \frac{1}{Yield_{Ethoh}} \frac{[\text{Ton}_{carbohydrate}]}{[\text{Ton}_{Ethoh}]} * \frac{1}{300} \frac{[\text{Ton}_{Ethoh}]}{[\text{Gal}_{Ethoh}]} = \frac{\\$}{\text{Gal}_{Ethoh}}$</p>

*\$Cost_{HST}: cost to harvest, store, and transport biomass, DM: dry matter, DML: dry matter loss, BCC_i: initial biomass carbohydrate concentration, Yield_{EtoH}: reaction product yield.

Equation 4.6: Feedstock contribution to ethanol production cost (FCEPC) equation

$$FCEPC = \frac{Cost_{HST}}{300 (BCC_i - DML)(Yield_{EtOH})} = \frac{\$}{Gal_{EtOH}}$$

where

$Cost_{HST}$ = cost to harvest, store, and transport 1 ton of fresh biomass (\$ ton⁻¹)

BCC_i = initial biomass carbohydrate concentration (fractional)

DML = dry matter loss (fractional)

$Yield_{EtOH}$ = reaction product yield ratio (fractional)

*300 represents a constant conversion of volume to mass (gal ton⁻¹)

Assumptions were applied to the four inputs to compare FCEPC for protected storage and field edge storage (Table 4.8). The loss of bale integrity with degradation in field edge storage poses concern if bales are unable to be transported or processed. The top and bottom bales lose the most integrity in uncovered field edge storage, therefore Equation 4.6 was also applied to scenarios where these bales cannot be processed (Table 4.8). $Cost_{HST}$ for the protected storage scenario (\$86/ton) is assumed from Dr. Darr's (2014) cost evaluation of a corn stover feedstock supply chain (Figure 2.6). Storage cost and one transportation cost were removed for the field edge storage scenarios, reducing cost to \$65/ton. All scenarios assume 70% initial carbohydrate for the corn stover biomass. DML varies based on storage types and ability to process bales. Okamoto (2014) measured fermentation yields of 0.32 to 0.40 g ethanol/g sugar for five carbon sugars and 0.45-0.49 g ethanol/g sugar for six carbon sugars. Lignocellulosic biomass carbohydrates contain a mix of five and six carbon sugars and must be released from carbohydrates before fermentation. For this analysis a reaction product yield ratio of 0.35 g ethanol/g carbohydrate is assumed for all scenarios. Such yields, in combination with assumed zero degradation and 70% BCC_i , measure a theoretical 70 gal per ton of dry matter. Industries are encouraged to apply their own product reactor yields to the given equation. With these

assumptions, if all material from field edge is processed, there is a potential \$0.18/gal savings in FCEPC in comparison to protected storage, reducing annual production cost by \$5.4M. If the top bales of field edge storage cannot be processed, there is a \$0.06/gal increase in FCEPC from protected storage, and an increase in annual production costs of \$1.8M. In a scenario where both the top bales and bottom bales cannot be processed the FCEPC increases by \$0.56/gal from protected storage, costing an extra \$17M in ethanol production costs annually.

Table 4.8: Comparing feedstock contribution to ethanol production cost (FCEPC) and annual FCEPC for protected storage and field edge storage

	Protected Storage (Transported to satellite location)	FE Uncovered (All bales make to plant)	FE Uncovered (Loose top bales)	FE Uncovered (Loose top and bottom bales)
	Input Assumptions	Input Assumptions	Input Assumptions	Input Assumptions
Cost _{HST}	\$86	\$65	\$65	\$65
BCC _i	70%	70%	70%	70%
DML	2.0%	9.5%	21.0%	35.0%
Yield _{EtoH}	35%	35%	35%	35%
Mass to volume	300	300	300	300
\$/gal	\$ 1.20	\$ 0.90	\$ 1.11	\$ 1.55
Annual FCEPC(\$) *	\$ 36,100,000	\$ 30,700,000	\$ 37,900,000	\$ 53,100,000

*Based on a 30M gal capacity

4.4 Conclusions

A one year long storage trial was implemented to evaluate both the magnitude and dynamic characteristics of biomass degradation during field edge storage. Degradation occurs if environmental conditions provide above freezing temperatures and adequate moisture to support microbial activity. Moisture content within a stack is dependent on its initial baled moisture content as well as its absorbance of external moisture. Bales with high initial moisture content will heat due to microbial activity. If these bales do not absorb external moisture and are allowed to release moisture through respiration, they will reach an equilibrium moisture content near 15-18%, and become stable. Stacks with material baled at moisture contents near the equilibrium range are below the microbial metabolism requirements initially.

External moisture is influenced by weather, coverage method, and timing of coverage. In order to preserve top bales, bales must be covered before significant rainfall occurs. Once partially saturated and covered, not able to remove moisture, the top bale will continue to degrade similar to an uncovered stack, although moisture will not penetrate the next bale down. An uncovered stack continues to absorb moisture, decreasing the amount of stable material and increasing dry matter loss. Wrapping the top bales in a stack provides protection from vertical moisture migration into the top bale. Water sheds off these wrapped bales, down the columns, and is absorbed by bale edges it contacts. Uncovered stacks absorb a small amount of moisture this way, but wrapped top bales provide the highest magnitude of horizontal penetration, increasing the overall moisture content of the stack. Field edge storage poses issues with bottom bales, regardless of the coverage method. Without developing land or providing ground protection, bottom bales of field edge stacks will see absorbance of moisture in 20% to 30% of

the bale. Ground barriers can be applied but must be safe to install, durable, and less costly than the loss of bottom bale material.

The moisture absorbed by a bale reflects the dry matter loss it experiences and the resulting structural integrity after one year of storage. Bale stacks stored on field edge will absorb ground moisture, and lose approximately 16% dry matter from their bottom bales. Dry bales in the center of stacks, regardless of coverage method, experience little to no dry matter loss. Top uncovered bales become saturated and lose upwards of 30% dry matter in one year. Bales within wrapped top bale stacks degrade horizontally with moisture migration. Bottom bales lose material quality where moisture wicking occurs. Degradation due to moisture absorption lessens the quantity and quality of material increasing the FCEPC for a biorefinery. In this study, if all biomass can be processed, uncovered field edge storage shows potential in significantly reducing FCEPC and annual production costs, approximately \$0.18/gal or \$5.4M/year. Degradation also poses problems to biorefineries in regards to material integrity and processing. Plants that require individual handling of bales, specific dimensions, or minimum structural integrity will struggle to process a large majority of bales after one year of field edge storage: uncovered top bales, bales within a wrapped top bale stack, bottom bales. Loss of integrity will also present problems in both handling and transportation of the material. If either top bales or both top and bottom bales of a field edge stack cannot be processed, field edge storage significantly increases the FCEPC and annual ethanol production cost. This study did not assess impact on plant cost beyond loss of carbohydrates. Degraded, wet material may have impact on grinding and reactor loading efficiencies as well as the water balance within a biorefinery. These potential issues should be evaluated to further understand the impact of field edge storage on FCEPC.

Corn stover supply chains must determine the correct balance of protection cost and material losses for the principles outlined. Field edge storage will eliminate many of the material costs of storage, but propose risks to feedstock quality. It is recommended that a combination of field edge and satellite storage be implemented to economically balance the storage cost to quality loss ratio. This balance will be heavily dictated by the capabilities of refineries processing the biomass. Field edge storage strategies should be determined based on historical weather patterns, but account for risk associated with late stack coverage. Overall storage of biomass must be flexibly designed to minimize risk to optimize long-term annual cost.

REFERENCES

- American Society of Agricultural and Biological Systems Engineers. 1988. "Moisture Measurement- Forages. ASABE Standard Procedure S358.2."
- Ankom Technology. 2000a. "Acid Detergent Fiber in Feeds - Filter Bag Technique (for A2000 and A2000I)." : 20–21.
- . 2000b. "Neutral Detergent Fiber in Feeds - Filter Bag Technique (for A2000 and A2000I)." : 2–3.
- AOAC. "Fiber (Acid Detergent) and Lignin in Animal Feed. AOAC Standard Procedures 973.18."
- Aro, Nina, Tiina Pakula, and Merja Penttilä. 2005. "Transcriptional Regulation of Plant Cell Wall Degradation by Filamentous Fungi." *FEMS Microbiology Reviews* 29(4): 719–39.
- Bajpai, Pratima. 2016. "Pretreatment of Lignocellulosic Biomass for Biofuel Production." : 86.
file:///C:/Users/rbearden/Downloads/9789811006869-c2.pdf.
- Brooker, Robert, J., P. Widmaier, Eric, E. Graham, Linda, and D. Stiling, Peter. 2011. "Cellular Respiration, Fermentation, and Secondary Metabolism." In *Biology For Bio 211 and 212*, New York: McGraw-Hill, 137–56.
- Brown, Robert, and Tristan Brown. 2014. *Biorenewable Resources- Engineering New Products from Agriculture*. 2nd ed. Ames.
- Chen, Hongzhang. 2014. *Biotechnology of Lignocellulose: Theory and Practice* *Biotechnology of Lignocellulose: Theory and Practice*.
- Darr, M.J., Keith Webster, and Rachel Bearden. 2015. *Biomass Storage Summary Report to DuPont Cellulosic Ethanol*.
- Darr, Matthew J. 2014. *Corn Stover Feedstock Supply Chain Cost Reduction Report to DuPont Cellulosic Ethanol*.

- Darr, Matthew J, Keith Webster, Jeremy Brue, and Rachel Bearden. 2015. *Annual Harvest Report to DuPont Cellulosic Ethanol*. Nevada, IA.
- Hubbe, Martin A., Mousa Nazhad, and Carmen Sanchez. 2010. "Composting as a Way to Convert Cellulosic Biomass and Organic Waste into High-Value Soil Amendments: A Review." *BioResources* 5(4): 2808–54.
- Iowa Environmental Mesonet. 2015. "Mesonet Dailey Weather."
<http://mesonet.agron.iastate.edu/>.
- Jang, Ming-feng, and Yi-shyong Chou. 2012. "Modeling and Optimization of Bioethanol Production via a Simultaneous Saccharification and Fermentation Process Using Starch." (November).
- Lee, DoKyoung, Vance N. Owens, Arvid Boe, and Peter Jeranyama. 2007. "Composition of Herbaceous Biomass Feedstocks." *Cellulose* (June): 16.
<http://scholar.google.com/scholar?hl=en&btnG=Search&q=intitle:Composition+of+herbaceous+biomass+feedstocks#0>
<http://scholar.google.com/scholar?hl=en&btnG=Search&q=intitle:Composition+of+Herbaceous+Biomass+Feedstocks#0>.
- Mourtzinis, Spyridon et al. 2014. "Distribution of Structural Carbohydrates in Corn Plants Across the Southeastern USA." *Bioenergy Research* 7(2): 551–58.
- Nutrition, Deer. 2003. "Near Infrared Reflectance Spectroscopy : Applications in Deer Nutrition." (July).
- Okamoto, Kenji, Atsushi Uchii, Ryuichi Kanawaku, and Hideshi Yanase. 2014. "Bioconversion of Xylose , Hexoses and Biomass to Ethanol by a New Isolate of the White Rot Basidiomycete *Trametes Versicolor*." : 1–9.

- Okpokwasili, G C, and C O Nweke. 2005. "Microbial Growth and Substrate Utilization Kinetics." 5(4): 305–17.
- Parker, Nathan (UC-Davis). 2016. *Epscor Series Seminar: Transition Cost for Cellulosic Biofuels*. Ames, IA.
- Rohr, Prof. Ph Rudolf von. 2016. "ETHzurich Transport Processes and Reactions Laboratory-Research." http://www.ltr.ethz.ch/en/research/green_chemistry.html.
- Schon, Brittany N. 2012. "Characterization and Measurement of Corn Stover Material Properties." Iowa State University.
- Schon, Brittany N, Matthew J Darr, Keith E Webster, and Nicole Jennett. 2013. "Analysis of Storage Methods and Tarping Practices for Corn Stover Bales."
- Schroeder, J.W. 2008. "Forage Nutrition for Ruminants." (June 2004): 1–22.
- Shah, A., M.J. Darr, K Webster, and C Hoffman. 2011. "Outdoor Storage Characteristics of Single-Pass Large Square Corn Stover Bales in Iowa." *Energies* (4): 1686–94.
- Shah, Ajay, and Keith Webster. 2014. "Corn Stover." *PM 3051E* (January): 1–2.
- Shinners, Kevin J et al. 2006. "Drying , Harvesting and Storage Characteristics of Perennial Grasses as Biomass Feedstocks." 0300(061012).
- Sluiter, A et al. 2005. "Determination of Ash in Biomass. National Renewable Laboratory."
- de Souza, Walter Rodrigo. 2013. "Microbial Degradation of Lignocellulosic Biomass." *Sustainable Degradation of Lignocellulosic Biomass - Techniques, Applications and Commercialization*: 207–48.
- Todar, Kenneth, Phd (University of Wisconsin). *Online Textbook of Bacteriology*. Online. http://textbookofbacteriology.net/nutgro_4.html.

Wang, Dr. Yu. 2016a. "Globalization & the Environment."

———. 2016b. "Peak Oil and Energy Security."

APPENDIX A. FEED ANALYSIS METHODOLOGY FOR ANALYZING CARBOHYDRATE STRUCTURE OF CORN STOVER

5.1 Laboratory Analysis of Forage

Forage materials are commonly analyzed for quality using wet chemistry feed analysis. Acid Detergent Fiber (ADF) and Neutral Detergent Fiber (NDF) are frequently used as standard forage tests to determine material fiber content, often to estimate fiber intake rates and digestibility for animal consumption. An Ankom NDF test estimates the amount of cell wall constituents, and the remaining residues are predominantly hemicellulose, cellulose, and lignin. The Ankom ADF test contains residues predominantly of cellulose and lignin. In many forage applications, the NDF and ADF values are the main values used to calculate feed rations. An Acid Detergent Lignin test, less utilized in feed rations, can be analyzed through a test that is commonly performed following an ADF test. Based on their residual components, these three tests and values: NDF, ADF, and AD Lignin should estimate the components of hemicellulose, cellulose, and lignin for forage material (Figure 5.1). Often for “cleaner” and consistent forage materials, detergent insoluble ash content is either estimated with a constant or may be low enough to exclude from the fiber calculations all together. Some, but not all labs include ash content testing in their ADF and NDF analysis. The following methods for ADF, NDF, and AD Lignin were performed by an external feed lab to determine composition of lignin, cellulose, hemicellulose, and total carbohydrate.

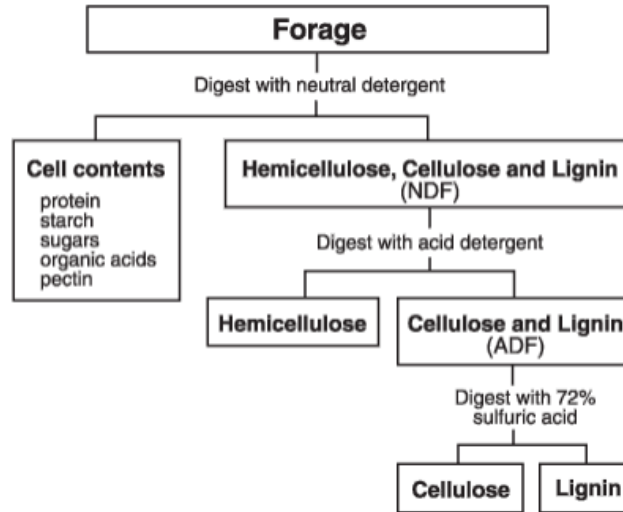


Figure 5.1: Forage analysis breakdown (Schroeder, 2008).

Proximate components	Chemical fraction	Van Soest fractions	
Ash ₁ ↔	Detergent soluble ash	Cell contents	
Ether extract ↔	Triglycerides Pigments		
Crude protein ↔	Protein NPN		
Nitrogen-free extract ↔	Sugar Starch Pectin		
Crude fiber ↔	Hemicellulose	Neutral detergent fiber (cell wall)	
	OH soluble		Acid detergent fiber
	OH insoluble Lignan		
Ash ₂ ↔	Cellulose		
	Detergent insoluble ash		

Figure 5.2: Forage fraction classification based on Van Soest method (Schroeder, 2008).

5.2 Sample Preparation for Structural Carbohydrate Analysis

All samples analyzed for carbohydrate content were first dried using ANSI/ASAE S358.3 standard (ASABE,1988) for moisture measurements of forage material to both capture final moisture content and dry the sample to be prepared. Each full sample was then ground through a 1mm using a Retch knife mill. The full sample was well mixed and a 25-50 g subsample was taken from the full ground sample, and sent to an external lab in a sealed zip lock bag for feed

analysis. Once delivered to the lab, the received sample was poured into a pan, mixed, and subsampled again. One 0.5 g subsample was taken for NDF analysis and a separate 0.5 g subsample was taken for sequential ADF and AD Lignin analysis.

5.3 Neutral Detergent Fiber Analysis

Neutral detergent fiber is a very common fiber measurement in feed analysis. It does not measure specific chemical compounds, but instead, a plant's structural components. The analysis for this research followed MWL FE 021 which is based on Ankom Technology method (Ankom Technology, 2000b). The method used takes the 0.5 g subsample and digests it in a detergent solution. The sample is then rinsed and dried and the remaining residue is considered the neutral detergent fiber and is reported on a percent bases of the original sample. Typically the structural components remaining are hemicellulose, cellulose, and lignin. Cell contents such as sugars, starch, pectin, and undamaged protein are dissolved in this process. The Ankom Technology method uses the following recorded values and Equation 5.1 to calculate the reportable %NDF on an as received basis.

W_1 = Bag tare weight

W_2 = Sample weight

W_3 = Dried weight of bag with fiber after extraction process

Equation 5.1: Reported percent neutral detergent fiber calculation

$$\% NDF = \frac{100 * (W_3 - W_1)}{W_2}$$

5.4 Acid Detergent Fiber Analysis

Acid detergent fiber analysis is also common in analyzing feed content quality. The carbohydrate analysis for this research followed MWL FE 022 which is based on Ankom

Technology method (Ankom Technology, 2000a). The method used digests the 0.5 g subsample in a detergent composed of sulfuric acid and cetyltrimethylammonium bromide (CTAB). The sample is rinsed and dried, and the remaining residue is reported as the ADF on a percent basis of the original sample. The cell contents dissolved in the NDF test are also dissolved in this ADF test, as well as hemicellulose. The remaining components are predominately cellulose and lignin. The Ankom Technology method uses the following recorded values and Equation 5.2 to calculate the reportable %ADF on an as received basis.

W_1 = Bag tare weight

W_2 = Sample weight

W_3 = Dried weight of bag with fiber after extraction process

Equation 5.2: Reported percent acid detergent fiber calculation

$$\% ADF = \frac{100 * (W_3 - W_1)}{W_2}$$

5.5 Acid Detergent Lignin Analysis

Determination of acid detergent lignin is less common in feed analysis, but is required to determine the composition of the three main lignocellulosic components. The analysis for this research followed MWL FE 025, which is based on AOAC 973.18 (AOAC, n.d.). In the methods used, lignin analysis is performed after an ADF test; the resulting ADF residues are the starting sample for the lignin test. These residues, already in their original sample bag, are digested in a 72% sulfuric acid bath to dissolve cellulose. The remaining bag and material is rinsed and dried. It is placed in a crucible and weighed. The bag and contents are burned for four hours and a final mass of the crucible and remaining contents are recorded. The method uses the following

recorded values and Equation 5.3 to calculate the reportable % Lignin on an as received basis. Lignin is calculated based on mass loss, not based on the remaining ash material.

W_1 = Sample Weight

W_2 = Crucible + Bag Contents

W_3 = Crucible + contents after ash

Equation 5.3: Reported percent Lignin calculation

$$\% \text{ Lignin} = \frac{100 * (W_3 - W_2)}{W_1}$$

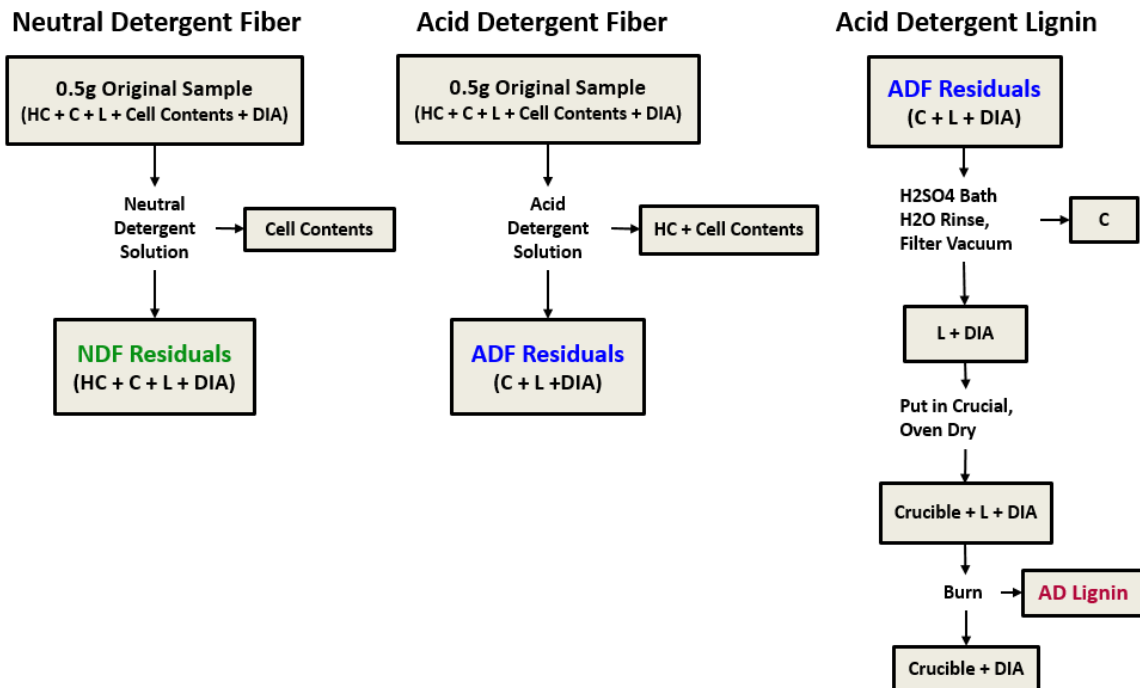


Figure 5.3: Summary flow chart of ADF, NDF, and AD Lignin analysis methods

5.6 Determination of Lignocellulosic Composition

The three reported values from the methods above: %NDF, %ADF, and %Lignin were used in Equations 5.4, 5.5, and 5.6 to determine the composition of hemicellulose, cellulose, and lignin respectfully for each sample examined. Total carbohydrate composition was determined using Equation 5.7.

Equation 5.4: Percent hemicellulose calculation

$$\% \text{ Hemicellulose} = \% \text{ NDF} - \% \text{ ADF}$$

Equation 5.5: Percent cellulose calculation

$$\% \text{ Cellulose} = \% \text{ ADF} - \% \text{ Lignin}$$

Equation 5.6: Percent lignin calculation

$$\% \text{ Lignin} = \% \text{ Lignin}$$

Equation 5.7: Percent total carbohydrate calculation

$$\% \text{ Total Carbohydrate} = \% \text{ Hemicellulose} + \% \text{ Cellulose}$$

5.7 Influence of Detergent Insoluble Ash

For “clean” forage materials; those with low non-structural ash and soil contamination, the above equations can generally be used as listed to analyze composition of hemicellulose, cellulose, and lignin. For those forage materials with high or variable ash contamination, the compositional values for the lignocellulosic components can be falsely inflated or deflated if ash content is not analyzed and used in the calculations. Most mineral ash inherent to plant material is dissolved during neutral detergent and acid detergent tests, and does not remain in the

measured residue. Insoluble ash on the other hand, silica for example, does not dissolve in either test and carries on within the residue.

An individual set of tests were performed to evaluate the influence of increased ash content in samples analyzed for carbohydrate structure with this method. 10 individual core samples, taken within the same day, from protected material were used for the tests. Material was bright in color and had not degraded. A 3 g subsample was taken from each lab sample, and ashed. The weight of the inorganic residue left behind was calculated and expressed as the % Total Ash Content. Seven of the samples had ash contents ranging from 7% to 11%, and three contained ash contents near 15%. Samples were then analyzed for the original NDF, ADF, and AD Lignin as described in the methodology above. A second 0.5 g subsample was taken from each, sent through the ADF process, and then ashed immediately. These samples were not analyzed for lignin content. The residue left after this ashing process was recorded as the detergent insoluble ash (DI) on a percent basis. A value of corrected % cellulose was determined by subtracting the lignin and detergent insoluble ash contents from the ADF content (Equation 5.8). This corrected value of % cellulose was used to determine the error in the original estimation of cellulose (Equation 5.9).

Equation 5.8: Corrected percent cellulose calculation

$$\text{Corrected \% Cellulose} = (\%ADF - \%AD \text{ Lignin} - \%DI \text{ Ash})$$

Equation 5.9: % Cellulose error calculated with the corrected cellulose content

$$\text{Cellulose Error Estimation} = \% \text{ Cellulose} - \text{Corrected \% Cellulose}$$

REPORT NUMBER [REDACTED]	 Midwest Laboratories [®] 13611 B Street • Omaha, Nebraska 68144-3693 • (402) 334-7770 www.midwestlabs.com	PAGE 6/6 <small>ISSUE DATE</small> Sep 27, 2016
<small>REPORT DATE</small> Sep 27, 2016 <small>RECEIVED DATE</small> Aug 22, 2016		
IOWA STATE UNIVERSITY RACHEL BEARDEN [REDACTED] BOONE IA 50036	REPORT OF ANALYSIS For: [REDACTED] IOWA STATE UNIVERSITY CARBOHYDRATE ANALYSIS CORN STOVER	
Detailed Method Description(s)		
<p>Acid Detergent Fiber Analysis follows MWL FD 021 which is based on Ankom Technology method. The sample is sealed in a small bag and the bag immersed in a solution that dissolves certain materials. The bag is washed and dried and re-weighed. The material remaining in the bag is reported as acid detergent fiber</p> <p>NDF Analysis follows MWL FD 022 which is based on Ankom Technology method. The sample is sealed in a small bag and the bag immersed in a solution that dissolves certain materials. The bag is washed and dried and re-weighed. The material remaining in the bag is reported as neutral detergent fiber</p> <p>Lignin Analysis follows MWL FD 025 which is based on AOAC 973.18. Samples are analyzed for ADF and remaining sample is digested in sulfuric acid for 4 hours and ashed. Weights are put in a program to determine % lignin.</p>		
<small>The result(s) issued on this report only reflect the analysis of the sample(s) submitted. Our reports and letters are for the exclusive and confidential use of our clients and may not be reproduced in whole or in part, nor may any reference be made to the work, the results, or the company in any advertising, news release, or other public announcements without obtaining our prior written authorization.</small>		

Figure 5.4: Description of carbohydrate analysis tests from Midwest Laboratories Inc.

APPENDIX B: MODELING MICROBIAL GROWTH AND SUBSTRATE UTILIZATION

Microbial systems generally follow their unique type of non-linear growth models. In batch microbial systems, growth occurs in four distinct phases: lag phase, log/exponential phase, stationary phase, and cell death phase (Figure 6.1). The system is often plotted on a logarithmic scale to distinguish the phases.

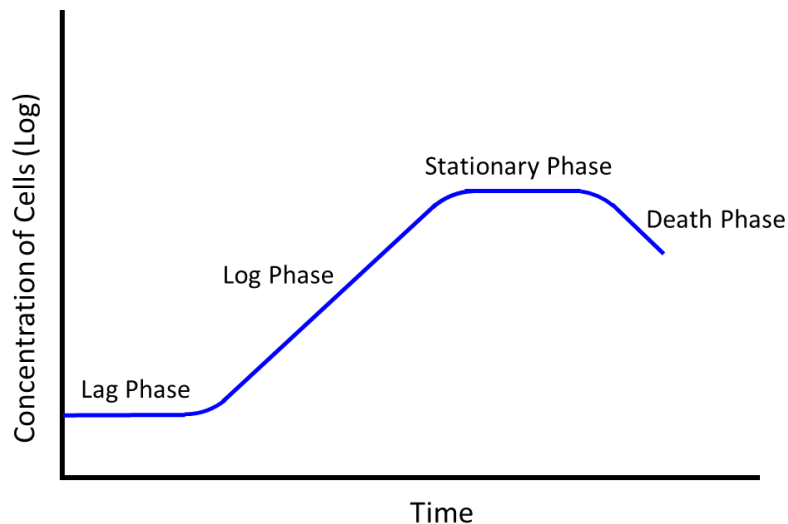


Figure 6.1: Microbial growth curve, log scale

The microbial growth within a simultaneous saccharification-fermentation reactor is dependent on kinetic characteristics of the organism itself, as well as influenced by the concentrations of microbes (X), enzymes (Enz), starch (S), glucose (G), and ethanol (E). The natural exponential growth experienced by microorganisms and inhibitory factors related to

substrate and product concentration cause the model to be non-linear (Figure 6.2).

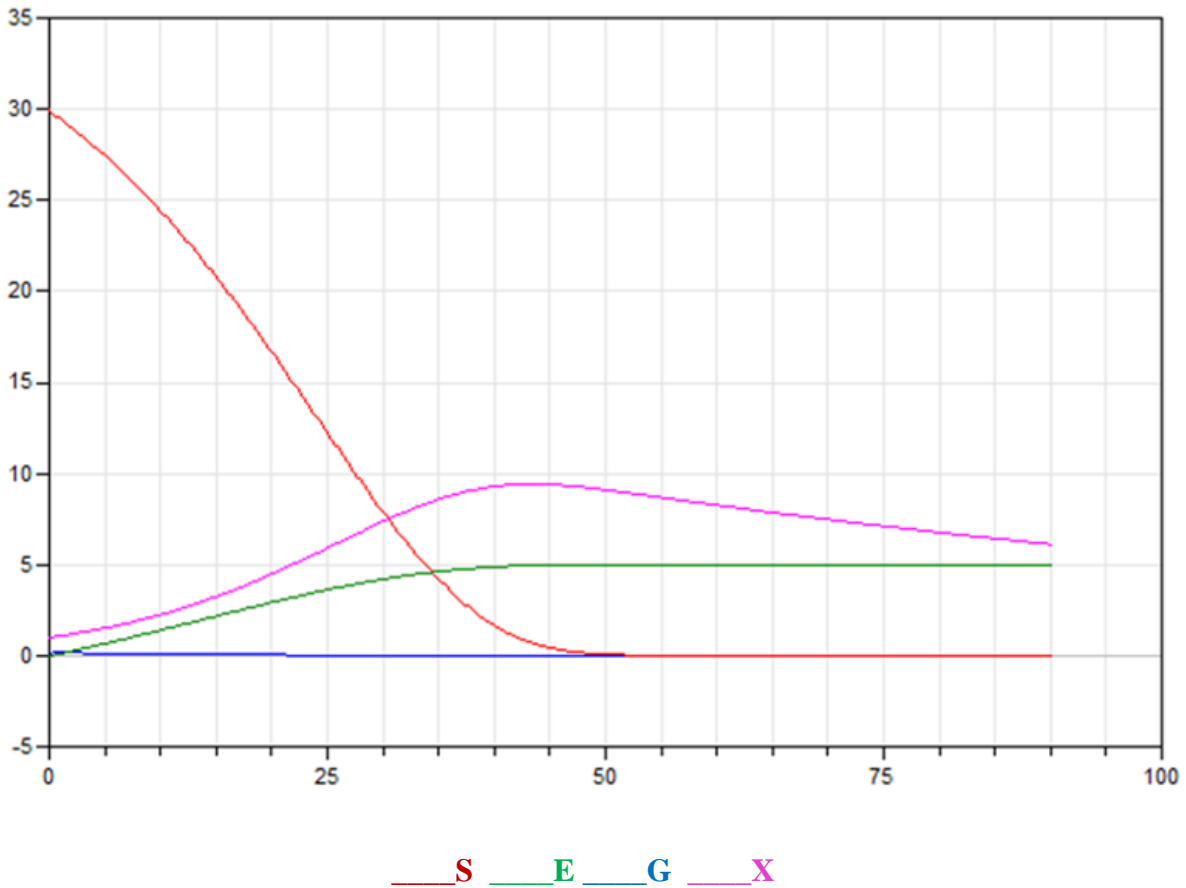


Figure 6.2: Modeling Simultaneous Saccharification/Fermentation reactor using (Jang and Chou, 2012) model. S: starch concentration, E: ethanol concentration, G: glucose concentration, and X: microbial concentration

The factors that an organism influences on its own growth are its concentration (X), maximum growth rate (μ_{max}), saturation growth constant (k_s), and cell death constant (k_d) (Equation 6.1). Growth is also dependent on the concentration of the utilized glucose substrate (G) and substrate inhibition constant (k_{ss}), as well as concentration of the ethanol product (E) and product inhibition constant (k_{ex}). The substrate inhibition constant can inhibit initial growth, shown in the lag phase. Lack of substrate, the product inhibition constant, and death constant cause microbial growth to experience the stationary and death phases. Starch substrate, glucose intermediate, and ethanol product concentrations have their own rate equations (Equations 6.2,

6.3, and 6.4) that are further dependent on the enzyme concentrations (Equation 6.5). Together these rate equations develop a real time model to estimate product yield, loading rates, and retention time.

Equation 6.1: Microbial growth rate equation (Jang and Chou, 2012)

$$\frac{dX}{dt} = \left[\left(\left(\frac{\mu_{max}G}{K_s + G + G^2/K_{SS}} \right) e^{-E/K_{ex}} \right) - K_d \right] X$$

Equation 6.2: Glucose rate equation (Jang and Chou, 2012)

$$\frac{dG}{dt} = 1.111R_sS - \left(\frac{1}{Y_{X/G}} * \frac{dX}{dt} \right) - \left(\frac{1}{Y_{E/G}} * \frac{dXE}{dt} \right)$$

Equation 6.3: Ethanol rate equation (Jang and Chou, 2012)

$$\frac{dE}{dt} = \left(\frac{q_{max}G}{k_{sp} + G + G^2/k_{ssp}} \right) e^{(-E/k_{ex})}$$

Equation 6.4: Starch rate equation (Jang and Chou, 2012)

$$\frac{dS}{dt} = \left[\frac{-k_h Enz}{k_m + \left(1 + G/K_G\right) + S^2/k_{starch} + S} \right] S$$

Equation 6.5: Enzyme rate equation (Jang and Chou, 2012)

$$\frac{dEnz}{dt} = \left[(\mu_{max} + \beta) \frac{Enz_{max}S}{k_{enz} + S} (\mu + \beta) \right] Enz$$

X = Microbial cell concentration	k_h = rate constant
G = Glucose concentration	k_m = Michaelis constant
E = Ethanol concentration	k_{starch} = starch inhibition constant
S = Starh concentration	k_G = glucose inhibition constant
Enz = Enzyme	k_s = saturation growth constant
μ_{max} = maximum specific growth rate	k_{ss} = substrate inhibition constant
q_{max} = maximum specific production rate	k_{sp} = saturation production constant
ENA_{max} = maximum enzyme concentration	k_{ssp} = substrate inhibition constant
$Y_{X/G}$ = yield coefficient of biomass growth	k_{ex} = product inhibition constant
$Y_{E/G}$ = yield coefficient of ethanol	k_d = cell death constant
β = enzyme degradation rate	k_{enz} = enzyme inhibition constant

Figure 6.3: Simultaneous Saccharification/Fermentation modeling variables (Jang, Chou 2012)